CHARACTERIZATION OF THE ROLE OF PCRK1 IN NORTIA-MEDIATED POLLEN TUBE RECEPTION

by

Rachel Danielle Flynn

A Thesis

Submitted to the Faculty of Purdue University

In Partial Fulfillment of the Requirements for the degree of

Master of Science

Department of Botany & Plant Pathology

West Lafayette, Indiana

December 2019

THE PURDUE UNIVERSITY GRADUATE SCHOOL
STATEMENT OF COMMITTEE APPROVAL

Dr. Sharon Kessler, Chair

Department of Botany & Plant Pathology

Dr. Leonor Boavida

Department of Botany & Plant Pathology

Dr. Chunhua Zhang

Department of Botany & Plant Pathology

Approved by:

Dr. Christopher Staiger

Head of the Graduate Program

This thesis is dedicated to my mother Susan Flynn (née Sarault) and my father Craig Flynn for helping shape the person I am today through their love and support.

ACKNOWLEDGMENTS

I would like to thank my advisor Dr. Sharon Kessler for giving me the opportunity to work in her lab and for all her guidance and support. I also want to thank my advisory committee members, Dr. Leonor Boavida and Dr. Chunhua Zhang for their advice and feedback.

Thanks to the current and past members during my time in the Kessler lab: Dr. Yan Ju, Cole Thomas Davis, Dr. Jing Yuan, Dr. Daniel Jones, Dr. Subramanian Sankaranarayanan, Daniel Cabada Gomez, Anna Donnelly, and Lindsey Berebitsky for their day-to-day lab support and for making the Kessler lab a fun environment to work in. I would especially like to thank Dr. Yan Ju and Cole Thomas Davis for taking the time to provide experimental training in the various molecular biology and microscopy techniques used. The training and advice provided by them and Dr. Sharon Kessler were essential to this work and has provided many useful skills which will be valuable to me going forward in my career.

TABLE OF CONTENTS

LIST OF TABLES

LIST OF FIGURES

ABSTRACT

Author: Flynn, Rachel, D. MS
Institution: Purdue University
Degree Received: December 2019
Title: Characterization of the Role of PCRK1 in NORTIA-Mediated Pollen Tube Reception
Committee Chair: Sharon Kessler

Cell-to-cell communication is the driving force behind successful reproduction in flowering plants. Extensive extracellular communication events occur between the male and female gametophytes during pollen tube reception to facilitate successful fertilization. These signaling events culminate into a product of great importance for both animals and plants: the seed. In this study, the pathogen defense regulator PATTERN-TRIGGERED IMMUNITY COMPROMISED RECEPTOR-LIKE CYTOPLASMIC KINASE 1 (PCRK1) was identified to function in pollen tube reception from both the male and female gametophytes in the flowering plant *Arabidopsis thaliana* using a forward genetic screen. A knockout of *pcrk1* suppresses the pollen tube overgrowth phenotype leading to infertility in *nortia* mutants. In addition, *pcrk1* pollen affected the pollen tube overgrowth phenotypes of pollen tube reception mutants *feronia* and *turan*. Shared molecular components of pollen tube reception and pathogen invasion have been reported. This study reveals another link between pathogen defense and pollen tube reception. By studying the links between fertility and disease in plants, we may be able to uncover potential trade-offs with fertility when breeding for pathogen resistance.

CHAPTER 1. INTRODUCTION

1.1 Reproduction in Flowering Plants

The evolutionary transition which allowed charophyte green algae to survive and reproduce above-water occurred over 470 million years ago and led to the diversification of terrestrial land plants as we know them today (Delwiche and Cooper, 2015; Gensel and Edwards, 2001). They are the basis for our life on Earth; providing food for humans, livestock, wildlife, insects, and microorganisms, important industrial products such as lumber, paper, and fibers, and secondary metabolites necessary for pharmaceutical drugs and pesticides (Delwiche and Cooper, 2015). In addition, dead land plants make up the primary source of stored carbon on Earth, by providing carbon to the soil and leading to the formation of coal (Delwiche and Cooper, 2015). Land plants consist of liverworts, hornworts, mosses, and vascular plants, and have a two-phase life cycle which alternates between diploid (2n) sporophytic and haploid (n) gametophytic life phases with many complex organs and tissue systems (Kenrick and Crane, 1997). Flowering plants, also known as angiosperms, differ from earlier land plants such as bryophytes in that their dominant life phase is the sporophytic generation. The angiosperm gametophyte is highly reduced, comprised of a few highly specialized cells which are buried within the flowers.

The floral framework of a typical flower consists of four concentric whorls of organs; the calyx, composed of sepals, the corolla, containing petals, the androecium with stamens, and the gynoecium which is comprised of the carpels (Fig. 1.1A, Ross, 1985). The outer whorl of sepals protects the developing flower bud, while the next inner whorl of petals function as pollinator attractants and provides a place for pollinators to land on the flower. The third inner whorl of stamens consists of the male reproductive organs which house the male gametophytes at maturity, and the fourth, most internal whorl develops into the female reproductive organs that contain the

female gametophytes. The female reproductive organs include the stigma, style, and carpels. The carpels house the transmitting tract and ovules (Fig. 1.1B). The ovules contain the female gametophyte and are the precursors of seed. The male gametophyte of flowering plants is the pollen grain. A pollen grain's purpose is to pass on its genetically encoded information to the next generation by delivering sperm cells to the female gametophyte, or embryo sac, in order for successful double fertilization to occur.

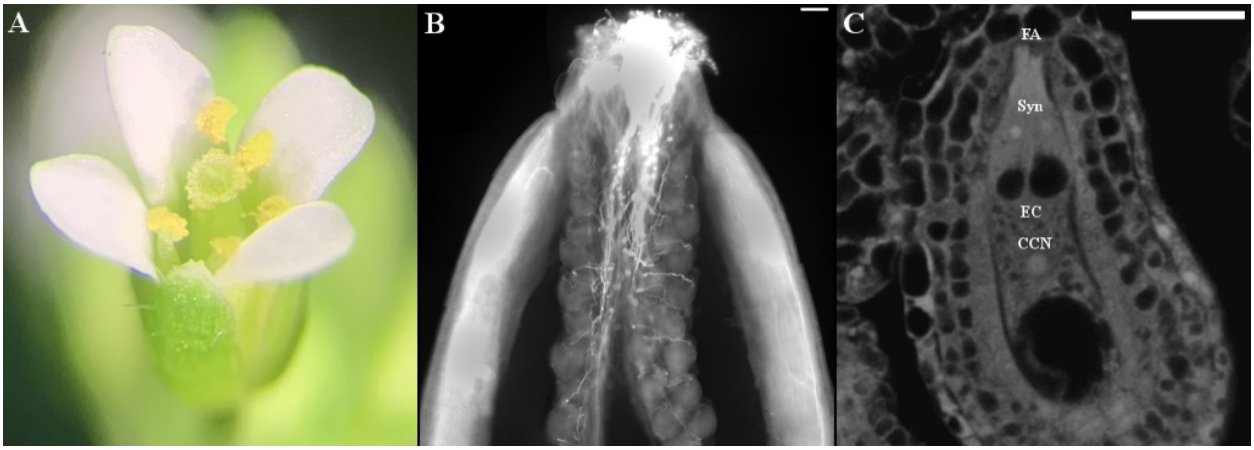

Figure 1.1 Sexual Reproduction in *Arabidopsis thaliana.*

(A) An *Arabidopsis thaliana* flower displaying the four whorls of floral development. (B) An epifluorescent image of an aniline blue stained pistil showing pollen tube growth through the transmitting tract and pollen tube attraction to ovules. (C) A confocal image of a mature *Arabidopsis* female gametophyte showing the filiform apparatus at the micropyle (FA), two synergid cells and their corresponding nuclei and vacuoles (Syn), the location of the egg cell (EC), and the central cell nucleus (CCN). Scale bars: 100µm (B), 25µm (C).

Arabidopsis thaliana is the "fruit fly of the plant world", meaning that it is a popular model organism frequently used for plant science research, just as the fruit fly is a popular model organism for research. *Arabidopsis thaliana* is a small flowering plant which is a member of the *Brassicaceae* or mustard family. It is often used as a model for understanding the genetic, cellular, and molecular biology of flowering plants. *Arabidopsi*s flowers are often utilized as a model system for angiosperm flowers in plant reproduction research and are used in this thesis. Using

Arabidopsis thaliana for research has many benefits such as a small, fully sequenced diploid genome, a large collection of T-DNA mutants and genomic resources, efficient transformation methods using *Agrobacterium tumefaciens,* and a large community of Arabidopsis researchers in academic, government, and industrial laboratories. *Agrobacterium tumefaciens* is a bacterial plant pathogen that has been modified for use as a tool. Molecular biologists take advantage of its natural ability to transfer DNA into the genome of another plant. *Arabidopsis thaliana* also has a short lifecycle, high seed production, and is easy to cultivate in limited spaces.

Over time, the morphology of flowers has evolved to allow for the attraction of pollinators and the efficient delivery of pollen by these pollinators. These adaptations are evident today in the large global diversity of angiosperm flower color and shape. Pollinators such as bees, birds, beetles, butterflies, flies, hummingbirds, and bats seek the nectar secreted by flowers which can be a nutritious food source for them. In return, the pollinator enables successful reproduction for the plant. When a pollinator enters a flower to find the nectar, pollen from the anthers sticks to the pollinator. As the pollinator travels from flower to flower, pollen is transferred to the female reproductive organs of another plant, facilitating pollination.

Cell-to-cell communication is the driving force behind mate selection and successful reproduction in flowering plants. Unlike in animals where mating selection is facilitated by pheromones, visual signals, and behavior, plants are sessile, therefore; their modes of interaction have evolved to be unique from animals (Preuss, 2002). Most higher plant cells are connected by rigid cell walls and often spend the duration of their lives alongside the same cells. One exception to this is the journey of pollen grains and subsequently, the pollen tube, during angiosperm reproduction (Preuss, 2002). There are various stages throughout this journey, each of which requires carefully orchestrated processes of extensive intercellular signaling events which enables

cell-to-cell communication. These signaling events culminate into a product of immense importance for animals and plants alike: the seed (Pajoro et al., 2014).

Sexual reproduction of flowering plants begins as a pollen grain lands on a female stigma. This can occur by either abiotic or biotic pollinators, or self-pollination. This is the first example of cell-to-cell communication between male and female tissues during plant reproduction. There are signaling mechanisms in place for the stigma to either accept or reject the pollen grain (Hiscock & Allen, 2008). If the pollen grain is accepted, it will hydrate and germinate a pollen tube (Hiscock & Allen, 2008). The pollen tube houses the two sperm cells which will eventually reach and fertilize the female gametophyte. The pollen tube grows downward into the stigma papillae cell and then into the transmitting tract (Fig. 1.1B) where it continues its downward growth until encountering attraction molecules secreted by the female ovules. One class of these attraction molecules were discovered in *Torenia fournieri*, called LUREs (Okuda et. Al., 2009). The pollen tube changes its direction of growth in the direction of attraction molecules, toward the ovule (Okuda et. Al., 2009). As the pollen tube reaches the ovule, it is guided toward and into the micropyle where it encounters the synergid cells of the female gametophyte, and their highly specialized region of invaginated plasma membrane, the filiform apparatus (Fig. 1.1C). Complex signaling occurs between the male pollen tube and the female synergid cells (Fig. 1.1C), leading to the slowed growth of the pollen tube as it reaches the micropyle. Eventually, the pollen tube grows into the female gametophyte, although whether it grows in or around one of two synergid cells is still debated. As both the pollen tube and the receptive synergid cell die, two sperm cells are released into the embryo sac, allowing gamete fusion and double fertilization to occur (Sandaklie-Nikolova, Palanivelu, King & Copenhaver, 2007; Huck, Moore, Federer, Grossniklaus, 2003; Rotman et al., 2003). One sperm cell fertilizes the egg cell of the embryo sac, and the other

fertilizes the central cell. Embryogenesis and endosperm development occur during the formation of a seed. This collective process of intricate signaling events is of immense importance for human agriculture and all life on land.

1.2 Female Gametophyte Development

The ovule is the precursor of a seed. The fertilized egg cell of the female gametophyte undergoes embryogenesis, and the fertilized central cell makes the endosperm. The ovule is made up of a nucellus, two integuments, and a funiculus (Reiser & Fischer, 1993). The inner and outer integuments initiate at the base of the nucellus during megasporogenesis and grow parallel to the developing embryo sac (Fig. 1.2B, Reiser & Fischer, 1993). They offer protection of the embryo sac and form the micropyle, the area between the integuments which is the site of pollen tube entry to the female gametophyte. The funiculus connects the base of the ovule at the chalaza to the ovary wall and contains vascular tissue. The chalaza is defined as the region from the base of the integuments to the funiculus attachment (Esau,1977). Megasporogenesis and megagametogenesis are the two stages of development involved in the formation of the mature embryo sac (Fig. 1.2). *Arabidopsis thaliana* undergoes the polygonum-type of embryo sac development, which is the most commonly observed form of embryo sac development, with seventy percent of species examined, including maize, undergoing this type of development (Reiser & Fischer, 1993; Russell, 1978; Mansfield et al., 1990; Webb & Gunning, 1990). During megasporogenesis, the megasporocyte undergoes meiosis I and II to form four megaspores (Fig. 1.2C). The three megaspores at the micropylar end degenerate, and one functional megaspore survives (Fig. 1.2D).

Megagametogenesis begins as the functional megaspore undergoes mitosis. Three rounds of mitosis, nuclear migration, and cellularization leads to the mature, seven-celled embryo sac (Fig. 1.2H). Starting at the chalazal end of the embryo sac and moving in the micropylar direction,

the first cells encountered are three antipodal cells. The function of these cells is not known but they are suspected to provide nutrients to the developing embryo. Next is the central cell which consists of two polar nuclei which fuse before maturity (Fig. 1.2G, Fig. 1.2H). The central cell fuses with one sperm cell to form the endosperm. The egg apparatus is located at the micropylar end of the embryo sac and consists of the egg cell and two synergid cells (Fig. 1.2H). The synergid cells are important for the attraction and reception of a pollen tube by the release of signaling molecules through the filiform apparatus, a region of invaginated plasma membrane at the micropylar end of the synergid cells.

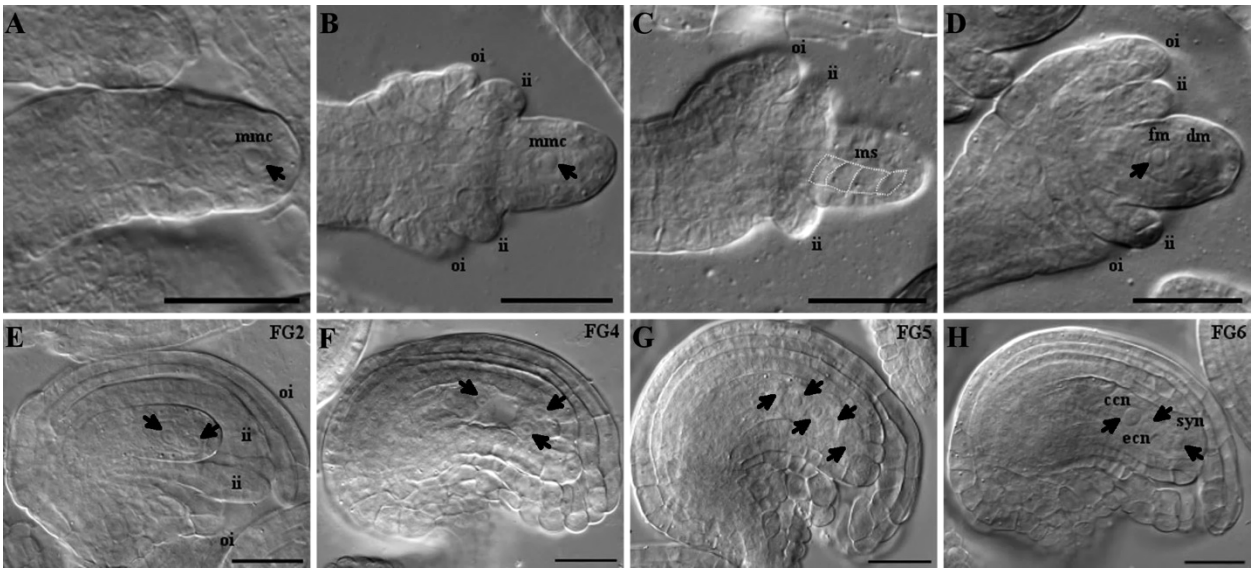

Figure 1.2 Polygonum-type Megasporogenesis and Megagametogenesis of the Female Gametophyte.

(A-D) Megasporogenesis of the female gametophyte. (A) Initiation of an ovule beginning with a single diploid megaspore mother cell (mmc). (B) The initiation of the outer and inner integuments (oi, ii). (C) The products of the mmc undergoing meiosis, four haploid megaspores. (D) The last stage of megasporogenesis, showing the functional megaspore (fm), degenerating megaspores (dm), and further developing outer and inner integuments (oi, ii). (E-H) Megagametogenesis of the female gametophyte. (E) FG2 stage of megagametogenesis. (F) An ovule at the FG4 stage of megagametogenesis. (G) The FG5 stage of megagametogenesis showing two unfused polar nuclei, the egg cell nucleus, and synergid cell nucleus. (H) An ovule with a mature female gametophyte showing a synergid cell nucleus (syn), egg cell nucleus (ecn), and central cell nucleus (ccn). Arrows point to nuclei. Scale bars: (A-H) 25 μm.

1.3 Female Regulation of Pollen Tube Reception

The series of signaling events which take place after the pollen tube has been successfully attracted to the micropyle as the pollen tube interacts with the female gametophyte is known collectively as pollen tube reception. The journey of the elongating pollen tube is highly collaborative between male and female tissues, and carefully orchestrated by complex intercellular signaling events. The communication events that occur between the pollen tube and female gametophyte during pollen tube reception facilitate the delivery of the sperm cells. Many female components originating from the female gametophyte involved in pollen tube reception have been characterized. The first female gametophytic pollen tube reception mutants identified in *Arabidopsis thaliana* are allelic, known as *sirène/feronia* (*srn*/*fer*; hereon referred to as *fer*) (Huck, Moore, Federer & Grossniklaus, 2003; Rotman et al., 2003; Escobar-Restrepo et al., 2007). In *fer* mutants, a majority of pollen tubes are successfully attracted to the ovules; however, they do not receive the signal to burst, leading to an unsuccessful release of sperm cells to the female gametophyte and consequently, unfertilized ovules and less seed. The fertility defect in *fer* is female gametophytic, as *fer* pollen is fertile (Grossniklaus, 2003; Rotman et al., 2003; Escobar-Restrepo et al., 2007). *fer* mutant pistils have a phenotype known as pollen tube overgrowth, which appears as a large growth of a pollen tube inside the female gametophyte of an unfertilized ovule (Fig. 1.3B). In addition, ultrastructural and cytological analyses have shown that the two synergids in *fer* mutants are normally differentiated, indicating that FER is involved in signaling during pollen tube reception (Escobar-Restrepo et al., 2007; Huck, Moore, Federer & Grossniklaus, 2003). FER is a synergid-expressed, plasma membrane-localized receptor-like kinase. It is one member of the plant-specific CrRLK1L-1 subfamily of protein kinases, and the first member of this subfamily to be assigned a function (Escobar-Restrepo et al., 2007). FER accumulates in the filiform apparatus, a specialized membrane-rich region at the micropylar end of the synergid cells

and is recognized as important for releasing signaling molecules to the pollen tube required for successful fertilization (Escobar-Restrepo et al., 2007). FER has since been characterized as being broadly expressed with many biological functions in plants, such as powdery mildew susceptibility, as well as a cell surface regulator for RAC/ROP activated ROS production mediating polarized root hair growth (Kessler et al., 2010; Duan, Kita, Li, Cheung & Wu, 2010). In this thesis, when discussing FER, I will mainly focus on FER's role in plant reproduction.

Another female-derived member of the pollen tube reception pathway is NORTIA (NTA). Like *fer*, *nta* mutant ovules have pollen tube overgrowth leading to a reduced number of fertilized ovules (Fig. 1.3B). Homozygous *nta* individuals have pollen tube overgrowth in 20-50 percent of ovules (Kessler et al., 2010, Jones et al., 2017). NTA, also known as AtMLO7, is one member of the Mildew Resistance Locus O (MLO) family in plants, a family of predicted seven transmembrane proteins originally described for their role in powdery mildew susceptibility in barley (Büschges et al., 1997). Conserved molecular components have been reported between fungal hyphae invasion and pollen tube reception, as both fungal hyphae and pollen tubes are tip-growing single cells, invade another cell after complex communication events, and involve the polar localization of MLO proteins in response to pollen tube and fungal hyphae arrival (Kessler et al., 2010; Bhat, Miklis, Schmelzer, Schulze-Lefert, Panstruga, 2005).

NTA localizes to Golgi-associated compartments in the synergid cells before pollen tube arrival (Jones et al., 2017). Upon arrival of a pollen tube, fluorescence of pNTA::NTA-GFP can be seen shifting its expression from the Golgi to the filiform apparatus of the synergid cells in a FER-dependent manner, while the Golgi is not (Kessler et al., 2010; Yuan and Ju et al., 2019). Whether this is due to trafficking of the NTA protein to the filiform apparatus, degradation, or some other mechanism is not known. A functional calmodulin (CaM) binding domain (CaMBD)

facilitates NTA movement from the Golgi to the filiform apparatus sometime between the pollen tube approaching the micropyle and pollen tube burst (Yuan and Ju et al., 2019). CaM and CaM-like proteins can bind the second messenger Ca^{2+}, which is involved in many signal transduction pathways in plants and may have a role in Ca^{2+} signal relay (Yuan and Ju et al., 2019). Similarly, Ca^{2+} levels oscillate in the synergids and pollen tubes during pollen tube reception (Denninger et al., 2014; Ngo et al., 2014) In *nta*, Ca^{2+} oscillations in synergids occur at lower magnitudes than in wild-type synergids, suggesting that *nta* may be involved in regulating Ca^{2+} signaling during pollen tube reception (Ngo et al., 2014).

Other female gametophyte-expressed regulators of pollen tube reception include ABSTINENCE BY MUTUTAL CONSENT (AMC), LORELEI (LRE), LRE-like GPI-AP1 (LLG1), early nodulin-like proteins (ENODLs, or Ens), TURAN (TUN), and EVAN (EVN) (Boisson-Dernier, Frietsch, Kim, Dizon & Shroeder, 2008; Capron et al., 2008; Li et al., 2015; Hou et al., 2016; Lindner et al., 2015). All these mutants also have the pollen tube overgrowth phenotype in ovules. The *amc* mutant has defects in pollen tube reception only when an *amc* mutant pollen tube interacts with an *amc* female gametophyte. AMC functions as a peroxin and is important for importing proteins into peroxisomes, implicating that peroxisomes have an important role in pollen tube reception. This possibly involves a diffusible signal exchanged between the gametophytes (Boisson-Dernier, Frietsch, Kim, Dizon & Shroeder, 2008). LORELEI, a synergid-expressed, putative glucosylphosphatidylinositol-anchored protein (GAP), shows defects in pollen tube reception when mutated (Capron et al., 2008). In addition, one null allele tested of *lre, lre-5* does not show synergid degeneration. A small fraction of ovules does not undergo embryogenesis but initiates endosperm development after central cell fertilization and are then aborted. This suggests that LRE also has a role in double fertilization and seed development

(Tsukamoto, Qin, Huang, Dunatunga & Palanivelu, 2010). GAPs have been shown to have various roles in cell-to-cell signaling and are anchored to the extracellular surface of the plasma membrane by their C termini (Capron et al., 2008). Another GPI-anchored protein, LLG1, binds to the extracellular region of FER, and this interaction is important for FER function as FER is retained in the ER in *llg1* mutants instead of at the plasma membrane of the filiform apparatus (Li et al., 2015). LRE was also shown to bind FER at the same extracellular region as LLG1 and requires FER for its function in pollen tube reception (Liu et al., 2016). In addition, LRE expressed in pollen tubes could rescue the pollen tube reception defect in *lre* mutants (Liu et al., 2016). Early nodulin-like proteins, or ENODLs, also have an important role in pollen tube reception. ENODLs belong to a separate family of GPI-anchored proteins than LRE and LLG1, 2, and 3 (Hou et al., 2016). ENODLs accumulate at the plasma membrane of the filiform apparatus, and quintuple loss-of-function *enodl* mutants have a pollen tube overgrowth phenotype (Hou et al., 2016). EN14 specifically interacts with the extracellular domain of FER, similar to LRE and LLG1 (Hou et al., 2016). GPI-anchored proteins similar to LRE, LLG1, and ENODLs have been identified to regulate key stages in mammal fertilization, although angiosperms and mammals have very different mechanisms for fertilization (Capron et al., 2008). Another similarity between angiosperm and animal egg-sperm interactions comes with the discovery that protein N-glycosylation is important for the interaction between the female and male gametophytes during pollen tube reception by the uridine diphosphate (UDP)-glycosyltransferase superfamily protein, TURAN, and the dolichol kinase, EVAN (Lindner et al., 2015). *tun* and *evn* mutants have pollen tube overgrowth at frequencies of 13.5% and 23%, respectively (Lindner et al., 2015).

In summary, various female gametophyte-expressed genes essential to the pollen tube reception pathway have been identified, although the underlying signaling pathways and

mechanisms are far from being understood. Notable characteristics are the similarities between animal and angiosperm gametophyte communications, as well as plant pathogen defense mechanisms and pollen tube reception.

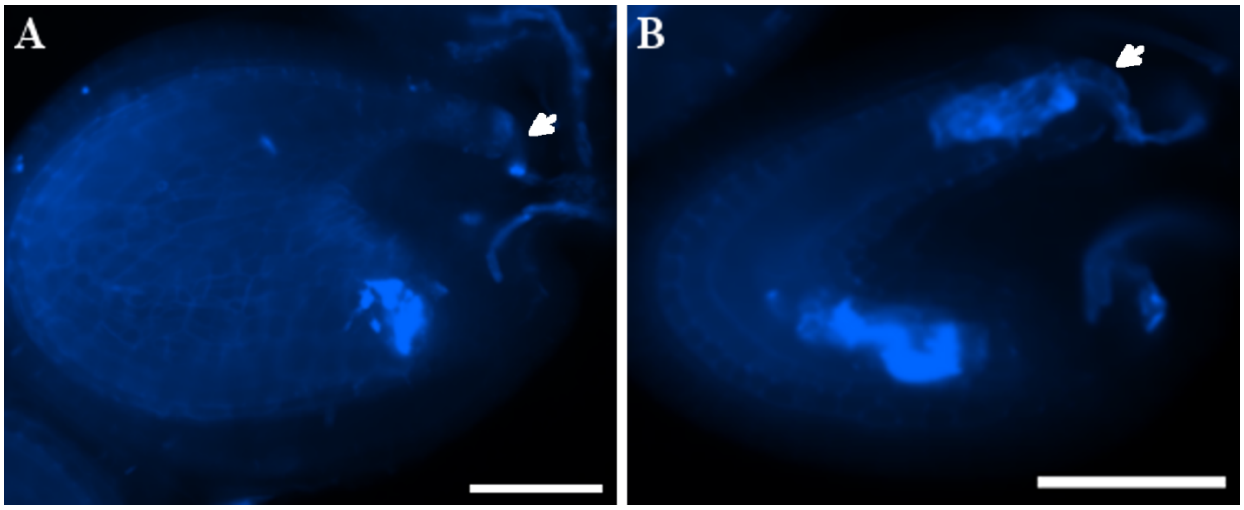

Figure 1.3 Pollen tube Overgrowth in a *nta-1* mutant.

(A) Epifluorescent image of an aniline blue-stained fertilized ovule forming a seed. (B) An aniline blue-stained unfertilized *nta-1* ovule with pollen tube overgrowth. Arrows point to pollen tubes entering the ovule. Scale bars: (A-B) 50µm.

1.4 Male Regulation of Pollen Tube Growth and Reception

During reproduction of flowering plants, the sperm cells must reach the female gametophyte for successful double fertilization to occur. Tip-growing pollen tubes germinate from compatible pollen grains on the stigma and are responsible for transporting the sperm cells down the stigma, through the transmitting tract, and to the micropyle of ovules where it reaches the synergid cells of the female gametophyte. The pollen tube then bursts to release and deliver the sperm cells to the egg and central cell. The delivery of sperm to the female gametophyte via the pollen tube is essential for successful fertilization; therefore, it is crucial for the fertility of the plant that its growth does not fail before reaching the female gametophyte.

Tip growth occurs in a small number of cell types, such as pollen tubes and root hairs in plants, fungal hyphae, and animal neurites (Cheung & Wu, 2008). Pollen tube tip growth shares fundamentally similar cellular activities and mechanisms that overlap with other expanding cells and polarity-dependent cellular processes, which makes it a useful model for understanding cell expansion, proliferation and differentiation (Cheung & Wu, 2008). Pollen tube elongation occurs rapidly at the tip, and an extensive signaling network of different pathways regulate this process (Guan, Guo, Li, & Yang, 2013). Exocytosis at the tip, a dynamic cytoskeleton, and vesicle trafficking are examples of coordinated processes required for tip growth (Guan, Guo, Li, & Yang, 2013). Cell wall materials as well as plasma membrane material must be rapidly supplied to the growing tip to maintain directional growth. Vesicles derived from the Golgi are delivered to the tip by cytoplasmic streaming. This process is dependent on actin filaments parallel to the direction of growth (Grebnev, Ntefidou, & Kost, 2017; Steer and Steer, 1989; Iwanami, 1956; Cheung et al., 2008). In addition, the cell wall is critical for maintaining the integrity of the elongating cell during tip growth. The growing pollen tube must be strong enough to maintain integrity under high turgor pressure, while being extensible enough at the tip to allow for cell expansion. The composition of the pollen tube cell wall is highly regulated to allow for this growth pattern, with pectins and callose making up the majority of the cell wall. Callose in the distal, or side region helps the pollen tube resist tension stress, and differentially-controlled pectin-esterification in the different regions of the pollen tube cell wall regulates the mechanical properties to maintain cell wall integrity while coordinating growth (Guan, Guo, Li, & Yang, 2013). Methyl-esterified pectin is secreted during exocytosis and surround the apical tip region of the pollen tube. As cell expansion occurs, cell wall-associated pectin methylesterases (PMEs) de-esterifiy pectins which increases rigidity in the wall as the pectins cross-link with calcium ions and form a matrix in the

flank of the pollen tube (Guan, Guo, Li, & Yang, 2013). Increasing or reducing the amount of PME activity in pollen tubes *in vitro* leads to reduced pollen tube growth rates, pollen tube burst, changes in morphology, and, *in vivo*, leads to reduced male transmission (Cheung & Wu, 2008; Jiang et al., 2005; Geitmann, 2005; Tian, Chen, Zaltsman and Citovsky, 2006).

Pollen tube integrity through the transmitting tract needs to be maintained until reaching the female gametophyte. Then, pollen tube burst delivers the sperm cells. Various regulators of pollen tube integrity as it grows through the transmitting tract have been identified, and many of them are tip-localized receptor kinases (Muro et al., 2018). Two homologs of FER, ANXUR1 (ANX1) and ANXUR2 (ANX2) are receptor-like kinases of the CrRLK1L subfamily which regulate pollen tube integrity during growth through the transmitting tract by regulating exocytosis and the accumulation of cell wall material (Boisson-Dernier et al., 2009, Boisson-Dernier et al., 2013). Null single mutants of *anx1* or *anx2* produce pollen tubes which are able to grow through the transmitting tract and fertilize ovules. However, *anx1 anx2* double mutant pollen tubes burst early, while overexpression of either ANX1-GFP or ANX2-GFP in wild-type pollen tubes leads to an arrest of pollen tube growth and a decrease in male transmission efficiency due to the overaccumulation of cell wall material (Boisson-Dernier et al., 2013). Two members of the respiratory burst oxidase homologue (Rboh) family act downstream of ANX1/2, generating oscillatory H_2O_2 at pollen tube tips, which functions to maintain a steady Ca^{2+} gradient during growth (Boisson-Dernier et al., 2013). One member of the Receptor-Like Cytoplasmic Kinase (RLCK) subfamily VIII, MARIS (MRI), is expressed in root hairs and pollen tubes, and coordinates cell wall integrity and tip growth. Mutant *mri* pollen tubes and root hairs have an early bursting phenotype, reminiscent of the *anx1 anx2* phenotype. Interestingly, an ethyl-methyl sulfonate (EMS)-induced MRI^{R240C}, resulting in a R240C amino acid substitution in the activation

loop of MRI partially rescues the *anx1 anx2* pollen tube bursting phenotype (Boisson-Dernier, Franck, Lituiev and Grossniklaus, 2015).

Two more CrRLK1L protein kinases, named BUDDHA'S PAPER SEAL 1 (BUPS1) and BUPS2 are also required for normal pollen tube growth. Like their homologs ANX1/2, BUPS1/2 are pollen tube-expressed, plasma membrane-localized protein kinases (Zhu et al., 2018). *bups1* null mutants show reduced transmission through the male gametophyte due to defects in pollen tube growth. *bups2* mutants have abnormal pollen tube morphology but are still able to fertilize ovules (Zhu et al., 2018).

Cysteine-rich peptides known as RAPID ALKALINIZATION FACTORs (RALFs) function as ligands for the CrRLK1L family. Two RALF signaling peptides, RALF4 and RALF19, maintain pollen tube integrity during growth by interacting with the ANX/BUPS receptors (Ge et al., 2017; Mecchia et al., 2017). These pollen-specific RALFs are hypothesized to be in competition with the female-derived RALF34 ligand, which is proposed to displace RALF4/19 on the pollen tube tip upon female-male gametophyte interaction and result in a loss of integrity, resulting in the pollen tube burst which delivers the sperm cells (Ge et al., 2017). In addition, the function of RALFs were found to be dependent on LEUCINE-RICH REPEAT EXTENSIN (LRX) family proteins (Mecchia et al., 2017). The pollen-specific LORELEI-LIKE GPI-ANCHORED PROTEINS 2 and 3 (LLG2/3) promote pollen tube growth *in vitro* and *in vivo* by interacting with ANX/BUPS in a RALF-concentration dependent manner (Ge et al., 2019). ANX/BUPS-LLG2/3 are thought to function in a receptor-coreceptor complex that acts as a chaperone for ANX/BUPS secretion to the plasma membrane. LLG2/3 may function as coreceptors to positively regulate ROS production in pollen tubes and coordinate their growth (Ge et al., 2019).

1.5 PCRK1's Role in Plant Pathogen Defense

Various mechanisms of pathogen defense have evolved in plants to protect them from disease. In order for plants to defend against pathogens, they must first be able to sense a pathogen attack. Similarly, during pollen tube reception, communication between the male and female gametophyte involves recognition to enable successful reproduction. As discussed in Section 1.3, the GPI-anchored protein, LLG1, functions as a FER co-receptor and binds to the extracellular region of FER (Li et al., 2015; Liu et al., 2016). This interaction is important for FER function in pollen tube reception (Li et al., 2015). LLG1 was found to function as a regulator of pattern recognition receptor (PRR) signaling during plant immune responses by associating with PRR FLAGELLIN-SENSING 2 (FLS2) and regulating its accumulation and signaling (Shen, Bourdais, Pan, Robatzek & Tang, 2017). In addition, FER mediates the ligand-induced complex of the immune receptor kinases EF-TU RECEPTOR (EFR) and FLS2 with the co-receptor BRASSINOSTEROID INSENSITIVE 1-ASSOCIATED KINASE 1 (BAK1) to initiate immune signaling (Stegmann et al., 2017). These studies reveal shared components between pollen tube reception and pathogen defense.

One mode of pathogen perception by plants is by damage-associated molecular patterns, or DAMPS. DAMPS are endogenous molecules which accumulate in intercellular space as a response to damage to the plant by pathogen attack, such as cell wall fragments or effectors induced by cell wall degradation, wounding, or elicitor recognition (Boller & He, 2009; Ryan et al., 2007; Huffaker et al., 2006). Another mode of pathogen perception involves the recognition of molecules which are distinct to pathogens, such as flagellin, cell wall components, and translation factors. These molecules can trigger plant immune responses and are referred to as microbe/pathogen-associated molecular patterns, or MAMPS/PAMPS. Pattern-triggered

immunity (PTI) refers to the early immune responses that are induced by recognition of MAMPS (Jones & Takemoto, 2004). MAMPS are perceived in plants by pattern-recognition receptors, or PRRs, located at the plasma membrane. In *Arabidopsis thaliana*, PRRs FLAGELLIN-SENSITIVE 2 (FLS2), EF-TU RECEPTOR (EFR), and CHITIN ELICITOR RECEPTOR KINASE 1 (CERK1) are receptor-like kinases (RLKs) that can directly bind and sense the peptides flg22, elf18, and chitin, respectively (Chinchilla *et al*., 2006; Zipfel *et al*., 2006; Miya *et al*., 2007; Yamaguchi *et al*., 2010). PTI leads to increased levels of Ca^{2+} in the cytoplasm, mitogen-activated protein kinase (MAPK) activation, deposition of callose at the cell wall, and reactive oxygen species (ROS) production (Gomez-Gomez et al., 1999). Later immune responses include the biosynthesis of three phytohormones which are known to have a large role in facilitating signal relay against biotrophic and necrotrophic pathogens during defense responses, either directly or indirectly through crosstalk between them. These hormones are jasmonic acid, ethylene, and salicylic acid (Tsuda et al., 2009).

Receptor-like Cytoplasmic Kinases, or RLCKs, have important roles during PTI responses. Specifically, the members of RLCK subfamily VII are overrepresented in genes induced during biotic stress responses (Lehti-Shiu *et al*., 2009). BOTRYTIS-INDUCED KINASE 1 (BIK1), avrPphB susceptible (PBS1), PBS1-LIKE 1 (PBL1), and PBS1-LIKE 27 (PBL27) are members of the RLCK Subfamily VII which directly interact with PRRs such as FLS2 and CERK1 (Lu *et al*., 2010; Zhang *et al*., 2010; Liu *et al*., 2013). BIK1 and PBL1 are phosphorylated and dissociate from the FLS2-BAK1 complex after recognition of flg22. BIK1 interacts with various PRRs and promotes ROS production by phosphorylating the NADPH oxidase D (Kong et al., 2016, Kadota et al., 2014, Li et al., 2014). Similarly, the RLCK BSK1 interacts with FLS2 and is needed for ROS production in response to flagellin perception (Kong et al., 2016, Shi et al., 2013).

BIK1 also phosphorylates FLS2 and BAK1 (Lu *et al*., 2010; Zhang *et al*., 2010). BIK1 and PBL1 are also reported to be involved in regulating CERK1-mediated chitin responses such as ROS accumulation and the activation of defense genes (Zhang et al., 2010).

Some pathogens have adapted effector proteins which function to disable PTI by cleaving various plant defense proteins. The plant is then in a state of effector-triggered susceptibility (ETS). In response, plants have evolved another mode of pathogen perception where specific proteins can perceive pathogen effector proteins or their products of effector activity, which then activates effector-triggered immunity (ETI) (Sreekanta et. Al., 2015; Jones & Dangl, 2006). RLCKs such as BIK1, PBL1, and PBS1 are targeted by bacterial effectors (Zhang et al., 2010).

PATTERN-TRIGGERED IMMUNITY COMPROMISED CYTOPLASMIC RECEPTOR-LIKE CYTOPLASMIC KINASE 1, or PCRK1, is another member of RLCK Subfamily VII that has a role in pathogen defense as a positive regulator of PTI responses, specifically against the bacterial pathogen *Pseudomonas syringae* pv. *Maculicola* ES4326 (*Pma* ES4326) (Sreekanta et al., 2015). Loss-of-function mutations in PCRK1 compromise early immune responses to *Pma* ES4326 during PTI after treatments with peptides derived from MAMPs flagellin (flg22), elongation factor-Tu (elf18), or the DAMP pep1 (Sreekanta et al., 2015). PCRK1 was reported to contribute to flg22-induced ROS burst and callose deposition, with both being reduced in the *pcrk1* mutant plants (Sreekanta et al., 2015). The same is true for *bik1*, *pbl1*, and *pbs1* mutants (Zhang et al., 2010). MAPK activation during PTI may be independent of PCRK1 function, which is consistent with other RLCK's such as *bik1*, *pbl1*, and *bsk1*. (Sreekanta et al., 2015). RBOHD-dependent ROS production during PAMP perception may occur independently or downstream of MAPK activation (Sreekanta et al., 2015; Zhang et al., 2007; Xu et al., 2014). The

shared roles of PCRK1 and FERONIA in pollen tube reception and pathogen defense signaling reveal more links between the two processes.

PCRK1 functions redundantly with its most closely related paralogue, PCRK2, to regulate salicylic acid (SA) biosynthesis by regulating pathogen-induced expression of two transcription factors and a key enzyme for salicylic acid biosynthesis, SARD1, CBP60g, and ICS1, respectively (Kong et al., 2016). Salicylic acid is a signaling molecule in plant pathogen defense which has important roles during local and systemic acquired resistance (SAR) (Gaffney et al., 1993; Delaney et al., 1994; Nawrath and Métraux, 1999; Nawrath et al., 2002). Both PCRK1 and PCRK2 were found to interact with the PRR FLS2, further giving evidence for their roles in pathogen defense (Kong et al., 2016). The kinase activity in PCRK1 and PCRK2 were found to be required for their functions in plant immunity (Sreekanta et al., 2015; Kong et al., 2016).

Jasmonic acid (JA) is another plant hormone which is critical for pathogen defense signaling. PCRK1 contributes to JA signaling during immune responses (Sreekanta, Haruta, Minkoff, Glazebrook, 2015). In addition to having a role in both SA and JA during defense responses, PCRK1 and PCRK2 were found to negatively regulate brassinosteroid (BR) signaling by inhibiting brassinolide (BL)-induced BES1 dephosphorylation, one transcription factor critical for BR signaling. (Huang et al., 2019).

1.6 Examining the Role of PCRK1 in Pollen Tube Reception

The signaling pathways underlying pollen tube reception, including the regulators of interactions between the male and female gametophytes are largely unknown. The goal of this thesis is to characterize a newly identified pollen tube reception regulator, which until now has only been described for its role in plant pathogen defense. The chapters of this thesis contribute to

our understanding of the genes underlying female and male interactions during pollen tube reception. In chapter two, I provide phenotypic and genetic evidence that this identified regulator, PCRK1, has a role in regulating pollen tube reception from both the male and female gametophyte. I also investigate genetic interactions between the male gametophyte expressed PCRK1 and other female PT reception regulators. By studying the links between fertility and disease in plants, such as the shared roles of FERONIA and MLOs in powdery mildew susceptibility and pollen tube reception, and now the dual role of PCRK1 in pathogen defense and pollen tube reception, we may be able to uncover important potential trade-offs with fertility when breeding for pathogen resistance.

1.7 References for Chapter One

Bhat, R. A., Miklis, M., Schmelzer, E., Schulze-Lefert, P., Panstruga, R. (2005) Recruitment and interaction dynamics of plant penetration resistance components in a plasma membrane microdomain. Proc. Natl. Acad. Sci. U.S.A. **102**, 3135 doi:10.1073/pnas.0500012102pmid:15703292

Boisson-Dernier, A., Franck, C. M., Lituiev, D. S., & Grossniklaus, U. (2015). Receptor-like cytoplasmic kinase MARIS functions downstream of CrRLK1L-dependent signaling during tip growth. *Proceedings of the National Academy of Sciences*, *112*(39), 12211–12216. doi: 10.1073/pnas.1512375112

Boisson-Dernier, A., Frietsch, S., Kim, T.-H., Dizon, M. B., & Schroeder, J. I. (2008). The Peroxin Loss-of-Function Mutation abstinence by mutual consent Disrupts Male-Female Gametophyte Recognition. *Current Biology*, *18*(1), 63–68. doi: 10.1016/j.cub.2007.11.067

Boisson-Dernier, A., Roy, S., Kritsas, K., Grobei, M. A., Jaciubek, M., Schroeder, J. I., & Grossniklaus, U. (2009). Disruption of the pollen-expressed FERONIA homologs ANXUR1 and ANXUR2 triggers pollen tube discharge. *Development*, *136*(19), 3279–3288. doi: 10.1242/dev.040071

Boisson-Dernier, A., Lituiev, D. S., Nestorova, A., Franck, C. M., Thirugnanarajah, S., & Grossniklaus, U. (2013). ANXUR Receptor-Like Kinases Coordinate Cell Wall Integrity with Growth at the Pollen Tube Tip Via NADPH Oxidases. *PLoS Biology*, *11*(11). doi: 10.1371/journal.pbio.1001719

Boller, T., and He, S. Y. (2009) Innate Immunity in plants: an arms race between pattern recognition receptors in plants and effectors in microbial pathogens. Science 324, 742–744

Büschges, R., Hollricher, K., Panstruga, R., Simons, G., Wolter, M., Frijters, A., … Schulze-Lefert, P. (1997). The Barley Mlo Gene: A Novel Control Element of Plant Pathogen Resistance. *Cell*, *88*(5), 695–705. doi: 10.1016/s0092-8674(00)81912-1

Capron, A., Gourgues, M., Neiva, L. S., Faure, J.-E., Berger, F., Pagnussat, G., … Sundaresan, V. (2008). Maternal Control of Male-Gamete Delivery in Arabidopsis Involves a Putative GPI-Anchored Protein Encoded by the LORELEI Gene. *The Plant Cell*, *20*(11), 3038–3049. doi: 10.1105/tpc.108.061713

Cass, D. D., Peteya, D. J., & Robertson, B. L. (1985). Megagametophyte development in Hordeum vulgare. 1. Early megagametogenesis and the nature of cell wall formation. *Canadian Journal of Botany*, *63*(12), 2164–2171. doi: 10.1139/b85-306

Cheung, A. Y. & Wu, H. M. (2008). Structural and signaling networks for the polar cell growth machinery in pollen tubes. *Annu. Rev. Plant Biol.* **59**, 547–572

Cheung, A. Y., Duan, Q. H., Costa, S. S., de Graaf, B. H., Di Stilio, V. S., Feijo, J., et al. (2008). The dynamic pollen tube cytoskeleton: live cell studies using actin-binding and microtubule-binding reporter proteins. *Mol. Plant.* 1, 686–702. doi: 10.1093/mp/ssn026

Chinchilla D, Zipfel C, Robatzek S, Kemmerling B, Nuernberger T, Jones JDG, Felix G, Boller T. 2007. A flagellin-induced complex of the receptor FLS2 and BAK1 initiates plant defence. *Nature* **448**: 497– 500.

Delaney TP, Uknes S, Vernooij B, Friedrich L, Weymann K, Negrotto D, Gaffney T, Gut-Rella M, Kessmann H, Ward E, et al. (1994). A central role of salicylic acid in plant disease resistance. Science 266: 1247–1250

Delwiche, C. F., & Cooper, E. D. (2015). The Evolutionary Origin of a Terrestrial Flora. *Current Biology*, *25*(19). doi: 10.1016/j.cub.2015.08.029

Denninger, P., Bleckmann, A., Lausser, A., Vogler, F., Ott, T., Ehrhardt, D. W., … Grossmann, G. (2014). Male–female communication triggers calcium signatures during fertilization in Arabidopsis. *Nature Communications*, *5*(1). doi: 10.1038/ncomms5645

Duan, Q., Kita, D., Li, C., Cheung, A. Y., & Wu, H.-M. (2010). FERONIA receptor-like kinase regulates RHO GTPase signaling of root hair development. *Proceedings of the National Academy of Sciences*, *107*(41), 17821–17826. doi: 10.1073/pnas.1005366107

Esau, K. (1997). *Anatomy of Seed Plants.* New York: John Wiley & Sons.

Escobar-Restrepo, J.-M., Huck, N., Kessler, S., Gagliardini, V., Gheyselinck, J., Yang, W.-C., & Grossniklaus, U. (2007). The FERONIA Receptor-like Kinase Mediates Male-Female Interactions During Pollen Tube Reception. *Science*, *317*(5838), 656–660. doi: 10.1126/science.1143562

Gaffney T, Friedrich L, Vernooij B, Negrotto D, Nye G, Uknes S, Ward E, Kessmann H, Ryals J. 1 993. Requirement of salicylic acid for the induction of systemic acquired resistance. Science **261**: 754–756

Ge, Z., Zhao, Y., Liu, M.-C., Zhou, L.-Z., Wang, L., Zhong, S., … Qu, L.-J. (2019). LLG2/3 Are Co-receptors in BUPS/ANX-RALF Signaling to Regulate Arabidopsis Pollen Tube Integrity. *Current Biology*, *29*(19). doi: 10.1016/j.cub.2019.08.032

Ge, Z., Bergonci, T., Zhao, Y., Zou, Y., Du, S., Liu, M.-C., … Qu, L.-J. (2017). Arabidopsispollen tube integrity and sperm release are regulated by RALF-mediated signaling. *Science*, *358*(6370), 1596–1600. doi: 10.1126/science.aao3642

Gensel, P.G., and Edwards, D. (2001). Plants Invade the Land: Evolutionary and Environmental Perspectives (Columbia University Press).

Gomez-Gomez L, Felix G, Boller T. 1999. A single locus determines sensitivity to bacterial flagellin in *Arabidopsis thaliana*. *Plant Journal* **18**: 277– 284.

Grebnev, G., Ntefidou, M., & Kost, B. (2017). Secretion and Endocytosis in Pollen Tubes: Models of Tip Growth in the Spot Light. *Frontiers in Plant Science*, *8*. doi: 10.3389/fpls.2017.00154.

Guan, Y., Guo, J., Li, H., & Yang, Z. (2013). Signaling in Pollen Tube Growth: Crosstalk, Feedback, and Missing Links. *Molecular Plant*, *6*(4), 1053–1064. doi: 10.1093/mp/sst070

Hiscock, S. J., & Allen, A. M. (2008). Diverse cell signalling pathways regulate pollen-stigma interactions: the search for consensus. *New Phytologist*, *179*(2), 286–317. doi: 10.1111/j.1469-8137.2008.02457.x

Hou, Y., Guo, X., Cyprys, P., Zhang, Y., Bleckmann, A., Cai, L., … Qu, L.-J. (2016). Maternal ENODLs Are Required for Pollen Tube Reception in Arabidopsis. *Current Biology*, *26*(17), 2343–2350. doi: 10.1016/j.cub.2016.06.053

Huang, G. Sun, J., Bai, J., Han, Y., Fan, F., Wang, S., … Lu, D. (2019) Identification of critical cysteine sites in brassinosteroid-insensitive 1 and novel signaling regulators using a transient expression system. *New Phytologist*. 222(3), 1405-1419. Doi:10.11

Huck, N., Moore, J. M., Federer, M., Grossniklaus, U. (2003). The Arabidopsis mutant feronia disrupts the female gametophytic control of pollen tube reception. *Development*, *130*(10), 2149–2159. doi: 10.1242/dev.00458

Huck, N., Moore, J. M., Federer, M., & Grossniklaus, U. (2003). The Arabidopsis mutant feronia disrupts the female gametophytic control of pollen tube reception. *Development*, *130*(10), 2149–2159. doi: 10.1242/dev.00458

Huffaker, A., Pearce, G., and Ryan, C. A. (2006) An endogenous peptide signal in *Arabidopsis* activates components of the innate immune response Proc. Natl. Acad. Sci. U.S.A. 103, 10098–10103

Iwanami, Y. (1956). Protoplasmic movement in pollen grains and tubes. *Phytomorphol* 6, 288–295.

Jiang, L., Yang, S.-L., Xie, L.-F., Puah, C. S., Zhang, X.-Q., Yang, W.-C., … Ye, D. (2005). VANGUARD1 Encodes a Pectin Methylesterase That Enhances Pollen Tube Growth in the Arabidopsis Style and Transmitting Tract. *The Plant Cell*, *17*(2), 584–596. doi: 10.1105/tpc.104.027631

Jones DA, Takemoto D. 2004. Plant innate immunity – direct and indirect recognition of general and specific pathogen-associated molecules. *Current Opinion in Immunology* **16**: 48– 62

Jones JDG, Dangl JL. (2006). The plant immune system. *Nature* **444**:323-329.

Jones, D. S., & Kessler, S. A. (2017). Cell type-dependent localization of MLO proteins. *Plant Signaling & Behavior*, *12*(11). doi: 10.1080/15592324.2017.1393135

Kenrick, P., & Crane, P. R. (1997). The origin and early evolution of plants on land. *Nature*, *389*(6646), 33–39. doi: 10.1038/37918

Kenrick, P., Wellman, C.H., Schneider, H., and Edgecombe, G.D. (2012). A timeline for terrestrialization: consequences for the carbon cycle in the Palaeozoic. Phil. Trans. R. Soc. B-Biol. Sci. 367, 519–536.

Kessler, S. A., & Grossniklaus, U. (2011). Shes the boss: signaling in pollen tube reception. *Current Opinion in Plant Biology*, *14*(5), 622–627. doi: 10.1016/j.pbi.2011.07.01

Kessler, S. A., Shimosato-Asano, H., Keinath, N. F., Wuest, S. E., Ingram, G., Panstruga, R., & Grossniklaus, U. (2010). Conserved Molecular Components for Pollen Tube Reception and Fungal Invasion. *Science*, *330*(6006), 968–971. doi: 10.1126/science.1195211

Kong, Q., Sun, T., Qu, N., Ma, J., Li, M., Cheng, Y.-T., … Zhang, Y. (2016). Two redundant receptor-like cytoplasmic kinases function downstream of pattern recognition receptors to regulate activation of SA biosynthesis in Arabidopsis. *Plant Physiology*. Doi: 10.1104/pp.15.01954

Lehti-Shiu MD, Zou C, Hanada K, Shiu S-H. 2009. Evolutionary history and stress regulation of plant receptor-like kinase/pelle genes. *Plant Physiology* **150**: 12– 26.

Li, C., Yeh, F.-L., Cheung, A. Y., Duan, Q., Kita, D., Liu, M.-C., … Wu, H.-M. (2015). Glycosylphosphatidylinositol-anchored proteins as chaperones and co-receptors for FERONIA receptor kinase signaling in Arabidopsis. *ELife*, *4*. doi: 10.7554/elife.06587

Lindner, H., Kessler, S. A., Müller, L. M., Shimosato-Asano, H., Boisson-Dernier, A., & Grossniklaus, U. (2015). TURAN and EVAN Mediate Pollen Tube Reception in Arabidopsis Synergids through Protein Glycosylation. *PLOS Biology*, *13*(4). doi: 10.1371/journal.pbio.1002139

Liu Z, Wu Y, Yang F, Zhang Y, Chen S, Xie Q, Tian X, Zhou J-M. 2013. BIK1 interacts with PEPRs to mediate ethylene-induced immunity. *Proceedings of the National Academy of Sciences, USA***110**: 6205– 6210.

Liu, X., Castro, C., Wang, Y., Noble, J., Ponvert, N., Bundy, M., … Palanivelu, R. (2016). The Role of LORELEI in Pollen Tube Reception at the Interface of the Synergid Cell and Pollen Tube Requires the Modified Eight-Cysteine Motif and the Receptor-Like Kinase FERONIA. *The Plant Cell*, *28*(5), 1035–1052. doi: 10.1105/tpc.15.00703

Lopes, A. L., Moreira, D., Ferreira, M. J., Pereira, A. M., & Coimbra, S. (2019). Insights into secrets along the pollen tube pathway in need to be discovered. *Journal of Experimental Botany*, *70*(11), 2979–2992. doi: 10.1093/jxb/erz087

Lu D, Wu S, Gao X, Zhang Y, Shan L, He P. 2010. A receptor-like cytoplasmic kinase, BIK1, associates with a flagellin receptor complex to initiate plant innate immunity. *Proceedings of the National Academy of Sciences, USA* **107**: 496– 501.

Mansfield, S. G., & Briarty, L. G. (1990). Early embryogenesis in Arabidopsis thaliana. II. The developing embryo. *Canadian Journal of Botany*, *69*(3), 461–476. doi: 10.1139/b91-063

Mansfield, S. G., Briarty, L. G., & Erni, S. (1990). Early embryogenesis in Arabidopsis thaliana. I. The mature embryo sac. *Canadian Journal of Botany*, *69*(3), 447–460. doi: 10.1139/b91-062

Mecchia, M. A., Santos-Fernandez, G., Duss, N. N., Somoza, S. C., Boisson-Dernier, A., Gagliardini, V., … Grossniklaus, U. (2017). RALF4/19 peptides interact with LRX proteins to control pollen tube growth inArabidopsis. *Science*, *358*(6370), 1600–1603. doi: 10.1126/science.aao5467

Meyerowitz, E. M., & Pruitt, R. E. (1985). Arabidopsis thaliana and Plant Molecular Genetics. Science, 229(4719), 1214–1218. doi: 10.1126/science.229.4719.1214

Miya A, Albert P, Shinya T, Desaki Y, Ichimura K, Shirasu K, Narusaka Y, Kawakami N, Kaku H, Shibuya N. 2007. CERK1, a LysM receptor kinase, is essential for chitin elicitor signaling in Arabidopsis. *Proceedings of the National Academy of Sciences, USA* **104**: 19613– 19618.

Muro, K., Matsuura-Tokita, K., Tsukamoto, R., Kanaoka, M. M., Ebine, K., Higashiyama, T., … Ueda, T. (2018). ANTH domain-containing proteins are required for the pollen tube plasma membrane integrity via recycling ANXUR kinases. *Communications Biology*, *1*(1). doi: 10.1038/s42003-018-0158-8

Nawrath C, Heck S, Parinthawong N, Métraux JP. (2002). EDS5, an essential component of salicylic acid-dependent signaling for disease resistance in Arabidopsis, is a member of the MATE transporter family. Plant Cell **14**: 275–286

Nawrath C, Métraux JP. (1999). Salicylic acid induction-deficient mutants of Arabidopsis express PR-2 and PR-5 and accumulate high levels of camalexin after pathogen inoculation. Plant Cell **11**: 1393–1404

Ngo, Q. A., Vogler, H., Lituiev, D. S., Nestorova, A., & Grossniklaus, U. (2014). A Calcium Dialog Mediated by the FERONIA Signal Transduction Pathway Controls Plant Sperm Delivery. *Developmental Cell*, *29*(4), 491–500. doi: 10.1016/j.devcel.2014.04.008

Okuda, S., Tsutsui, H., Shiina, K., Sprunck, S., Takeuchi, H., Yui, R., … Higashiyama, T. (2009). Defensin-like polypeptide LUREs are pollen tube attractants secreted from synergid cells. *Nature*, *458*(7236), 357–361. doi: 10.1038/nature07882

Pajoro, A., Biewers, S., Dougali, E., Valentim, F. L., Mendes, M. A., Porri, A., … Angenent, G. C. (2014). The (r)evolution of gene regulatory networks controlling Arabidopsis plant reproduction: a two-decade history. *Journal of Experimental Botany*, *65*(17), 4731–4745. doi: 10.1093/jxb/eru233

Parre, E., & Geitmann, A. (2004). Pectin and the role of the physical properties of the cell wall in pollen tube growth of Solanum chacoense. *Planta*, *220*(4), 582–592. doi: 10.1007/s00425-004-1368-5

Preuss, D. (2002). Sexual Signaling on a Cellular Level: Lessons from Plant Reproduction. *Molecular Biology of the Cell*, *13*(6), 1803–1805. doi: 10.1091/mbc.es-01-0001

Reiser, L., & Fischer, R. L. (1993). The Ovule and the Embryo Sac. *The Plant Cell*, *5*(10), 1291. doi: 10.2307/3869782

Ross, J.D. (1985) The Physiology of Flowering Plants - Their Growth and Development, 3rd Edition - Street,He, Opik,H. Nature **314:** 42-43

Rotman, N., Rozier, F., Boavida, L., Dumas, C., Berger, F., & Faure, J.-E. (2003). Female Control of Male Gamete Delivery during Fertilization in Arabidopsis thaliana. *Current Biology*, *13*(5), 432–436. doi: 10.1016/s0960-9822(03)00093-9

Rotman, N., Rozier, F., Boavida, L., Dumas, C., Berger, F., & Faure, J.-E. (2003). Female Control of Male Gamete Delivery during Fertilization in Arabidopsis thaliana. *Current Biology*, *13*(5), 432–436. doi: 10.1016/s0960-9822(03)00093-9

Russell, S. D. (1978). Fine structure of megagametophyte development in Zea mays. *Canadian Journal of Botany*, *57*(10), 1093–1110. doi: 10.1139/b79-134

Ryan, C. A., Huffaker, A., and Yamaguchi, Y. (2007) New insights into innate immunity in Arabidopsis. Cell Microbiol. 9, 1902–1908

Sandaklie-Nikolova, L., Palanivelu, R., King, E. J., Copenhaver, G. P., & Drews, G. N. (2007). Synergid Cell Death in Arabidopsis Is Triggered following Direct Interaction with the Pollen Tube. *Plant Physiology*, *144*(4), 1753–1762. doi: 10.1104/pp.107.098236

Shen, Q., Bourdais, G., Pan, H., Robatzek, S., & Tang, D. (2017). Arabidopsisglycosylphosphatidylinositol-anchored protein LLG1 associates with and modulates FLS2 to regulate innate immunity. *Proceedings of the National Academy of Sciences*, *114*(22), 5749–5754. doi: 10.1073/pnas.1614468114

Shinya T, Yamaguchi K, Desaki Y, Yamada K, Narisawa T, Kobayashi Y, Maeda K, Suzuki M, Tanimoto T, Takeda J, et al. 2014. Selective regulation of chitin-induced defense response by the Arabidopsis receptor-like cytoplasmic kinase PBL27. *Plant Journal* **79**: 56– 66.

Sreekanta, S., Haruta, M., Minkoff, B. B., & Glazebrook, J. (2015). Functional characterization of PCRK1, a putative protein kinase with a role in plant immunity. Plant Signaling & Behavior, 10(10). doi: 10.1080/15592324.2015.1063759

Sreekanta, S., Bethke, G., Hatsugai, N., Tsuda, K., Thao, A., Wang, L., … Glazebrook, J. (2015). The receptor-like cytoplasmic kinase PCRK1 contributes to pattern-triggered immunity againstPseudomonas syringaeinArabidopsis thaliana. *New Phytologist*, *207*(1), 78–90. doi: 10.1111/nph.13345

Steer, M., and Steer, J. (1989). Pollen tube tip growth. *New. Phytol.* 111, 323–358. doi: 10.1111/j.1469-8137.1989.tb00697.x

Stegmann, M., Monaghan, J., Smakowska-Luzan, E., Rovenich, H., Lehner, A., Holton, N., … Zipfel, C. (2017). The receptor kinase FER is a RALF-regulated scaffold controlling plant immune signaling. *Science*, *355*(6322), 287–289. doi: 10.1126/science.aal2541

Tian, G.-W., Chen, M.-H., Zaltsman, A., & Citovsky, V. (2006). Pollen-specific pectin methylesterase involved in pollen tube growth. *Developmental Biology*, *294*(1), 83–91. doi: 10.1016/j.ydbio.2006.02.026

Tsuda K, Sato M, Glazebrook J, Cohen JD, Katagiri F. 2008. Interplay between MAMP-triggered and SA-mediated defense responses. *Plant Journal* **53**: 763– 775.

Tsukamoto, T., Qin, Y., Huang, Y., Dunatunga, D., & Palanivelu, R. (2010). A role for LORELEI, a putative glycosylphosphatidylinositol-anchored protein, in Arabidopsis thaliana double fertilization and early seed development. *The Plant Journal*, *62*(4), 571–588. doi: 10.1111/j.1365-313x.2010.04177.x

Tsukamoto, T., Qin, Y., Huang, Y., Dunatunga, D., & Palanivelu, R. (2010). A role for LORELEI, a putative glycosylphosphatidylinositol-anchored protein, in Arabidopsis thaliana double fertilization and early seed development. *The Plant Journal*, *62*(4), 571–588. doi: 10.1111/j.1365-313x.2010.04177.x

Webb, M., & Gunning, B. (1990). Embryo sac development in Arabidopsis thaliana. *Sexual Plant Reproduction*, *3*(4). doi: 10.1007/bf00202882

Xu J, Xie J, Yan C, Zou X, Ren D, Zhang S. 2014. A chemical genetic approach demonstrates that MPK3/MPK6 activation and NADPH oxidase-mediated oxidative burst are two independent signaling events in plant immunity. *Plant Journal* **77**: 222– 234.

Yamaguchi Y, Huffaker A, Bryan AC, Tax FE, Ryan CA. 2010. PEPR2 Is a second receptor for the Pep1 and Pep2 peptides and contributes to defense responses in Arabidopsis. *Plant Cell* **22**: 508– 522.

Yuan, J., Ju, Y., Jones, D. S., Zhang, W., Lucca, N., Staiger, C. J., & Kessler, S. A. (2019). Redistribution of NORTIA in response to pollen tube arrival facilitates fertilization in Arabidopsis thaliana. BioRxiv doi: 10.1101/621599

Zhang J, Li W, Xiang T, Liu Z, Laluk K, Ding X, Zou Y, Gao M, Zhang X, Chen S, et al. 2010. Receptor-like cytoplasmic kinases integrate signaling from multiple plant immune receptors and are targeted by a *Pseudomonas syringae* effector. *Cell Host Microbe* **7**: 290– 301.

Zhang J, Shao F, Cui H, Chen L, Li H, Zou Y, Long C, Lan L, Chai J, Chen S, et al. 2007. A *Pseudomonas syringae* effector inactivates MAPKs to suppress PAMP-Induced immunity in plants. *Cell Host Microbe* **1**: 175– 185.

Zhu, L., Chu, L.-C., Liang, Y., Zhang, X.-Q., Chen, L.-Q., & Ye, D. (2018). The Arabidopsis CrRLK1L protein kinases BUPS1 and BUPS2 are required for normal growth of pollen tubes in the pistil. *The Plant Journal*, *95*(3), 474–486. doi: 10.1111/tpj.13963

Zipfel C, Kunze G, Chinchilla D, Caniard A, Jones JD, Boller T, Felix G. 2006. Perception of the bacterial PAMP EF-Tu by the receptor EFR restricts Agrobacterium-mediated transformation. *Cell* **125**: 749– 760.

CHAPTER 2. FORWARD GENETIC SCREEN REVEALED A NOVEL ROLE OF PCRK1 DURING PLANT REPRODUCTION

2.1 A Forward Genetic Screen in a *nta-1* background to Identify Members of the Pollen Tube Reception Pathway

Forward genetic screens are powerful tools to identify specific genes underlying a phenotype of interest. They begin with a phenotype, and various screening methods are used to identify the causative gene which has a role in the process of interest. This thesis work builds on a mutagenesis-based forward genetic screen for *nta-1* enhancers and suppressors started by Dr. Sharon Kessler.

The goal of this genetic screen is to identify new members of the pollen tube reception pathway using the pollen tube overgrowth phenotype of *nta-1*. Ethyl methanesulfonate (EMS) was used as the mutagen in the screen. EMS induces nucleotide substitutions in genetic material, which consists mainly of cytosine to thymine substitutions (Kim, Shumaker & Zhu, 2006). Therefore, mutations throughout the plant genomes were induced. The goal of the screen was to identify new mutations that modify the *nta-1* phenotype as enhancers or suppressors. The mutagen will cause a single nucleotide polymorphism (SNP) in an uncharacterized gene involved in pollen tube reception. If the SNP has an effect on the amino acid sequence of the corresponding protein, a premature STOP codon, or alternative splice junction, we may be able to see a change in our phenotype of interest. In this genetic screen, plants were screened for either an increase or decrease in the level of fertility and pollen tube overgrowth compared to *nta-1* plants. Plants with an increase in pollen tube overgrowth likely have an enhancer mutation which has affected its function in pollen tube reception. This results in an increase in the pollen tube overgrowth phenotype compared to *nta-1*. Similarly, a decrease in the level of pollen tube overgrowth suggests the presence of a suppressor mutation. A suppressor mutation tends to be a gene functioning in the

same molecular pathway. An enhancer mutation could indicate the gene is working in the same pathway or in a parallel pathway. Any genes identified as either suppressors or enhancers will have a genetic interaction with NORTIA. The regulators underlying the pollen tube reception pathway are largely unknown. Identifying and characterizing new members of the pollen tube reception pathway can help us to elucidate the pathways and mechanisms underlying plant reproduction, which can have important implications in plant breeding.

2.2 Materials and Methods

2.2.1 Plant Growth and Materials

Seeds were sterilized in 30% sodium hypochlorite, 0.1% Triton-X 100 for ten minutes, washed two timed with sterile, double-distilled water, then incubated in 70% ethanol for 3-4 minutes, and washed with sterile water two more times. Sterilized seeds were plated on ½ Murashige and Skoog (MS) media with 0.6% phytoagar, stratified at 4°C for two days, then moved to a lighted growth chamber. Seeds from transformed lines were sterilized and plated on ½ MS plate with 20mg/L hygromycin for selection of transgenic seedlings. Seedlings were transplanted to soil after 7 days and grown at 21-22°C in long day conditions of 16 hours of light followed by 8 hours of darkness.

2.2.2 *nta-1* Enhancer Screen Methods

Most *nta-1* enhancer screen methods were not performed by me. Only the T-DNA screening of enhancer candidates as described in Section 2.4.1 were performed by me. However, I will describe the enhancer screen methods since the screen led to the identification of the pollen tube reception regulator characterized in this thesis. First, *nta-1* mutant seed was mutagenized with ethyl methanesulfonate (EMS). M1 plants were screened for an increase or decrease in fertility

compared to *nta-1* plants. The plants with a change in the level of fertility had their levels of pollen tube overgrowth measured by counting with aniline blue staining. After plants with an enhancer phenotype were identified, the plants were backcrossed to *nta-1* females three times. The progeny of each backcross was screened for the enhancer phenotype, and sequential backcrosses were performed on the backcrossed plants. Backcrossing the plants and screening the progeny allows mutations which are unlinked to the phenotype to be segregated out of the enhancer plants.

After backcrossing, whole genome sequencing by next generation sequencing was performed. The resulting genome sequence was aligned to the wild-type sequence. The candidate SNPs were identified as cytosine to thymine nucleotide substitutions at allele frequencies near 50% due to the enhancer mutations being heterozygous. This allows researchers to see exactly where the SNPs are in the plant's genome, and what type of corresponding amino acid change is induced by the SNP. The location of each SNP gives us a list of candidate genes which may be the enhancer gene functioning in pollen tube reception.

2.2.3 Microscopy

- Ovule Clearing

DIC microscopy of pistils was performed by first fixing overnight in 9:1 ethanol:acetic acid. Pistils were rehydrated in 70%, 50%, 30% ethanol for thirty minutes to one hour each at room temperature. Pistils were cleared in chloral hydrate for at least one hour and visualized with a Nikon Eclipse Ti2-E inverted microscope.

- Aniline Blue Staining of Pollen Tubes

Pollinated pistils one to two days after pollination were fixed in 9:1 ethanol:acetic acid overnight at 4°C or for 1-2 hours at room temperature. Pistils were rehydrated in 70%, 50%, 30% ethanol for 10 minutes each at room temperature. Pistils were incubated in a chloral hydrate

clearing solution (4g/mL chloral hydrate, 10% glycerol) for five minutes at 60°C, then washed in 100mM phosphate buffer pH 7.0 and incubated in 5M sodium hydroxide for 10 minutes at 60°C. Pistils were washed twice with 100mM phosphate buffer at pH 7.0, then mounted in 0.1% aniline blue in pH 8.0 phosphate buffer. A Nikon Eclipse Ti2-E inverted microscope was used to visualize samples by exciting with 370 nm light and fluorescence was detected at 510nm.

For the pollen tube length measurements in the transmitting tract, Col-0 pistils were pollinated two days after emasculation with either Col-0 pollen or *pcrk1* pollen. I then collected and fixed samples overnight in 9:1 ethanol:acetic acid at 2, 4, 6, and 8 hours after pollination for aniline blue staining of pollen tubes..

- Confocal Microscopy of Cleared Ovules

Confocal microscopy of ovules for embryo sac analysis was performed as described by Christensen et al., 1997. Emasculated or pollinated pistils taken 7.5 hours after pollination were dissected using a needle to cut both sides of the pistil replum, then fixed in 4% glutaraldehyde, 12.5mM cocadylate pH 6.9 for two hours at room temperature, with the first 15-30 minutes of fixation under vacuum at .3 bar. Pistils were then dehydrated in 30%, 50%, 70%, 85%, 100% ethanol for 10 minutes each at room temperature (samples were sometimes stored in 70% ethanol overnight at 4°C). Samples were cleared in a 2:1 mixture of benzyl benzoate:benzyl alcohol for 2 hours, then mounted in immersion oil. Images were captured using a Zeiss LSM 880 confocal microscope under 40x water objective. Samples were excited using a 561nm laser.

-Confocal of GFP Signal

Images of GFP fluorescence in pollen tubes were captured using a Nikon A1Rsi inverted confocal microscope under a 40x water objective. Samples were excited using a 488nm laser. Approximately 150 µL of pollen germination media, consisting of 5 mM KCl, 1 mM $MgSO_4$, 0.01%

(w/v) H_3BO_3, 5 mM $CaCl_2$, 20% sucrose, 1.5% agarose, and adjusted pH to 7.5 with KOH was poured into a Glass Bottom Culture Petri Dish (MatTek Corporation, P35G-1.0-20-C) and spread out by tilting the dish. Pollen was placed on the germination media, and a damp kim wipe was folded and placed on the side of the dish to maintain humidity. The dish was sealed with filter tape, which was moistened with water. The dish was placed in a humid chamber made of a damp paper towel placed into a pipette box and allowed to grow overnight. Pollen tubes were imaged the next day.

2.2.4 *nta-1 pcrk1* Complementation Assay

A plasmid vector containing PCRK1 fused to GFP under its native promoter (pPCRK1::PCRK1-GFP) was obtained by courtesy of Dr. Yuelin Zhang at the University of British Columbia (Kong et al., 2016). pPCRK1::PCRK1-GFP was transformed to *Agrobacterium tumefaciens* strain GV3101 and transformed into genotyped *nta pcrk1* mutant plants by inoculation using the floral dipping method (Bent, 2006). Ten independent insertion lines were grown to the T2 generation. Three independent insertion line's T2 plants were screened for homozygosity using fluorescence microscopy. Unfertilized versus fertilized ovule counts from manually and self-pollinated flowers were measured in multiple plants of each insertion line and compared to manually and self-pollinated *nta-1* and *nta pcrk-1* plants. Ovule counts were statistically analyzed using Prism (www.graphpad.com). A Student's *t*-test was used for determining significance between the genotypes.

2.2.5 Transmission Efficiency

Transmission Efficiency was measured by first genotyping plants for the desired genotypes (See table 2.1 for primer list). Selected flowers from each plant were emasculated by removing all immature anthers and pistils were allowed to mature for two days. Emasculated branches were

marked with colored tape. Plants with emasculated flowers were separated from other plants to prevent pollen contamination. Crosses were performed with the genotypes described in Tables (2.3, 2.4). Seeds were collected after maturity. Seeds from each cross were sterilized and plated. Seedlings were transplanted to soil after seven days. Genomic DNA was extracted, and polymerase chain reaction (PCR) was used to identify the genotype of each F1 plant. Genotypes from each cross were totaled.

Table 2.1 Primers Used for Genotyping

Primer Number	Primer Name	Locus	Mutant Allele	Primer Sequence
1058	RDF8LP	*PCRK1*	*pcrk1-2 (SALK_145629)*	TCCATAACTTGCCAAACCAAC
1444	PCRK1_Paste_FP2	*PCRK1*	*pcrk1-2 (SALK_145629)*	CATTGACCTCTATCTTCTCTGACC
464	SALK-LBb1.3	SALK T-DNA Insertion		ATTTTGCCGATTTCGGAAC
1322	*nta*1_LP	*NORTIA*	*nta-1*	ATGCAGCTACATCACTCTCC
1323	*nta*1_RP	*NORTIA*	*nta-1*	GCTCCACACACCATTTCATC
952	*fer*4_LP2	*FER*	*fer-4 (CS69044/GABI_106A06)*	GATCGATGAAGATCACAGAGGGACGATTC
953	*fer*4_RP2	*FER*	*fer-4 (CS69044/GABI_106A06)*	CTGCGGTAAGCACCAAACACACAAAAC
1123	o8474	GabiKat T-DNA Insertion		ATAATAACGCTGCGGACATCTACATTTT
1364	SAIL_129_D02_FP	*PCRK2*	CS866962	ATGAAAACTCCGTATCCCCAC
1365	SAIL_129_D02_RP	*PCRK2*	CS866962	ATATCAGTGGAGGAACCTCGG
1362	SAIL_416_A03_FP	*PCRK3*	CS862947	GAGGCTGGTTTCATCTAAGGC
1363	SAIL_416_A03_RP	*PCRK3*	CS862947	GATGTTCTGCTCGTTTCTTGG
1364	LB1	Sail T-DNA Insertion		GCCTTTTCAGAAATGGATAAATAGCCTTGCTTCC
1056	RDF7LP	AT1G43100(M)	SAIL_348_A06(CS873375)	CGGAAAGCTCTTGCTACATTG
1057	RDF7RP	AT1G43100(M)	SAIL_348_A06(CS873375)	ACCCTAGGGACATTAAGCAGG
1060	RDF9LP	AT3G11964(H)	CS480000(GK_834C08)	TTGAAACTGGTAAAGGCGTTG
1061	RDF9RP	AT3G11964(H)	CS480000(GK_834C08)	GGCGTGTACGAGAGAACAGAG
1062	RDF10LP	AT3G15870(H)	SALK_142406C	CCATCATATGCAATAGGACCG
1063	RDF10RP	AT3G15870(H)	SALK_142406C	AATTTACCGGCCATGGATAAG
1064	RDF11LP	AT5G10470(M)	SALK_014609	TTCGGATTCAACTTCGACATC
1065	RDF11RP	AT5G10470(M)	SALK_014609	CTCTCCTTCTCCAACAGCTCC
1066	RDF12LP	AT3G42990(H)	SALK_036970	TTCGGATTCAACTTCGACATC
1067	RDF12RP	AT3G42990(H)	SALK_036970	CTTCGGGATAAAATGGCTAGG

Transmission efficiency of the mutant alleles was calculated by dividing the number of mutant alleles by the number of total alleles. This was multiplied by 100 to obtain the mutant allele percentage. The mutant allele percentage was divided by the expected mutant allele percentage under normal transmission, 25% or .25. This allows a comparison of mutant allele transmission to normal transmission to be reflected in the final percentage.

Transmission Efficiency: {[(Mutant Alleles/Total Alleles) *100]/Expected Mutant Allele Percentage Under Normal Transmission (.25)}

2.3 Results and Discussion

2.3.1 Enhancer Candidate Screening

After identifying candidate genes from the screen, genes were filtered by three criteria. The first criterium was whether the SNP caused a high effect or a moderate effect on the gene. SNPs that were classified as a high effect cause an early stop codon, leading to a truncated protein, or alternative splicing. SNPs categorized as causing a moderate effect lead to a nonsynonymous amino acid change in the protein, which could affect the protein's function in the plant. The second criterium was whether the gene had been reported as expressed in the synergid cells of the female gametophyte, using publicly available microarray data (Wuest et al., 2010). The third criterium was the predicted function of the protein encoded by the gene. For example, many of the genes found to be involved in plant reproduction are kinases. Therefore; we would likely choose to screen any kinase candidates before candidate genes with unknown functions.

Using these selection criteria, six candidate genes from one sequenced enhancer line ntaE-14E-6 were selected to be screened. T-DNA insertion lines from the Salk Institute were ordered for the corresponding genes (Table 2.2). The plants were genotyped by PCR (See Table 2.1 for primers used for genotyping) and the percentage of unfertilized versus fertilized ovules were counted using a dissection microscope (Fig. 2.1). We expected that some enhancer mutants could have fertility defects caused by pollen tube overgrowth, or that the double mutant combination with *nta-1* would be required to see an enhancement of pollen tube overgrowth. Two candidate lines, *rrp5* and *ads3.2* showed higher than Col-0 infertility (Fig. 2.1). Aniline blue staining of these T-DNA lines revealed that they did not have pollen tube overgrowth in the single mutants, and that the infertility was caused by other reasons not related to pollen tube reception. These T-DNA lines were crossed with homozygous *nta-1* plants. T2 plants were genotyped and double mutants were characterized. The number of unfertilized ovules was compared to *nta-1* plants grown under

the same conditions. In addition, aniline blue staining of *nta-1* and double *nta-1 enhancer candidate* plants was used to count the percentage of pollen tube overgrowth. All six double mutant combinations with the various mutant enhancer candidates did not show an enhancement of pollen tube overgrowth compared to *nta-1*. However, one double mutant, *nta pcrk1* was identified to have an increase in fertilized ovules and a reduction in pollen tube overgrowth, indicating that it acts as a suppressor.

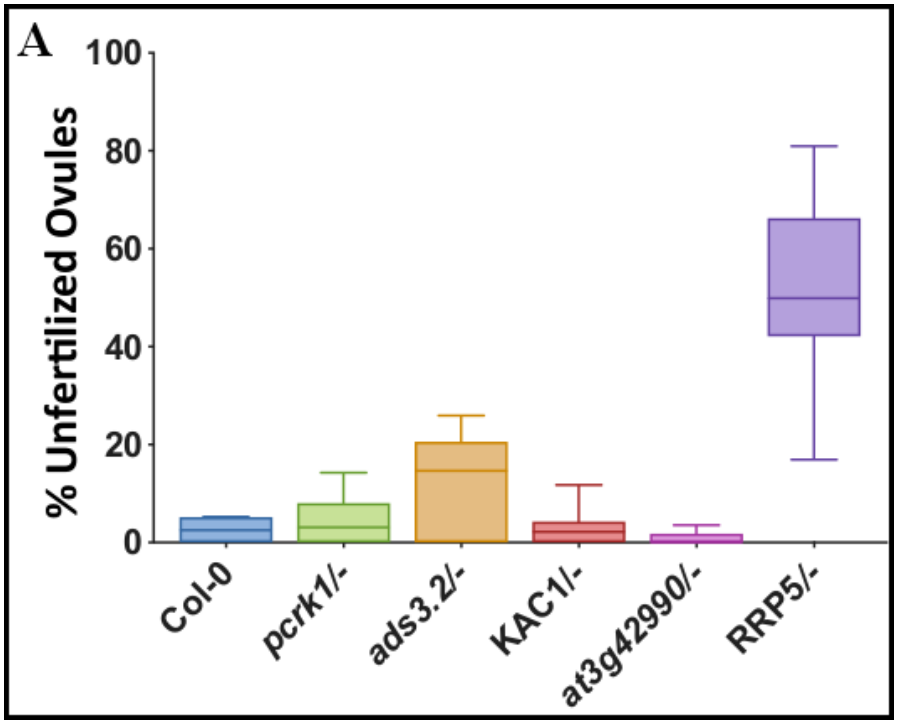

Figure 2.1 Percentage of Unfertilized Ovules in T-DNA Insertion Lines of the Enhancer Candidates.

(A) Boxplot displaying the unfertilized ovule percentages for wild-type Col-0 plants and homozygous or heterozygous single mutant enhancer candidate plants.

Table 2.2 Enhancer Candidate Genes Screened by T-DNA insertion.

Gene ID	Gene Name	SNP Classification	Stock Number	Ecotype
AT3G09830	*PCRK1*	Medium	Salk_145629	Col-0
AT5G10470	*KAC1*	Medium	Salk_014609	Col-0
AT3G42990	Unknown	High	Salk_036970	Col-0
AT3G15870	*ADS3*	High	Salk_142406C	Col-0
AT3G11964	*RRP5*	High	Gk_834C08	Col-0

It was surprising to identify a suppressor of *nta* pollen tube overgrowth while searching for an enhancer. One possibility for this unexpected result is that the T-DNA insertion mutant behaves differently than the EMS-derived mutant. Notably, The SNP in PCRK1^{L164F} is a "moderate effect" SNP that causes an amino acid change of leucine to phenylalanine in the kinase domain. PCRK1 could be the enhancer gene identified from the screen. We thought that the differential effects caused by a single amino acid change in the PCRK1 protein, versus a complete knockout of the gene could be the reason there are different phenotypes occurring between the enhancer plant and the T-DNA double mutant knockout. One notable example of this occurring in plant reproduction research is during the study of MARIS (MRI) from Boisson-Dernier, Franck, Lituiev & Grossniklaus, 2015. The authors identified the MRI^{R240C} allele in a suppressor screen of the *anx1 anx2* pollen tube bursting phenotype. This allele acts as an overactive version of the protein. The knockout of *mri* causes the opposite phenotype of early pollen tube bursting. MARIS is a member of the cytoplasmic receptor-like kinase (RLCK) subfamily VIII. This is one subfamily away from PCRK1, which is a member of RLCK subfamily VII. I thought it was plausible, given this information, that a similar situation could be occurring with the PCRK1 protein.

To test this, a segregating population of plants with the enhancer phenotype were grown. The number of unfertilized versus fertilized ovules in each plant were determined, and the percentages were compared to *nta-1* plants grown at the same time (Fig. 2.1). Plants with infertility higher than *nta-1* were categorized as likely to be heterozygous or homozygous for the enhancer SNP. As expected, I found a large range of unfertilized ovules in the plants, indicating a segregating enhancer SNP. To test whether the SNP in PCRK1 is causing the enhancer phenotype, three plants were selected which could be either heterozygous or homozygous for the enhancer mutation, and three which were thought to have a *nta-1* phenotype based on their infertility. PCR

amplification of the region of *PCRK1* containing the SNP were generated for each plant. Sanger sequencing was used to obtain the sequences of these plants (Fig. 2.2). They were aligned to the wild-type sequence. If *PCRK1* is the enhancer gene, we would expect to see the *PCRK1* SNP to be present in the three plants with high infertility. We would also expect to see no SNP in the plants with low infertility. The result showed no SNP in *PCRK1* in any of the plants sequenced. This indicated to us that *PCRK1* is likely not the enhancer gene from the genetic screen. Although my evidence suggested that *PCRK1* is not the enhancer from the ntaE-14E-6 line, I decided to continue investigating the pollen tube overgrowth suppression phenotype in *nta pcrk1* plants. PCRK1's potential function in pollen tube reception in addition to plant pathogen defense made me want to continue investigating this double mutant since shared components between pollen tube reception and pathogen defense have been reported (Kessler et al., 2010).

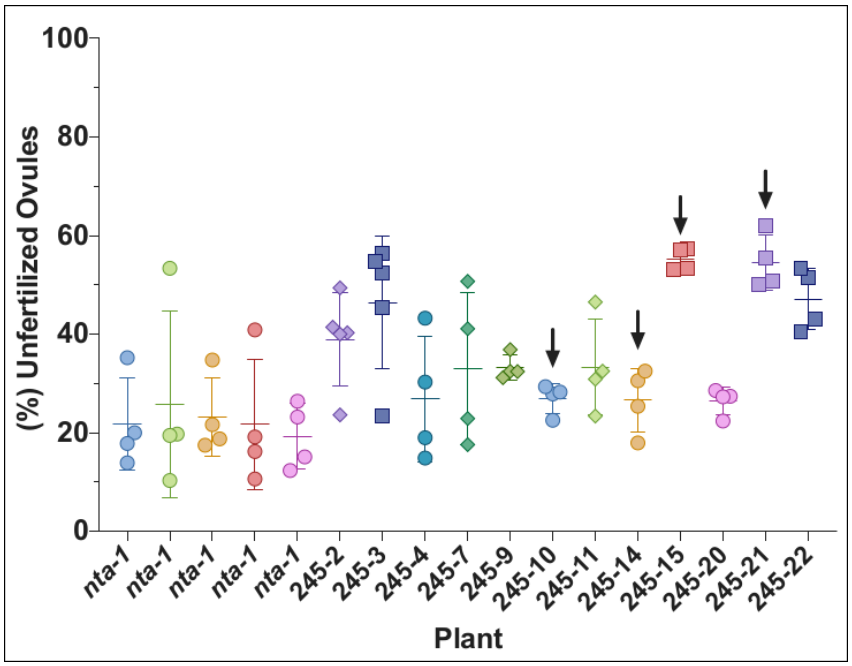

Figure 2.2 Unfertilized Ovule Percentages in a Segregating Enhancer Line ntaE-14E-6 Population Compared to *nta-1*.

Graph of unfertilized ovules in RDF245. RDF245 represents a segregating population of the enhancer mutation. Each data point represents the percentage of unfertilized ovules from one silique of each plant. Black arrows indicate plants chosen for sequencing of PCRK1.

2.3.2 PCRK1 Functions in the Male Gametophyte as a Suppressor of NTA During PT Reception

In single *nta-1* mutants, ovules remain unfertilized due to pollen tube overgrowth (Kessler et al., 2010). Self-pollinated double mutants of *nta-1 pcrk1* have significantly reduced percentages of unfertilized ovules when compared to unfertilized ovules in *nta-1* single mutants under the same growth conditions (Fig. 2.3A). We hypothesized that the increased fertility is due to a decrease in the level of pollen tube overgrowth occurring in these double mutants. Aniline blue staining of *nta-1 pcrk1* pollinated siliques revealed that there is a significant decrease in the amount of pollen tube overgrowth occurring in *nta pcrk1* double mutant plants compared to the level of pollen tube overgrowth in *nta-1* single mutants, and confirmed that suppression of pollen tube overgrowth was the reason for the increased fertility (Fig. 2.3B). In order to determine whether the *pcrk1* suppression of *nta-1* pollen tube overgrowth was being derived from the female or male gametophytic or sporophytic tissues, reciprocal crosses with wild-type were performed using *nta-1*, Col-0, and *nta-1 pcrk1* genotypes. In this thesis, where crosses are listed, the genotype used as the female is always listed first, and the male genotype is listed second. These reciprocal crosses revealed that the *pcrk1* suppression of *nta-1* pollen tube overgrowth is male gametophytic (Fig. 2.3D). Pollen tube overgrowth is significantly decreased in ovules of a *nta* x *pcrk1* cross, though the level of unfertilized ovules remains the same, suggesting that fertilization is still hindered (Fig. 2.3E, D). In addition, these reciprocal crosses revealed a phenotype from the female sporophytic or gametophytic tissues which is not seen in the self-pollinated double mutant plants. This female phenotype will be discussed in section 2.4.3. Together, the phenotypic results of these manual reciprocal crosses, combined with the self-pollinated fertility phenotype suggests that the suppression of *nta-1* pollen tube overgrowth is the dominant phenotype, as the female-side phenotype is not seen in a *nta-1 pcrk1* self-pollinated cross. My results suggest that *nta-1* must be

mutated on both female and male sides to see a suppression of *nta-1* infertility. *nta pcrk1* crossed by wild-type pollen results in the unusual female phenotype. Therefore, the female side infertility phenotype may not be present in a selfed double mutant because the unknown fertilization barrier is suppressed in selfed plants. Based on my transmission efficiency results, this appears to be the case for both *nta pcrk1* x *nta* and *nta* x *nta pcrk1* crosses.

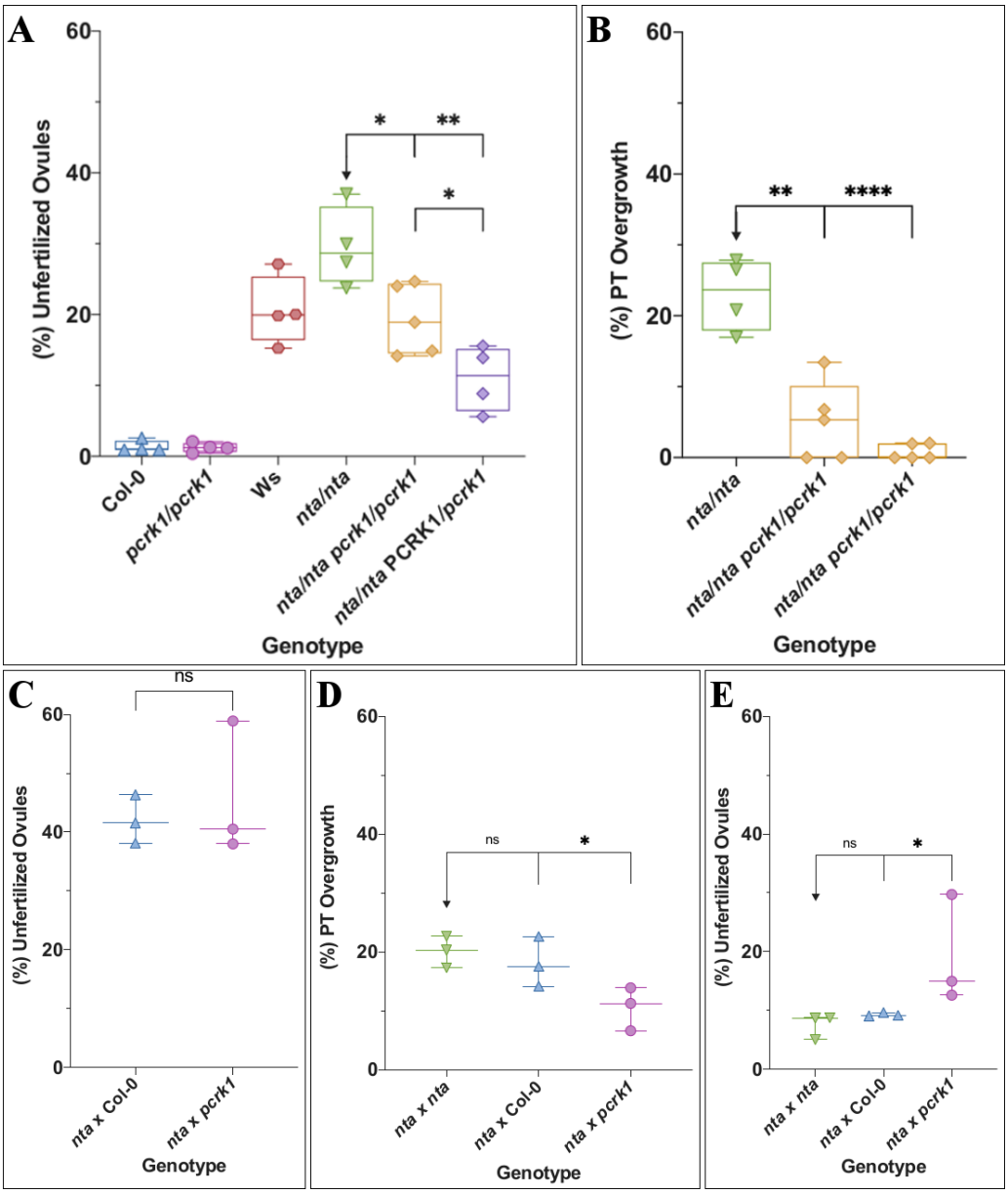

Figure 2.3 *pcrk1* Pollen Suppresses *nta-1* Pollen Tube Overgrowth.

(A-B) Self-pollinated plants. (A) Percentage of unfertilized ovules counted with a dissection microscope in self-pollinated plants. Each data point represents an average of five siliques from one plant. (B) Percentage of pollen tube overgrowth in aniline-blue stained self-pollinated siliques. Each data point represents one silique from a single plant. The two *nta pcrk1* categories represent different plants of the same genotype and line. (C-E) Manually pollinated plants. (C) Percentage of unfertilized ovules. Each data point represents an average of three siliques from one plant. (D) Percentage of pollen tube overgrowth in aniline blue stained siliques. Each data point represents an average of ovule counts from four siliques. (E) Percentage of unfertilized ovules without a pollen tube in aniline-blue stained manually pollinated siliques. Each data point represents an average of four siliques from one plant. P values: ≥0.1234 (ns), ≤ 0.0332 (*), ≤ 0.0021 (**), ≤ 0.0002 (***), ≤ 0.0001 (****).

The male *pcrk1* suppression of *nta-1* was further tested by measuring male transmission efficiency. *pcrk1* transmission through the male gametophyte was measured by crossing pollen from the genotype *pcrk1*/PCRK1 in a *nta-1* background. 50% of haploid pollen grains will contain wild-type PCRK1, and 50% will contain mutant *pcrk1*. 100% is the expected transmission rate of an allele following normal mendelian segregation. Deviations from 100% represent segregation distortion of a specific allele. *pcrk1* was transmitted at a rate of 190% through the male gametophyte (Table 2.3). This suggests that the *pcrk1* mutant allele was transmitted 90% higher than expected compared to the wild-type PCRK1 allele. Taking into account the manual crosses which revealed that *nta* x *pcrk1* does not lead to a decrease in the number of unfertilized ovules, the results of this male transmission efficiency test suggest that *nta-1* must be mutated on both the female and male sides to see the suppression effect. This is interesting since a single *nta-1* mutant does not have adverse effects on fertility when transmitted through the male gametophyte (Kessler et al., 2010). This result provides genetic evidence for *pcrk1* suppression of *nta-1* pollen tube overgrowth through the male gametophyte, since pollen tubes with the *pcrk1* genotype in a *nta-1* background are much more likely to fertilize ovules and produce seeds. In addition, it may provide evidence that *nta-1* functions in pollen tubes, though a phenotype is not observed unless *pcrk1* is mutated in the same plant.

Table 2.3 Male Transmission Efficiency of *pcrk1* and *nta-1* in reciprocal mutant backgrounds.

Transmission	**Cross (Female x Male)**	***pcrk1*/*PCRK1***	***PCRK1*/*PCRK1***	***pcrk1*/*PCRK1*:Total %**	**TE (Expected)**	**X^2 (P) for**
Male	*nta/nta PCRK1/PCRK1 x nta/nta pcrk1/PCRK1*	42	2	95.45	190 (100)	0.0000
Transmission	**Cross (Female x Male)**	***nta*/*NTA***	***NTA*/*NTA***	***nta*/*NTA*:Total %**	**TE (Expected)**	**X^2 (P) for**
Male	*pcrk1/pcrk1 NTA/NTA x nta/NTA pcrk1/pcrk1*	22	26	45.83	92 (100)	0.6831

The *nta-1* allele has reduced transmission through the female gametophyte (Kessler et al., 2010). The pollen tube overgrowth phenotype in *nta-1* is a partial phenotype which varies under different environmental conditions with 20-50% of ovules having pollen tube overgrowth. Therefore, with complete suppression of *nta-1* PT overgrowth of a specific allele, we may expect the transmission of the *pcrk1* allele compared to PCRK1 to increase to a maximum of around 150%. Considering this, it was surprising to us that the transmission of *pcrk1* was so high through the male gametophyte at 190% (Table 2.3). One reason for this could be that only around fifty plants were genotyped for each cross. Another possibility for this high transmission efficiency is that *pcrk1* pollen tubes outcompete the wild type by growing faster or being attracted to ovules more efficiently. The *in-vivo* length of *pcrk1* pollen tubes through the transmitting tract of Col-0 pistils was measured using various time points after manual pollination (Fig. 2.4A). Aniline blue staining was used to visualize the pollen tubes in the transmitting tract. *pcrk1* pollen tubes were observed lower in the transmitting tract than Col-0 pollen tubes at two hours after pollination (Fig. 2.4A). *pcrk1* pollen tubes were not observed significantly longer than Col-0 in the transmitting tract between 4 and 8 hours after pollination (Fig. 2.4A). This experiment should be repeated with a larger sample size, especially to confirm whether there is a significant difference in the growth of Col-0 and *pcrk1* between 0 and 2 hours after pollination. Although this experiment did not reveal

many significant differences between *pcrk1* and Col-0 growth, we hypothesized that the nature of the experiment could be the reason we don't see much of an effect. First, my transmission efficiency data was measured in a *nta-1* background. The reason for the highly increased transmission may be dependent on having *nta* also mutated in the plants. My data suggests that this is the case. In this experiment, I was measuring pollen tubes still in the transmitting tract. Another possible reason I may not be able to observe the cause of the increased transmission from my experiment is because it may not be accurately measured by this method. For example, if *pcrk1* pollen tubes are better attracted to wild-type ovules, those pollen tubes would leave the transmitting tract, and would not be included in my measurements. The reason for the large increase of *pcrk1* male transmission still needs to be investigated.

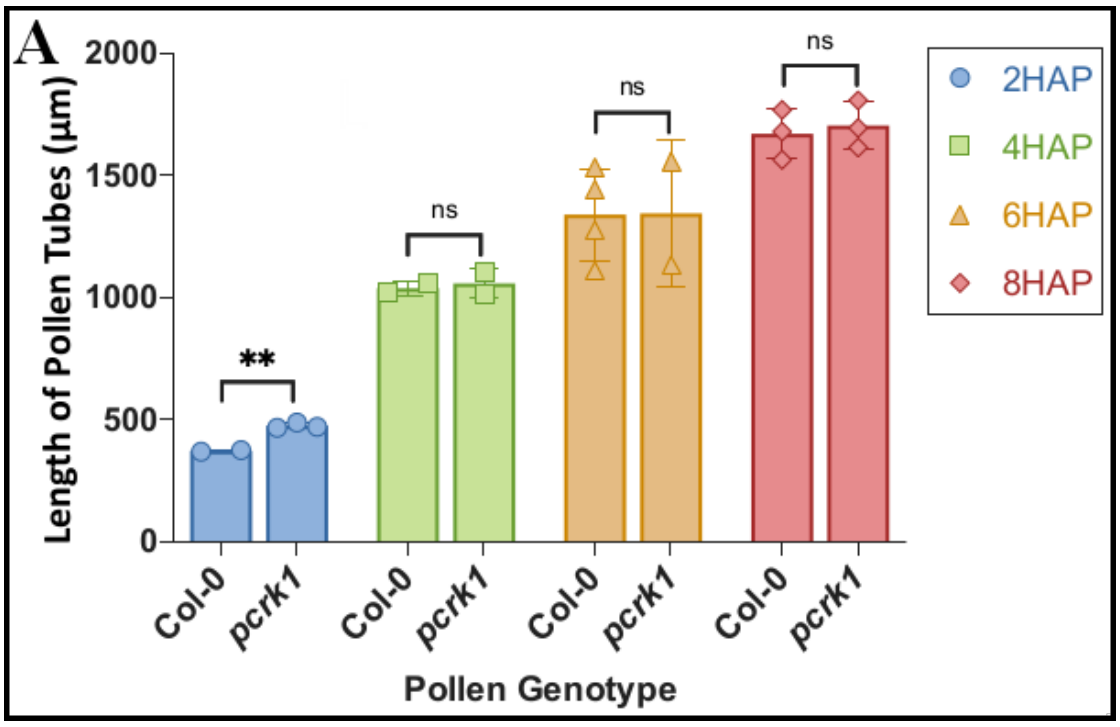

Figure 2.4 *pcrk1* Pollen Tubes are Further Down the Transmitting Tract Than Col-0 at 2 Hours After Pollination.

(A) Bar graph showing the pollen tube length in the transmitting tract for both Col-0 and *pcrk1* pollen tubes at 2, 4, 6, and 8 hours after pollination (HAP). Each data point represents a single measurement from one silique. P values: ≥0.1234 (ns), ≤ 0.0332 (*), ≤ 0.0021 (**), ≤ 0.0002 (***), ≤ 0.0001 (****).

The male gametophytic suppression of *nta-1* by *pcrk1* suggests that PCRK1 is expressed in pollen tubes. In addition, publicly available microarray data reported PCRK1 as being expressed in mature pollen (Wuest et al., 2010). A binary vector containing the native PCRK1 promoter-driven GFP fusion of PCRK1, named pPCRK1::PCRK1-GFP, was transformed to *Agrobacterium tumefaciens.* Col-0 plants were inoculated using the floral-dip method (Bent, 2006). GFP fluorescence was detected in T2 pollen tubes (Fig. 2.5). This provides more evidence that PCRK1 is expressed and functioning in pollen tubes. PCRK1 has been reported to localize in the cytoplasm of a cell, with reported association to plasma membranes (Sreekanta et al., 2015). Co-localization experiments with reporter lines could be performed in the future to determine its localization in pollen tubes.

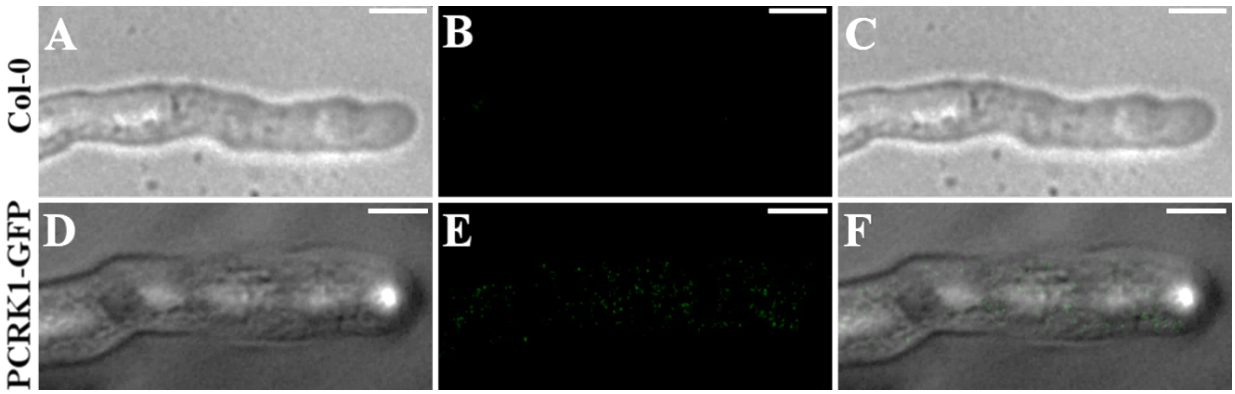

Figure 2.5 pPCRK1::PCRK1-GFP is Expressed in Col-0 pollen tubes.
(A-C) Col-0 pollen tube. (A) DIC image of a Col-0 pollen tube. (B) GFP image of a Col-0 pollen tube showing no fluorescence. (C) Merged DIC and GFP image. (D-F) pPCRK1::PCRK1-GFP in a Col-0 pollen tube. (D) DIC image of a PCRK1-GFP pollen tube. (E) GFP fluorescence of a PCRK1-GFP pollen tube indicating gene expression. (F) Merged DIC and GFP channels. Scale bars: 5µm.

If the absence of functional *nta-1* and *pcrk1* in pollen tubes causes the suppression of *nta-1* PT overgrowth in the *nta pcrk1* double mutant plants, then the addition of functional copies of PCRK1 to the double mutant plants should complement the suppression phenotype. This would return pollen tube overgrowth to *nta-1* levels. T1 seeds of pPCRK1::PCRK1-GFP in Col-0 were

screened for hygromycin resistance in the female gametophyte and pollen tubes, which indicates that the plant was successfully transformed with the modified Ti plasmid. T1 fertility counts revealed that ½ of T1 plants had high levels of infertility, and ½ had levels of unfertilized ovules between *nta-1* and *nta pcrk1* (Fig. 2.6A). Aniline blue staining of pistils from these T1 plants with high infertility revealed that many female gametophytes in the ovules of these plants were defective with no pollen tubes attracted to them (Fig. 2.6B, C). Since PCRK1 is expressed in the female gametophyte, one half of the T1 haploid female gametophytes should contain a single copy of the transgene. If the transgene is causing the high infertility in half of the T1 plants, I may still observe the infertility rise above 50% due to *nta-1* pollen tube overgrowth in these plants. All of the T2 segregation ratios from the lines with high infertility deviated from the expected 3:1 Hyg^R:Hyg^S ratio if there was one copy of the transgene. However, three out of five T2 lines from T1 plants with expected fertility ranges between *nta-1* and *nta pcrk1* matched the expected 3:1 Hyg^R:Hyg^S ratios. I hypothesize that PCRK1 expression levels higher than wild type could cause the infertility in ½ of the T1 plants. The level of gene expression after *Agrobacterium* transformation can be highly variable. This result suggests that *PCRK1* gene expression over a certain threshold could cause the female gametophytes to develop improperly or to die. Some segregation ratios of the highly infertile lines differ greatly from each other. For example, T2 progeny of RDF208 segregated in a 0:16 Hyg^R:Hyg^S ratio (Table 2.4). This could be because ovules containing the transgene were not transmitted to the T2 generation, or because the T1 line was not actually Hyg^R. In contrast, the T1 line RDF207 had 69% unfertilized ovules and a Hyg^R:Hyg^S ratio of 6:1 (Table 2.4). It's important to consider that many seeds did not germinate on the media for all T2 lines (Table 2.4). The reason for low germination rates is unknown, however, it could influence the Hyg^R:Hyg^S ratios of each line. RDF207 had a Hyg^R:Hyg^S ratio of

6:1, however, only seven seeds germinated while twenty-eight seeds did not. The T2 progeny of RDF 201 segregated 18:1 with a T1 infertility of 11.4%. This extreme number of Hyg^R plants could be due to multiple T-DNA insertions in the plants, or an inaccurate segregation ratio due to ungerminated seeds. While an obvious relationship between the Hyg^R:Hyg^S ratios and the infertility of the T1s isn't clear from these results, it is clear that most of the T1 plants in the expected fertility range below 40% have the expected 3:1 Hyg^R:Hyg^S ratio. Future experiments to investigate the cause of the infertility and unusual Hyg^R:Hyg^S ratios in these T1 and T2 lines could involve measuring PCRK1 gene expression levels of T2 plants and comparing it to the infertility and Hyg^R:Hyg^S ratios.

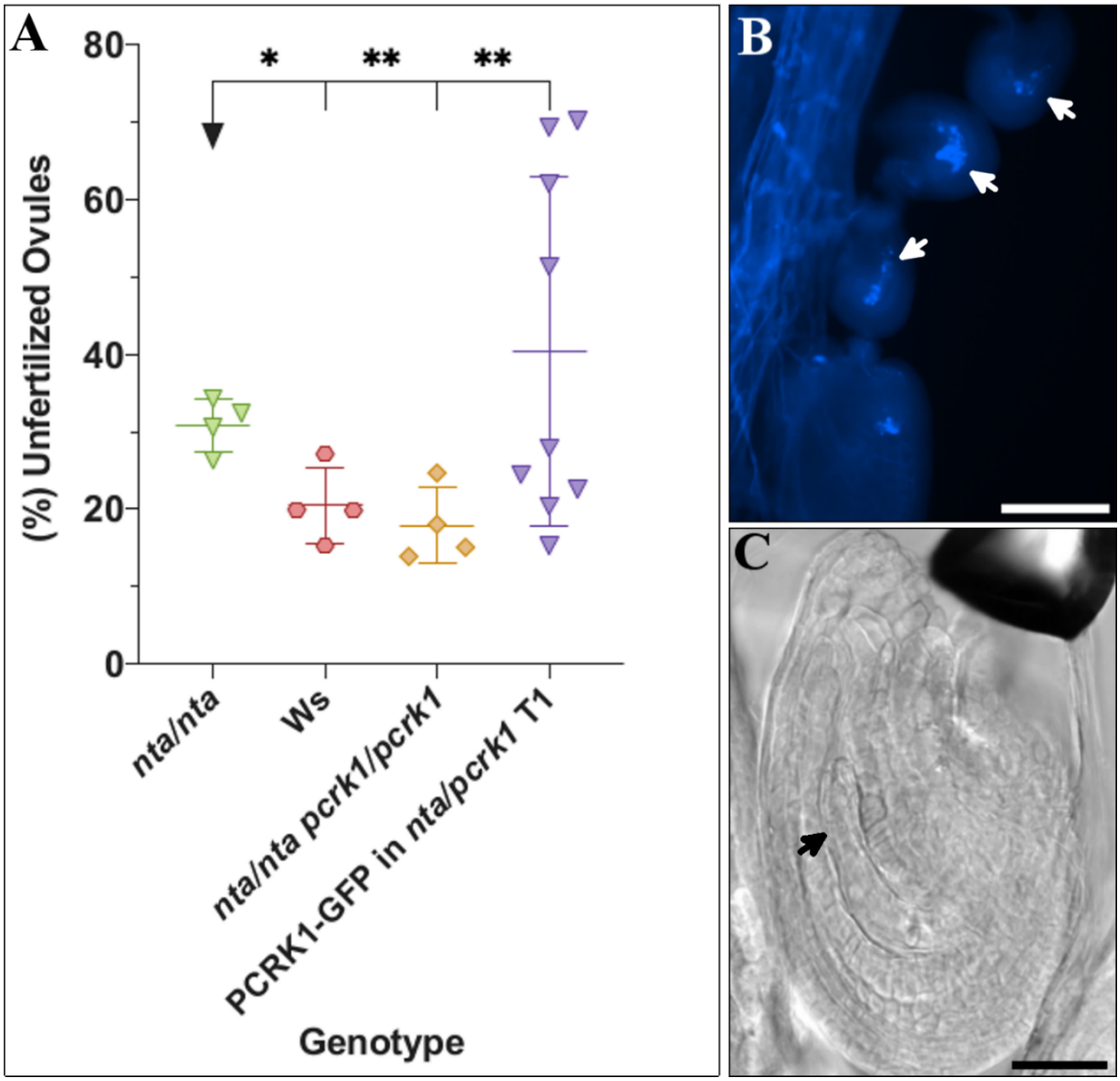

Figure 2.6 One Half of T1 Plants Have High Percentages of Unfertilized Ovules Due to Defective Embryo Sacs.

(A) Percentage of unfertilized ovules in self-pollinated plants. Each data point represents an average of five siliques from one plant. (B) Aniline blue staining image of callose in the dying embryo sacs. (C) DIC image of a defective embryo sac in a T1 line. Arrows point to defective embryo sacs. P values: ≥0.1234 (ns), ≤ 0.0332 (*), ≤ 0.0021 (**), ≤ 0.0002 (***), ≤ 0.0001 (****). Scale bars: 100µm (B), 25µm (C).

Table 2.4 T2 Hyg^R Segregation Ratios for *nta pcrk1* with pPCRK1::PCRK1-GFP Complemented Lines

ID	T1 Unfertilized Ovules (%)	Hyg^R:Hyg^S Ratio in T2 Plants	Ungerminated Seed #
RDF201	11.4	18:1	18
RDF202	70	23:10 (≈2:1)	10
RDF203	62	31:7 (≈4:1)	7
RDF204	24.5	24:7 (≈3:1)	13
RDF205	20.5	20:7 (≈3:1)	8
RDF206	22.6	20:6 (≈3:1)	9
RDF207	69.4	6:1	28
RDF208	51.4	0:16	16
RDF209	15.3	28:12 (≈2:1)	8
RDF210	28	12:3 (≈4:1)	24

Gray rows indicate lines chosen for complementation testing.

Since the complemented T1 generation are hemizygous for pPCRK1::PCRK1-GFP, progeny from each T2 generation with one copy of the transgene should segregate in a 3:1 Hyg^R:Hyg^S ratio. I counted the Hyg^R:Hyg^S ratios for each of my T2 lines (Table 2.4). Three T2 lines which had a 3:1 Hyg^R:Hyg^S ratio were selected and screened for homozygous GFP using the GFP fluorescence present in the female gametophyte. The transgenic pollen was crossed onto *nta-1* mutant plants and the number of fertilized versus unfertilized ovules were counted. The infertility was compared to the manually self-pollinated *nta-1* plants and *nta pcrk1* plants (Figure 2.7). The level of PCRK1-GFP in the double mutant pollen of these lines was sufficient to complement the suppression phenotype, bringing the level of infertility to *nta-1* levels. Aniline blue staining confirmed *nta-1*-like levels of PT overgrowth in these crosses (Fig. 2.7B).

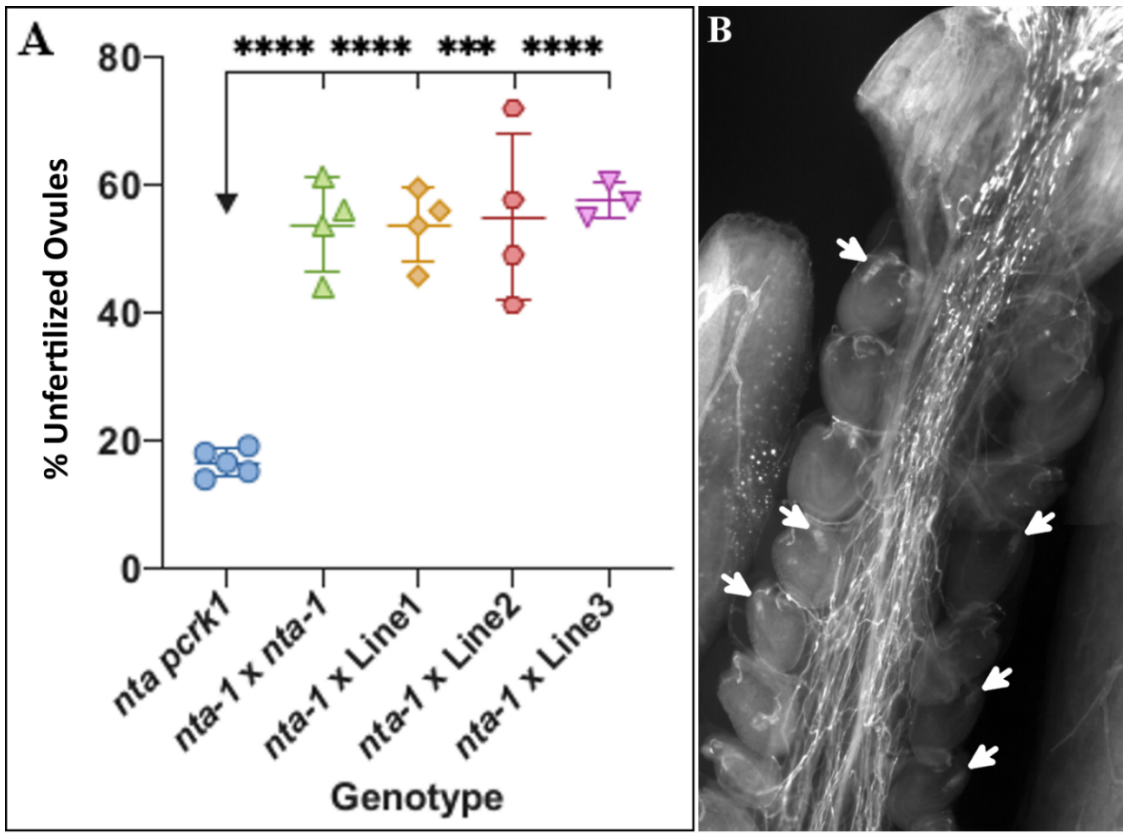

Figure 2.7 pPCRK1::PCRK1-GFP Complements the *nta-1* Suppression Phenotype of *nta-1 pcrk1* Pollen.

(A) *nta pcrk1* pollen transformed with pPCRK1::PCRK1-GFP complements the suppression phenotype and returns unfertilized ovule numbers to *nta-1* levels. Line1, Line2, and Line3 represent individual T1 lines. Each data point represents an average of four siliques from one plant. (B) Aniline blue stained image showing pollen tube overgrowth returns to *nta-1* levels in the siliques crossed with complemented pollen. P values: ≥0.1234 (ns), ≤ 0.0332 (*), ≤ 0.0021 (**), ≤ 0.0002 (***), ≤ 0.0001 (****).

A solid foundation of evidence for *pcrk1* suppression of *nta-1* PT overgrowth has been collected. The suppression of *nta* pollen tube overgrowth phenotype could be due to either a result of a change in direct signaling between the male and female gametophytes, or the result of a change in the mechanics of the growing pollen tube. This could be similar to the *anx1, anx2* mutant defects in the biosynthesis of cell wall materials (Boisson-Dernier et al., 2009). One hypothesis is that *pcrk1* PTs may be weaker and more likely to burst regardless of NTA levels, and that this could

influence the level of pollen tube overgrowth occurring in *nta-1* mutants. Although *pcrk1* pollen tubes cause a decrease in the level of *nta* pollen tube overgrowth, the number of unfertilized ovules appears to only decrease when *nta* is also mutated on the male side (Fig. 2.3A, Table 2.3). This was surprising since NTA has not been reported to be expressed or function in the male gametophyte.

2.3.3 PCRK1 Functions in the Female Gametophyte During PT Reception

As discussed in section 2.3.2, reciprocal crosses with wild-type were performed to determine whether the *pcrk1* suppression of *nta-1* pollen tube overgrowth was from the female or male gametophyte. Crosses with *nta pcrk1* as the female and either Col-0 or Ws ecotype pollen revealed an unusual pollen tube reception phenotype. Aniline blue-stained pistils of these crosses have higher levels of ovules with pollen tube overgrowth, however, unlike in *nta-1* pollen tube overgrowth, these ovules consistently enlarge, resembling a fertilized ovule (Fig. 2.8C, E). The large sized ovules and pollen tube overgrowth phenotype in these pistils indicate that pollen tube attraction occurs successfully to these ovules from this cross. Fertility counts of *nta pcrk1* x Ws siliques revealed that 40% of the ovules appear to abort during seed development (Fig. 2.8H). I was not able to observe any embryo or endosperm development in these ovules, which suggests that fertilization in these ovules is not successful. Next, ovule enlargement was investigated. In mutants with pollen tube overgrowth, ovules remain unfertilized and remain small and white. Ovules which abort after the initiation of seed development appear larger and white or brown. Kasahara et al., 2016 first described ovule enlargement and seed coat initiation in the absence of fertilization, a phenomenon they named pollen tube-dependent ovule enlargement morphology (POEM). They concluded that pollen tube contents (PTC) is sufficient to induce POEM, and that it occurs independent of fertilization. I hypothesized that POEM is occurring in these aborted-

looking ovules which lack evidence of fertilization. Vanillin staining, which stains the seed coat marker proanthocyanidin, was performed on *nta pcrk1* x Ws siliques. This revealed staining at the micropylar end of the ovule, which is consistent with the POEM phenotype (Fig. 2.8E). Together, these results suggest that pollen tube overgrowth occurs in these ovules, the pollen tubes eventually burst, but fertilization does not occur.

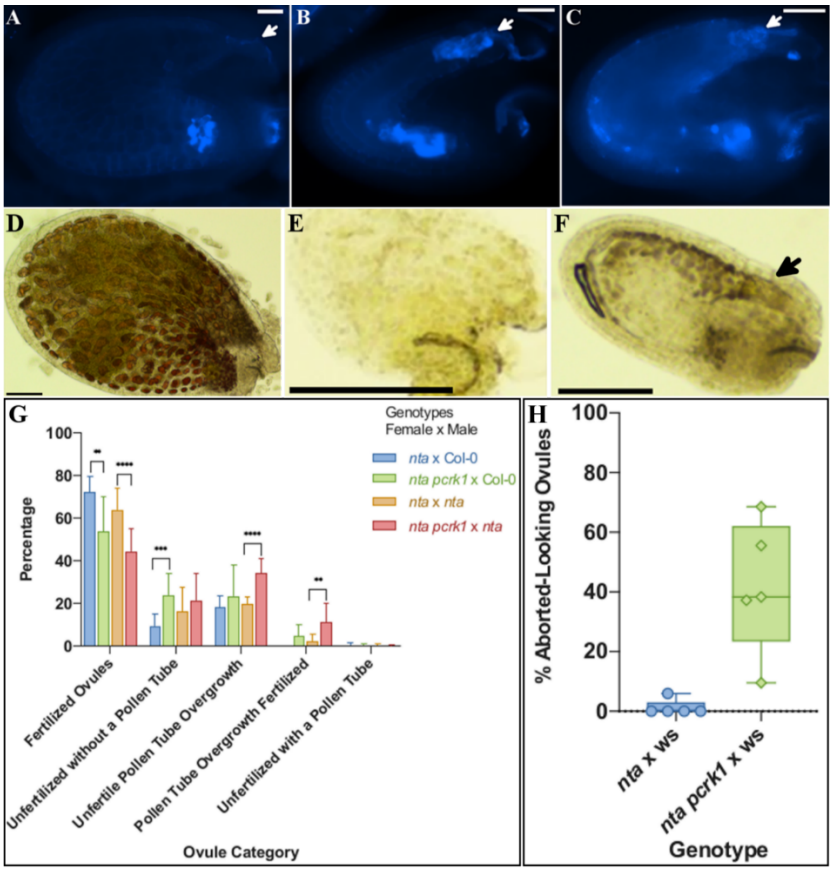

Figure 2.8 *nta pcrk1* Crossed by Wild-Type Pollen Results in Increased Pollen Tube Overgrowth and a POEM phenotype.

(A-C) Aniline blue stained images of ovules with pollen tubes (arrows). (A) Normal pollen tube reception in a fertilized ovule. (B) Pollen tube overgrowth in a *nta-1* ovule. (C) Pollen tube overgrowth and ovule enlargement in a *nta pcrk1* x Ws ovule. (D-F) Vanillin stained ovules six days after pollination. (D) Seed coat staining in a fertilized Col-0 ovule. (E) No staining in an unfertilized Col-0 ovule. (F) POEM phenotype with seed coat staining near the micropyle of a *nta pcrk1* x Ws ovule. (G) Quantification of ovule phenotypes observed from each cross. (H) Quantification of the *nta pcrk1* x ws POEM phenotype based on ovule size. P values: ≥0.1234 (ns), ≤ 0.0332 (*), ≤ 0.0021 (**), ≤ 0.0002 (***), ≤ 0.0001 (****). Scale bars: 25µm (A-C), 100µm (D-F).

The female transmission efficiency of *pcrk1* was measured in a *nta* mutant background. The transmission was 157%, suggesting that *pcrk1* in a *nta* background was transmitted to the next generation more than the *PCRK1* allele (Table 2.5). However, the control transmission efficiencies of *pcrk1/PCRK1* crossed by wild-type, and *nta/nta pcrk1/PCRK1* crossed by wild-type were not collected, and therefore a strong conclusion cannot be made about the transmission of *pcrk1* in a *nta* background.

Table 2.5 Female Transmission Efficiency of *nta* and *pcrk1* in Reciprocal Mutant Backgrounds.

Transmission	Cross (Female x Male)	*pcrk1*/*PCRK1*	*PCRK1*/*PCRK1*	*pcrk1*/*PCRK1*:Total%	TE (Expected)	X^2 (P)
Female	*nta/nta pcrk1/PCRK1 x nta/nta PCRK1/PCRK1*	43	12	78.18	157 (100)	0.0031
Transmission	**Cross (Female x Male)**	***nta*/*NTA***	***NTA*/*NTA***	***nta*/*NTA*:Total%**	**TE (Expected)**	**X^2 (P)**
Female	*nta/NTA x NTA/NTA*	24	34	41.38	82.8 (100)	0.3532
Female	*nta/NTA pcrk1/pcrk1 x NTA/NTA pcrk1/pcrk1*	20	38	34.48	69 (82.8)	0.4166
Female	*nta/NTA pcrk1/pcrk1 x NTA/NTA PCRK1/PCRK1*	24	46	34.29	69 (82.8)	0.3537

The female transmission efficiencies of *nta-1*, *nta-1* in a *pcrk1* background, and *nta-1* crossed by wild-type pollen were collected. The transmission efficiency of *nta-1* was 82.8%, which, if the same method of calculation is used, matches the transmission efficiency of *nta-1* previously reported (Kessler et al., 2010, Table 2.5). Self-pollinated *nta pcrk1* plants have higher fertility than *nta-1* plants due to a suppression of pollen tube overgrowth. However, *nta pcrk1* pistils crossed by wild-type pollen of ecotypes Ws and Col-0 result in the POEM phenotype as previously described. Therefore, I wondered if the *pcrk1* mutation in pollen prevented the POEM phenotype in the self-

pollinated plants. If this is true, I expected a high female transmission of the *nta-1* allele in a *pcrk1* background. I thought I may see a low female transmission of the *nta-1* allele in *nta/NTA pcrk1/pcrk1* crossed by wild-type pollen, which would be indicative of the POEM phenotype. However, my results showed a decreased *nta-1* transmission from both crosses, indicating that *nta pcrk1* crossed by *pcrk1* pollen does not cause the high fertility observed in *nta pcrk1* mutant plants (Table 2.5). It is possible that *nta pcrk1* crossed by either *nta-1* or *nta-1 pcrk1* in pollen is required to see the high fertility and suppression phenotype. Since I genotyped each individual plant by PCR for this experiment, lower than ideal numbers have been collected, and this experiment should be repeated. *pcrk1* control crosses should be added as discussed above, as well as a *nta*/NTA *pcrk1/pcrk1* x *nta/nta* cross for a more complete experiment. A future investigation into which mutant combinations in the female and male gametophytes lead to high fertility of selfed plants should be performed by the repetition of these transmission efficiency crosses, as well as fertility counts of each cross.

Since it appeared that PCRK1 functions in the female gametophyte, used Col-0 plants transformed with PCRK-GFP under its native promoter to look for GFP expression in the female gametophyte. Gene expression analysis using confocal microscopy showed *PCRK1* gene expression in the central cell of the female gametophyte (Fig. 2.9B). This matched previously reported *PCRK1* expression in the central cell (Wuest et al., 2010).

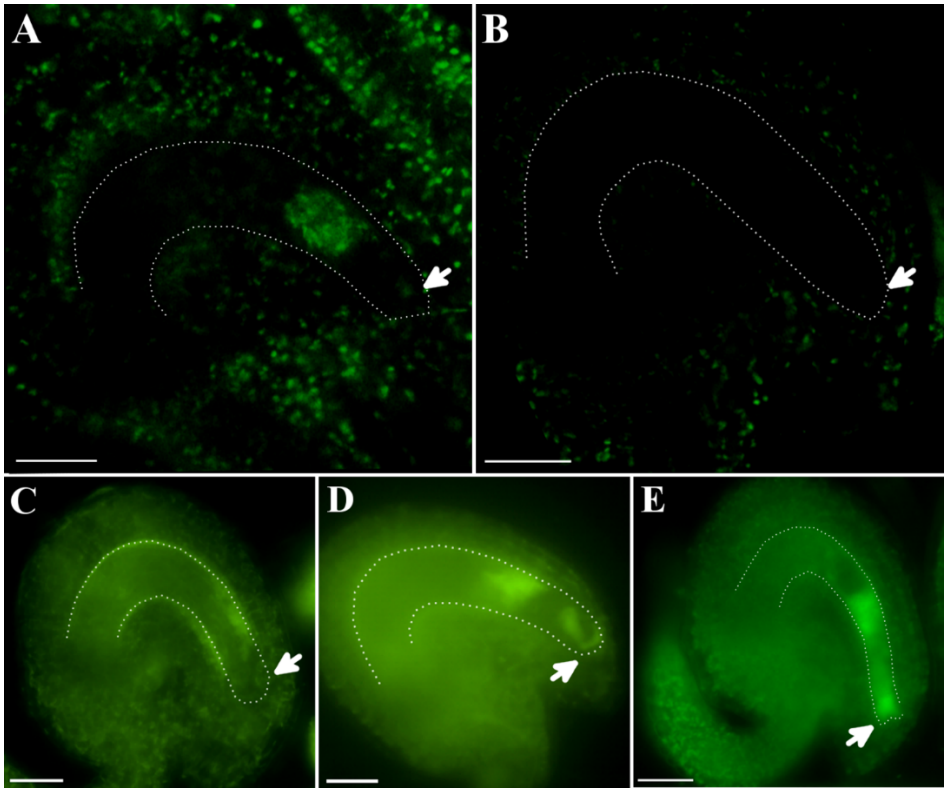

Figure 2.9 PCRK1 is expressed in the central cell of the embryo sac.

(A-B) Confocal laser-scanning microscope images. (A) pPCRK1::PCRK1-GFP expression in the central cell region of the embryo sac. (B) No GFP expression in the embryo sac of a Col-0 ovule. (C-E) Epifluorescent microscope images. (C) Embryo sac of a Col-0 ovule. (D) Fluorescence in the central cell and synergid cell regions of a T1 Col-0 ovule transformed with pPCRK1::PCRK1-GFP embryo sac. (E) Fluorescence spanning the egg cell apparatus and central cell region in a T2 *nta pcrk1* ovule transformed with pPCRK1::PCRK1-GFP. Dotted lines outline the embryo sacs. Arrows indicate the micropylar end of the embryo sac. Scale bars: 25µm.

During pollen tube reception, a form of programmed cell death known as synergid degeneration is an important step. The synergid which interacts with the pollen tube and induces it to burst is known as the receptive synergid cell. It undergoes cell death around the time of pollen tube burst (Wang et al., 2017; Drews & Yadegari, 2002; Kessler et al., 2010; Leydon et al., 2015). The second synergid cell, known as the persistent synergid, remains alive until the egg cell and central cell facilitate its death via ethylene signaling (Marayuama et al., 2015; Pereira, Lopes & Coimbra, 2016). Synergid cell death in Arabidopsis may be regulated by vacuolar acidification

mediated by AP1G and V-ATPases (Wang et al., 2017). *ap1g* mutants are impaired in pollen tube reception and in receptive synergid cell death (Wang et al., 2017).

Putative autofluorescence and a strange synergid shape was observed at maturity in these ovules (Fig. 2.9D). This reminded me of the dying synergid characteristics as described in Sandaklie-Nikolova, Palanivelu, King, Copenhaver, and Drews, 2007. Using confocal microscopy, I did not observe GFP expression in the synergids of Col-0 plants transformed with PCRK1-GFP under its native promoter. The putative auto fluorescence observed, coupled with a strange synergid shape may indicate a dying synergid cell. I hypothesize that at least one of the synergid cells of these putative overexpression plants may be undergoing early cell death in the absence of pollination. However, the evidence for this is very preliminary, and much more testing of synergid health in these plants will need to be performed to make a conclusion. Another possibility is that the synergids observed were not healthy due to other environmental reasons such as light exposure from the fluorescence microscopy. However, as mentioned before, the central cell has been shown to regulate synergid cell death via ethylene signaling (Marayuama et al., 2015; Pereira, Lopes & Coimbra, 2016). Given that PCRK1 is expressed in the central cell, it's possible that it has a role in synergid cell death. In *Arabidopsis thaliana*, synergid and filiform apparatus health before pollination have been shown to be essential for successful attraction and reception of pollen tubes (Kasahara, Portereiko, Sandaklie-Nikolova, Rabiger, and Drews, 2005). Therefore, it would be surprising if early synergid degeneration was occurring in these plants and maintained high levels of fertility. Again, this evidence this is very preliminary, and more testing of synergid health in these plants will need to be performed to make a solid conclusion.

If PCRK1 is involved in regulating synergid cell death in the female gametophyte, I hypothesized that delayed synergid death in the double mutant could be involved in the POEM

phenotype seen in a *nta pcrk1* x wild-type cross. Embryo sacs from emasculated *nta-1*, *nta-1* x Ws, and *nta-1 pcrk1* x Ws pistils were visualized using the confocal microscopy method described in Christensen, 1997. Sandaklie-Nikolova, Palanivelu, King, Copenhaver, and Drews, 2007 reported using the same CLSM method that 72% of synergids were degenerated at 8 hours after pollination, and 22% were slightly degenerated, suggesting that pollen tube reception has occurred in these ovules. My results showed that the synergid cells of unpollinated *nta-1* siliques showed no degeneration (Fig. 2.11A). Synergids of *nta-1* x Ws ovules 7.5 hours after pollination showed highly degenerating synergid cells (Fig. 2.11B). However, degenerating synergids were only seen in about three ovules from a *nta pcrk1* x Ws cross 7.5 hours after pollination (Fig. 2.11C). Although pollen tube attraction appears to occur successfully in pistils from this cross, the timing of pollen tube reception has not been measured. Using this CLSM method, I was unable to tell whether pollen tubes have successfully reached the ovule. However, this preliminary evidence suggests a clear difference in synergid health between the *nta* x Ws and *nta pcrk1* x Ws crosses. It is possible that the pollen tubes haven't yet reached the *nta pcrk1* x Ws ovules at 7.5 hours after pollination. Another possibility is that the receptive synergid cell has delayed or an absence of cell death compared to *nta* x Ws. In either case, the difference between the crosses may relate to the POEM phenotype observed in the *nta pcrk1* x Ws ovules.

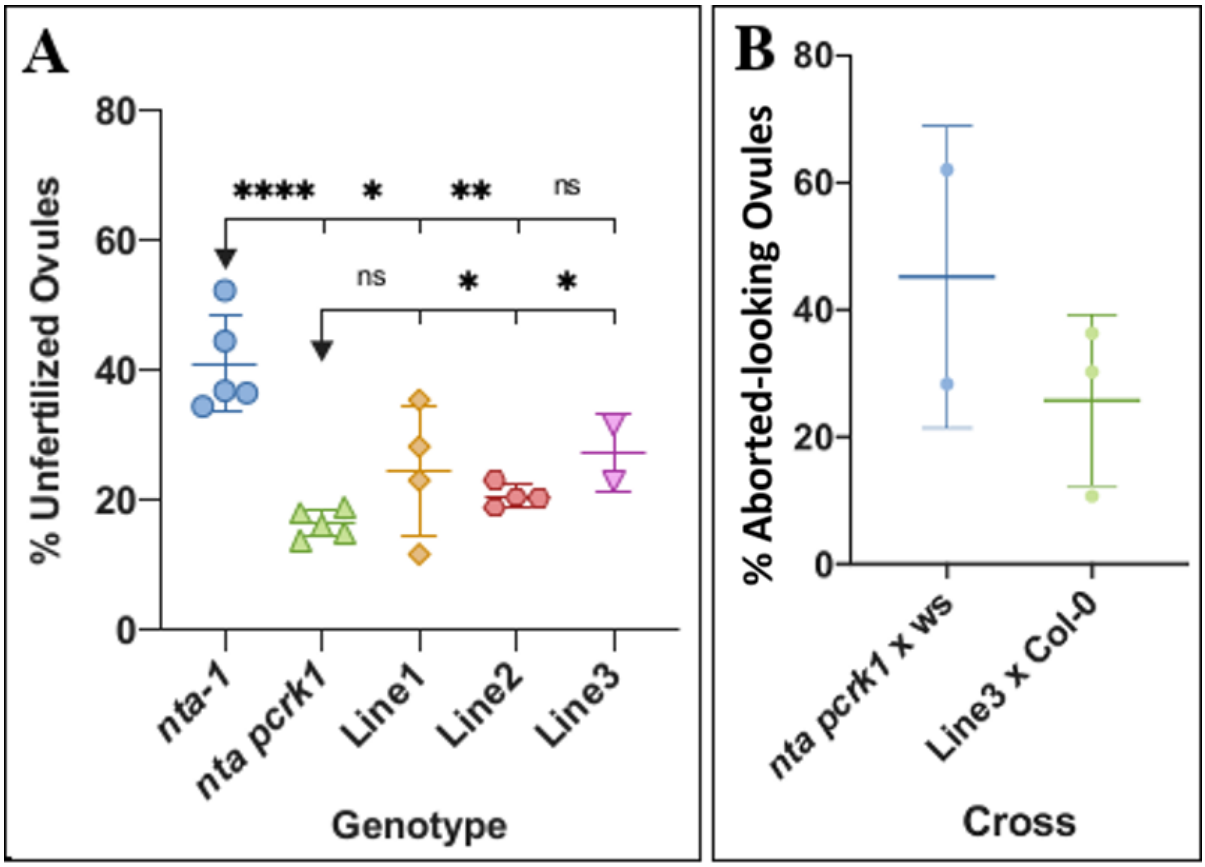

Figure 2.10 *nta pcrk1* Female-Side Phenotype is Partially Complemented by pPCRK1::PCRK1-GFP.

(A) Percentage of unfertilized ovules of self-pollinated plants. (B) Percentage of aborted-looking ovules in manually crossed siliques. P values: ≥0.1234 (ns), ≤ 0.0332 (*), ≤ 0.0021 (**), ≤ 0.0002 (***), ≤ 0.0001 (****).

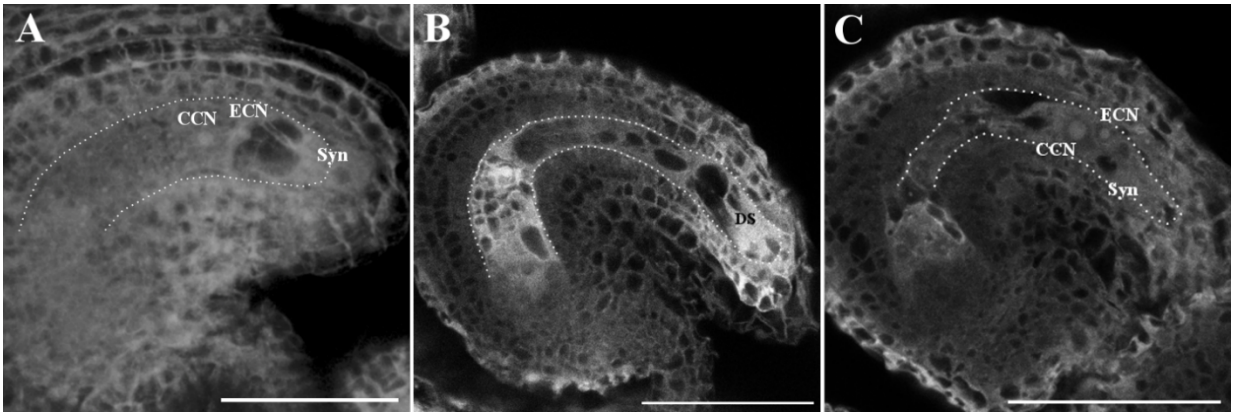

Figure 2.11 *nta pcrk1* x Ws Synergids are Not Degenerated at 7.5 Hours After Pollination.

(A-C) Confocal laser scanning microscopy images of ovules. (A) Unpollinated mature *nta* pistil showing an ovule with no synergid degeneration. (B) *nta* x ws ovule at 7.5 HAP with synergid degeneration. (C) *nta pcrk1* x ws ovule at 7.5 HAP with no synergid degeneration. Dotted lines outline the embryo sacs. Central Cell Nucleus (CCN), Egg Cell Nucleus (ECN), Synergid Cells (Syn), Degenerating Synergids (DS). Scale bars: 50µm

Complementation testing was utilized to see if PCRK1 under its native promoter fused to GFP could complement the POEM phenotype and return the phenotype to pollen tube reception of *nta pcrk1* double mutants. The same independent transformants that complemented the *pcrk1* pollen phenotype only partially complemented the female-side phenotype (Fig. 2.10). The self-pollinated complemented plants had lower levels of unfertilized ovules compared to *nta-1*, suggesting that neither the female nor male side complemented enough to act as single mutant *nta-1* plants. However, the pollen complemented enough to return the suppression phenotype to *nta-1* levels of infertility and pollen tube overgrowth.

Further inspection of the GFP fluorescence in these plants showed GFP expression was altered in the female gametophyte. Either GFP expression or autofluorescence extended from the synergid to the central cell area of the female gametophyte (Fig. 2.9E). Expression specific to the central cell was not observed as it was in transgenic Col-0 plants. In addition, crosses of wild type pollen onto these pistils showed the POEM phenotype, further confirming that the female-side

phenotype of these double mutant *nta-1 pcrk1* plants was not fully complemented (Fig. 2.10B). This could be for various reasons. One reason could be that *nta-1* is disrupting the native expression of PCRK1-GFP in the female gametophyte. Evidence of an altered expression pattern was observed (Fig. 2.9E). Another reason could be that differing levels of expression between wild-type and these transgenic plants could be preventing the rescue of the phenotype.

Together, the complementation results on the male and female sides suggest that the *pcrk1* phenotype in pollen was fully complemented, but the female gametophyte phenotype was only partially complemented (Fig. 2.5, Fig. 2.10). If the complemented pollen of these plants acted like wild type pollen, I would expect the self-pollinated complemented plants to display the POEM phenotype since the female-side did not appear to fully complement. Since it didn't, I believe the pollen may have complemented enough to rescue the suppression of *nta-1* pollen tube overgrowth back to *nta-1* levels, but the expression may have been too dissimilar to behave like wild-type pollen.

The results of my experiments indicate that *pcrk1* mutated on either the female or male side causes pollen tubes to burst more easily during pollen tube reception, even without the female signals of the NORTIA-mediated pollen tube reception pathway. Vanillin staining revealed seed coat staining near the micropylar end of the female gametophyte. This, coupled with the ovule enlargement, resembles the POEM phenotype described in Kasahara et al., 2016. The lack of embryo or endosperm formation in ovules with this phenotype suggests that fertilization does not occur in these ovules. If POEM is occurring in these ovules, the pollen tubes are bursting and releasing pollen tube contents. The ovules enlarge and initiate seed coat formation in response, but fertilization does not occur. Pollen tubes could be seen growing around the female gametophyte of these ovules, suggesting that overgrowth is occurring in these ovules. The absence of

fertilization may be because although the pollen tubes are able to burst, the sperm cells are not released in the correct location to fuse with the egg and central cell.

Not much is known about pollen tube entry to a female gametophyte or its route of growth after entry. It was always thought that the filiform apparatus is a pollen tube's site of entry into the female gametophyte, however, some have reported a site of entry away from the filiform apparatus (Leshem, Johnson & Sundaresan, 2013). It isn't known whether the pollen tube is guided to a specific position before pollen tube bursting in order for the gametes to fuse with the egg and central cell. The central cell has been implicated in micropylar guidance in Arabidopsis (Chen et al., 2007). Specific signals or conditions could be required for guidance of a pollen tube after entering the female gametophyte in order for bursting in the proper place for successful gamete fusion. Sperm cell contact with the female gametes occurs directly before gamete fusion (Mori, Igawa, Tamiya, Miyagishima & Berger, 2014). The gamete fusion in this POEM phenotype could be hindered by the incorrect placement of bursting by these overgrowing pollen tubes.

2.3.4 The Effects of PCRK1 Pollen on other PT Reception Mutant Phenotypes

Mutations in several different genes (discussed in Chapter 1 Section 1.3) cause pollen tube overgrowth. I wanted to test whether the *pcrk1* pollen tube overgrowth suppression and POEM phenotypes are specific to *nta,* or also occur in these other mutants. FER is a synergid-expressed, plasma membrane-localized receptor-like kinase, a member of the CrRLK1L-1 subfamily of protein kinases, and a putative cell wall sensor (Escobar-Restrepo et al., 2007). FER accumulates in the filiform apparatus, a specialized membrane-rich region at the micropylar end of the synergid cells and is recognized as important for releasing signaling molecules to the pollen tube required for successful fertilization (Escobar-Restrepo et al., 2007). FER seems to act upstream of NTA, since redistribution of NTA-GFP is compromised in *fer* mutants (Kessler et al., 2010).

The genetic interaction between PCRK1 and NTA made me curious if I would see a similar genetic interaction with other female pollen tube reception mutants. I wondered whether *pcrk1* pollen would have any effect on the pollen tube overgrowth phenotype of the *fer-4* mutant, which is in the Col-0 ecotype background. I compared crosses of *fer-4*/*fer-4* x Col-0, *fer-4*/*fer-4* x *pcrk1*, Col-0 x *pcrk1*, and Col-0 x Col-0, and found that the *fer-4* x *pcrk1* cross resulted in an aborted-looking large ovule phenotype which resembled the POEM phenotype of a *nta pcrk1* x wild type cross, and that this phenotype occurred at around 25% of ovules (Fig. 2.12, Fig. 2.8). Vanillin staining of these siliques revealed the POEM phenotype in these ovules, which was not observed in a *fer-4* x Col-0 cross (Fig. 2.12). The number of fertilized ovules decreased, as well as the number of unfertilized ovules. This result indicates a genetic interaction between FER and PCRK1 which leads to a change in the *fer-4* pollen tube overgrowth phenotype to include ovules with POEM.

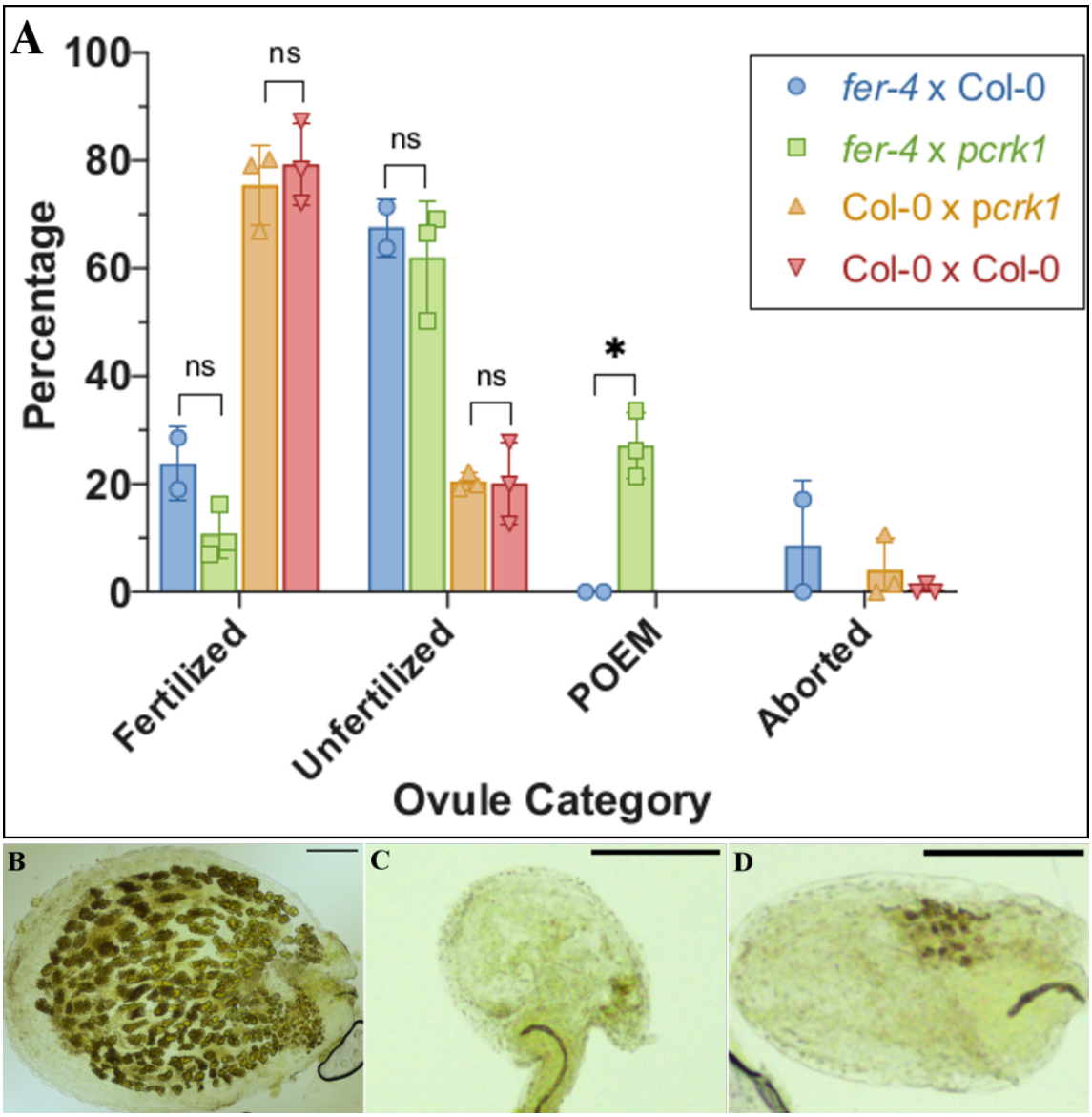

Figure 2.12 *fer-4* Crossed by *pcrk1* Pollen Results in a POEM Phenotype.

(A) Percentage of ovules from each ovule category after manual pollinations. (B-D) Vanillin stained ovules. (B) Fertilized ovule from a *fer-4* x Col-0 cross. (C) Unfertilized ovule from a *fer-4* x Col-0 cross. (D) POEM Phenotype in a *fer-4* x pcrk1 cross. Scale bars: 100µm

fer has been reported to have defects in synergid cell death during pollen tube reception (Ngo, Vogler, Lituiev, Nestorova & Grossniklaus, 2014). Given my observation that *nta pcrk1* ovules crossed by wild type pollen have delayed or absent synergid cell death, I wonder if this parallel between *fer* and *nta pcrk1* ovules is involved in the POEM phenotype seen in both ovule

genotypes. Future experiments could involve a larger quantification of *fer* synergid cell death defects, along with a greater quantification of the frequency of POEM in *fer-4* x *pcrk1* crosses to see if the levels of each correlate with the other.

We also tested whether there was a genetic interaction between the pollen tube reception regulator TURAN and PCRK1. TURAN was previously discussed in Chapter 1, Section 1.3. *turan* mutants are male sterile with an early pollen tube bursting phenotype, therefore, homozygous mutants cannot be acquired (Lindner et al., 2015). Ovules of *turan* mutants have a pollen tube overgrowth phenotype (Lindner et al., 2015). I compared the crosses of *turan*/+ x *turan*/+, *turan*/+ x *pcrk1*, Col-0 x *pcrk1*, and Col-0 x Col-0, and observed that the *turan*/+ x *pcrk1* cross resulted in aborted-looking large ovules which resembled the POEM phenotype seen from a *nta pcrk1* x wild-type cross (Fig. 2.13, Fig. 2.8). I let *turan*/+ plants self-pollinate for my experiment since the ovules will only receive wild-type pollen tubes. Vanillin staining revealed that the POEM phenotype was occurring in these ovules (Fig. 2.13D). This experiment revealed a genetic interaction between TURAN ovules and PCRK1 pollen which leads to a change in the pollen tube overgrowth phenotype. The change in phenotype is similar to the one observed in the *fer-4* x *pcrk1,* and *nta pcrk1* x wild-type crosses. However, this phenotype was not observed from a *nta* x *pcrk1* cross.

This data suggests that *pcrk1* suppresses the absent pollen tube bursting phenotype in *fer-4* and *turan*/*TURAN* ovules. However, an unknown reason prevents successful fertilization of these ovules. My hypothesis for this POEM phenotype was discussed in Section 2.4.3.

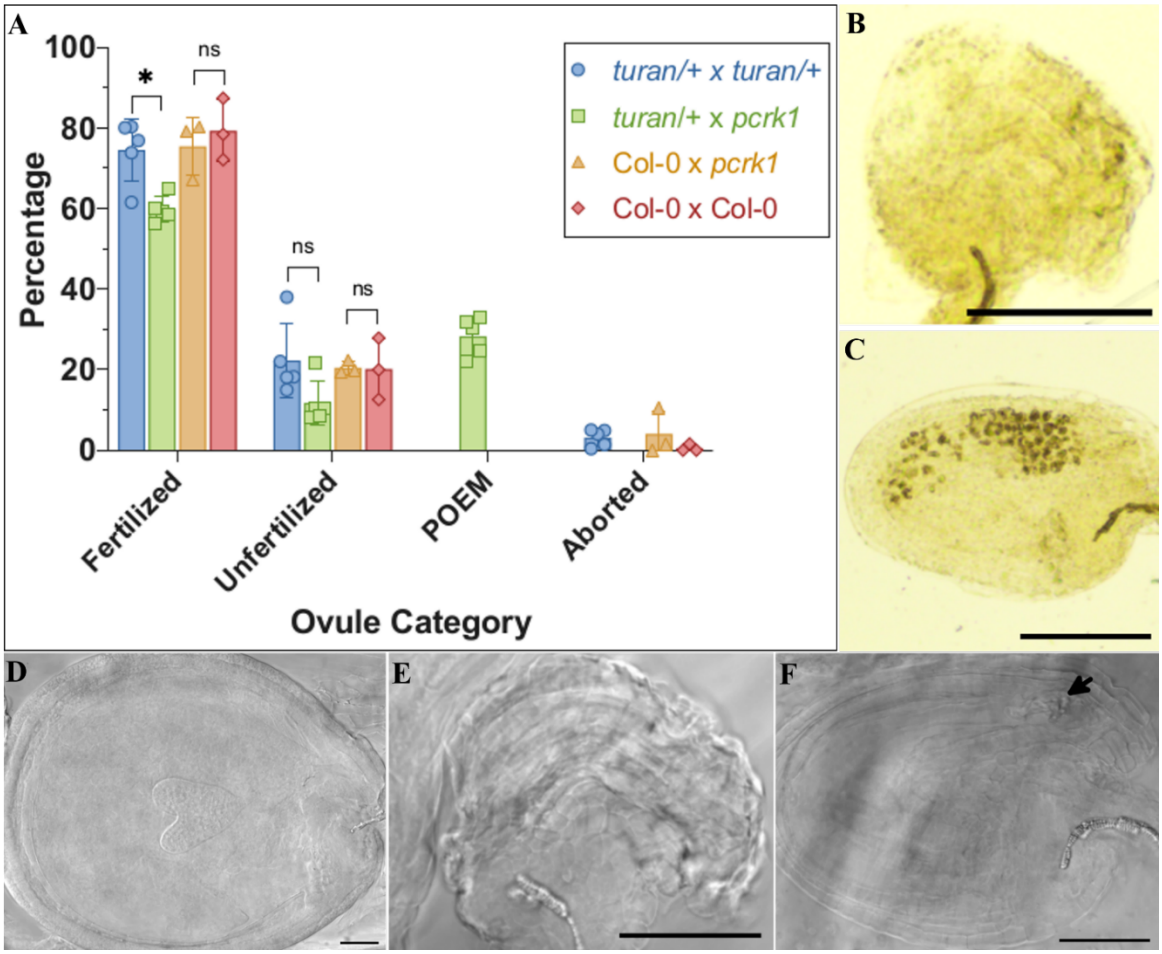

Figure 2.13 *turan* Crossed by *pcrk1* Pollen Results in a POEM phenotype.

(A) Percentages of ovule types from manual pollinations. (A-B) Vanillin staining of ovules at five days after pollination. (B) An unfertilized ovule in a *turan*/TURAN pistil. (C) A POEM phenotype in a *turan*/TURAN x pcrk1 ovule. (D-F) DIC images of ovules at five days after pollination (D) A DIC image of a fertilized ovule at the heart stage of embryo development from a *turan*/TURAN x *pcrk1* cross. (E) An unfertilized ovule from a *turan*/TURAN pistil. (F) POEM phenotype in an ovule from a *turan*/TURAN x *pcrk1* cross. Arrow indicates pollen tube overgrowth while the ovule has no evidence of embryo or endosperm development. Scale bars: 100µM.

2.7 References for Chapter Two

Bent A (2006) Arabidopsis thaliana Floral Dip Transformation Method. In K Wang, ed, Methods in Molecular Biology, Vol 343. Humana Press Inc., Totowa, NJ

Boisson-Dernier, A., Franck, C. M., Lituiev, D. S., & Grossniklaus, U. (2015). Receptor-like cytoplasmic kinase MARIS functions downstream of CrRLK1L-dependent signaling during tip growth. *Proceedings of the National Academy of Sciences*, *112*(39), 12211–12216. doi: 10.1073/pnas.1512375112

BoissonDernier, A., Roy, S., Kritsas, K., Grobei, M.A., Jaciubek, M., Schroeder, J.I., Grossniklaus, U. (2009). Disruption of the pollen-expressed FERONIA homologs ANXUR1 and ANXUR2 triggers pollen tube discharge. Development **136**: 3279–3288.

Chen, Y.-H., Li, H.-J., Shi, D.-Q., Yuan, L., Liu, J., Sreenivasan, R., … Yang, W.-C. (2007). The Central Cell Plays a Critical Role in Pollen Tube Guidance in Arabidopsis. *The Plant Cell*, *19*(11), 3563–3577. doi: 10.1105/tpc.107.053967

Drews, G. N., & Yadegari, R. (2002). Development and Function of the Angiosperm Female Gametophyte. *Annual Review of Genetics*, *36*(1), 99–124. doi: 10.1146/annurev.genet.36.040102.131941

Escobar-Restrepo, J.-M., Huck, N., Kessler, S., Gagliardini, V., Gheyselinck, J., Yang, W.-C., & Grossniklaus, U. (2007). The FERONIA Receptor-like Kinase Mediates Male-Female Interactions During Pollen Tube Reception. *Science*, *317*(5838), 656–660. doi: 10.1126/science.1143562

Kasahara, R. D., Notaguchi, M., Nagahara, S., Suzuki, T., Susaki, D., Honma, Y., … Higashiyama, T. (2016). Pollen tube contents initiate ovule enlargement and enhance seed coat development without fertilization. Science Advances, 2(10). doi: 10.1126/sciadv.1600554

Kasahara, R. D., Portereiko, M. F., Sandaklie-Nikolova, L., Rabiger, D. S., & Drews, G. N. (2005). MYB98 Is Required for Pollen Tube Guidance and Synergid Cell Differentiation in Arabidopsis. The Plant Cell, 17(11), 2981–2992. doi: 10.1105/tpc.105.034603

Kessler, S. A., Shimosato-Asano, H., Keinath, N. F., Wuest, S. E., Ingram, G., Panstruga, R., & Grossniklaus, U. (2010). Conserved Molecular Components for Pollen Tube Reception and Fungal Invasion. *Science*, *330*(6006), 968–971. doi: 10.1126/science.1195211

Kim, Y., Schumaker, K. S., & Zhu, J.-K. (2006). EMS Mutagenesis of *Arabidopsis*. *Arabidopsis Protocols*, 101–104. doi: 10.1385/1-59745-003-0:101

Leshem, Y., Johnson, C., & Sundaresan, V. (2013). Pollen tube entry into the synergid cell of Arabidopsis is observed at a site distinct from the filiform apparatus. *Plant Reproduction*, *26*(2), 93–99. doi: 10.1007/s00497-013-0211-1

Leydon, A. R., Tsukamoto, T., Dunatunga, D., Qin, Y., Johnson, M. A., & Palanivelu, R. (2015). Pollen Tube Discharge Completes the Process of Synergid Degeneration That Is Initiated by Pollen Tube-Synergid Interaction in Arabidopsis. *Plant Physiology*, *169*(1), 485–496. doi: 10.1104/pp.15.00528

Lindner, H., Kessler, S. A., Müller, L. M., Shimosato-Asano, H., Boisson-Dernier, A., & Grossniklaus, U. (2015). TURAN and EVAN Mediate Pollen Tube Reception in Arabidopsis Synergids through Protein Glycosylation. PLOS Biology, 13(4). doi: 10.1371/journal.pbio.1002139

Maruyama, D., Völz, R., Takeuchi, H., Mori, T., Igawa, T., Kurihara, D., … Higashiyama, T. (2015). Rapid Elimination of the Persistent Synergid through a Cell Fusion Mechanism. *Cell*, *161*(4), 907–918. doi: 10.1016/j.cell.2015.03.018

Mori, T., Igawa, T., Tamiya, G., Miyagishima, S.-Y., & Berger, F. (2014). Gamete Attachment Requires GEX2 for Successful Fertilization in Arabidopsis. *Current Biology*, *24*(2), 170–175. doi: 10.1016/j.cub.2013.11.030

Ngo, Q. A., Vogler, H., Lituiev, D. S., Nestorova, A., & Grossniklaus, U. (2014). A Calcium Dialog Mediated by the FERONIA Signal Transduction Pathway Controls Plant Sperm Delivery. *Developmental Cell*, *29*(4), 491–500. doi: 10.1016/j.devcel.2014.04.008

Pereira, A. M., Lopes, A. L., & Coimbra, S. (2016). JAGGER, an AGP essential for persistent synergid degeneration and polytubey block in Arabidopsis. *Plant Signaling & Behavior*, *11*(8). doi: 10.1080/15592324.2016.1209616

Sandaklie-Nikolova, L., Palanivelu, R., King, E. J., Copenhaver, G. P., & Drews, G. N. (2007). Synergid Cell Death in Arabidopsis Is Triggered following Direct Interaction with the Pollen Tube. *Plant Physiology*, *144*(4), 1753–1762. doi: 10.1104/pp.107.098236

Sreekanta, S., Bethke, G., Hatsugai, N., Tsuda, K., Thao, A., Wang, L., … Glazebrook, J. (2015). The receptor-like cytoplasmic kinase PCRK1 contributes to pattern-triggered immunity againstPseudomonas syringaeinArabidopsis thaliana. *New Phytologist*, *207*(1), 78–90. doi: 10.1111/nph.13345

Wang, J.-G., Feng, C., Liu, H.-H., Feng, Q.-N., Li, S., & Zhang, Y. (2017). AP1G mediates vacuolar acidification during synergid-controlled pollen tube reception. *Proceedings of the National Academy of Sciences*, *114*(24). doi: 10.1073/pnas.1617967114

Wuest, S. E., Vijverberg, K., Schmidt, A., Weiss, M., Gheyselinck, J., Lohr, M., … Grossniklaus, U. (2010). Arabidopsis Female Gametophyte Gene Expression Map Reveals Similarities between Plant and Animal Gametes. Current Biology, 20(6), 506–512. doi: 10.1016/j.cub.2010.01.051

CHAPTER 3. CONCLUSIONS AND FUTURE DIRECTIONS

3.1 Introduction

By further elucidating the molecular processes of plant reproduction, scientists can better understand how to breed plants which have improved reproductive success and increased agricultural productivity. Gaining more insight into the process of pollination is valuable for understanding how plants perceive beneficial invasions such as a pollen tube's entrance to an ovule and prevent detrimental ones such as pathogen invasions.

This thesis focused on characterizing the role of PCRK1 in pollen tube reception. Phylogenetic analysis revealed that PCRK1 has two paralogues, PCRK2 and PCRK3 (Rao et al., 2018, Figure 3.1). Paralogues likely originated from a single ancestral gene which underwent a gene duplication event. Gene paralogues may have differences in sequence and their biological functions. As discussed in Chapter 1, they have been reported to function redundantly in pattern-triggered immune responses and in brassinosteroid signaling (Kong et al., 2016; Huang et al., 2019). PCRK1 has been reported as expressed in the central cell of the female gametophyte and in pollen, which matches the results from this research (Wuest et al., 2010; Fig. 2.9A). However, PCRK2 was not reported to be expressed in either the female or male gametophytes from the same study. Interestingly, PCRK3 was reported to be expressed in the synergid cells of the female gametophyte and in pollen (Wuest et al., 2010). Single T-DNA insertion mutants of *pcrk2* and *pcrk3* did not have any fertility defects, nor did double mutants of *pcrk1 pcrk2*. Considering that the synergid cells are highly specialized cells functioning in pollen tube attraction and reception, it is possible that PCRK3 also has a role in pollen tube reception. Though PCRK3 has not been reported to function redundantly with either PCRK1 or PCRK2, PCRK3 and PCRK1 are identical

in sixty percent of their amino acid sequences. Future studies should investigate the role of PCRK2 and PCRK3 in plant reproduction.

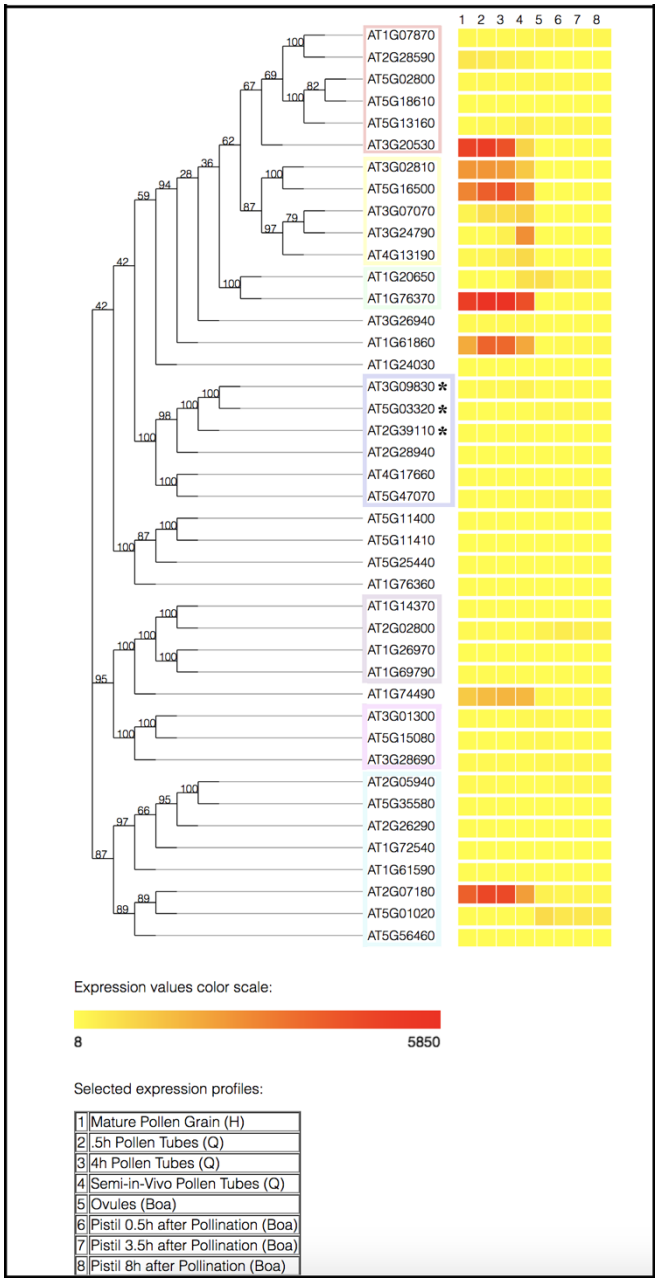

Figure 3.1 Phylogenetic Tree of PCRK1 and Gene Expression Heat Map.

Phylogenetic tree of PCRK1 assembled using aramemnon (http://aramemnon.botanik.uni-koeln.de/) and the Arabidopsis Heat Tree Viewer (http://arabidopsis-heat-tree.org/). * indicate PCRK1 (AT3G09830), PCRK2 (AT5G03320), and PCRK3 (AT2G39110), respectively.

3.2 *pcrk1* Male Gametophytic Suppression of *nta-1* Pollen Tube Overgrowth

In this thesis, I showed that a knockout of PCRK1 in pollen tubes suppresses the pollen tube overgrowth phenotype of *nta-1* mutants. My data suggests that *nta-1* must be mutated in both the female and male gametophyte for *pcrk1* to suppress *nta-1* infertility. This implicates that NTA may have a role in pollen tubes, but a phenotype is not present unless *pcrk1* is mutated as well. Since the mutant *pcrk1* pollen tubes appear to burst more easily and suppress *nta*-1 pollen tube overgrowth, PCRK1 may be involved in negatively regulating pollen tube bursting.

The receptor-like cytoplasmic kinase MARIS functions with many other receptor-like kinases in the pollen tube integrity pathway during pollen tube growth through the transmitting tract (Boisson-Dernier, Franck, Lituiev and Grossniklaus, 2015). Cell wall integrity pathway mutants lead to early pollen tube bursting phenotypes and male sterility (Boisson-Dernier et al., 2009). Ge et al., 2017 hypothesized that this integrity pathway may be switched off as a pollen tube bursting mechanism during pollen tube reception. Since *pcrk1* pollen tubes appear to burst more easily, future experiments should explore whether PCRK1 is a member of the pollen tube integrity pathway. The receptor-like kinases involved in the pollen tube integrity pathway often involve functionally redundant proteins, such as in the case of ANX1/2 and BUPS1/2. Double mutants of these receptor-like kinases are required to see an early pollen tube bursting phenotype. Single *anx1/2* mutants have altered cell walls, but the pollen tubes are still able to grow and fertilize ovules. Similarly, *pcrk1*, *pcrk2,* and *pcrk3* single mutants produce very fertile siliques. A similar situation as in *anx1/2* pollen tube cell walls could be occurring with *pcrk1* pollen tubes. It would make sense if pollen tubes with weaker cell walls are able to burst more easily. PCRK1 and its paralogues, PCRK2 and PCRK3 could be functioning redundantly in the pollen tube integrity pathway. The integrity of the pollen tube cell wall could be influencing the pollen tube's likelihood of bursting after reaching the female gametophyte, leading to a suppression of the pollen tube

overgrowth phenotypes of pollen tube reception mutants such as *nta*. PCRK1 and PCRK3 transcripts are present in the male and female gametophytes (Wuest, 2010). This microarray expression data should be used as a tool but not solely relied upon, since inaccuracies may exist. The fertility of the triple mutant *pcrk1 pcrk2 pcrk3* should be measured to investigate if they are acting functionally redundant in plant reproduction. In addition, mutants or overexpression lines with altered pollen tube cell walls such as in single *anx1/2* mutants, or the overactive version of MARIS, MRI^{R240C} should be crossed to female gametophytic pollen tube reception mutants to investigate whether the altered cell wall integrity has an effect on pollen the tube overgrowth phenotype of pollen tube reception mutants.

PCRK1 has been characterized as a negative regulator of brassinosteroid signaling by inhibiting dephosphorylation of the transcription factor BES1. Dephosphorylated BES1 is its biologically active form which allows it to transcriptionally regulate the expression of genes. *In-vitro* pollen tube growth supplemented with 10µM epibrassinolide showed a five-fold increase in growth rate (Vogler, Schmalzl, Englhart, Bircheneder & Sprunck, 2014). *In-vivo* experiments of the brassinosteroid biosynthesis mutant *cpd* showed pollen tubes were shorter compared to Col-0 in the transmitting tract (Zhang et al., 2018). The BES1 transcription factor regulates CPD. Additionally, brassinosteroids have reported effects on pollen number, viability, and release efficiency (Ye et al., 2010). Another hypothesis for male suppression of pollen tube overgrowth by *pcrk1* is that the upregulation of brassinosteroid signaling in pollen tubes may cause cell wall changes leading to a change in growth due to weaker pollen tube cell walls in *pcrk1*. This may cause suppression of pollen tube overgrowth. Although *pcrk1* pollen tube length in the transmitting tract did not show significant differences 4-8 hours after pollination, it did show a significant

difference at 2 hours after pollination (Fig. 2.4). The experiment should be repeated with a higher sample size with some samples in a *nta-1* background in order to make strong conclusions.

Interestingly, *pcrk1* pollen tubes crossed with *fer* and *turan* female gametophytes resulted in a POEM phenotype. I believe that *pcrk1* pollen tubes are suppressing by bursting more easily in *fer* ovules, but an unknown barrier is preventing fertilization of some ovules. Hypotheses for this were discussed in Chapter 2, Section 2.4.3.

3.3 PCRK1's Role in the Female Gametophyte

PCRK1 functions in the female gametophyte during pollen tube reception. The female transmission efficiency result suggests that PCRK1 has a role in regulating pollen tube bursting from the female gametophyte and can suppress the *nta-1* pollen tube overgrowth phenotype. Similar to *pcrk1* suppression of *nta* pollen tube overgrowth in the male gametophyte, these results indicate that *nta-1* must be mutated in both the female and male gametophytes for the suppression of *nta-1* infertility. When *nta pcrk1* is crossed to wild-type pollen, a POEM phenotype is observed. It appeared that delayed or absent synergid cell death was observed in *nta pcrk1* x Ws ovules, although I was unable to tell if a pollen tube had reached those ovules using that method. In addition, putative autofluorescence and a strange synergid shape provided evidence of early synergid cell death in Col-0 plants transformed with PCRK-GFP under its native promoter. I believe this could be an overexpression phenotype. This could be tested using the CLSM method from Christensen, 1997 on PCRK1-GFP in Col-0 emasculated ovules compared to Col-0 ovules. Future experiments such as this should address whether PCRK1 regulates synergid cell death in the female gametophyte.

The POEM phenotype observed in *nta pcrk1* x wild-type crosses indicates that the pollen tubes are bursting, but another unknown barrier prevents fertilization of the ovule. Considering

that the pollen tubes are bursting, it was surprising to still observe pollen tube overgrowth in these ovules. Pollen tube bursting appears successful, but the pollen tubes are still growing around the female gametophyte. It's possible that the bursting is severely delayed, or a signal to slow pollen tube growth at the micropyle is not being received. Another possibility involves PCRK1's role in negative regulation of brassinosteroid (BR) signaling as discussed in Section 3.2. If PCRK1's negative regulation of BR signaling is involved in its role in reproduction, I would expect an increase in BR signaling in *pcrk1* mutant plants in both the male and female gametophytes. I discussed possible effects on the male gametophyte in Section 3.2. If BR signaling is important at the micropyle of the female gametophyte, it could affect pollen tubes in a similar way as my hypothesis for the male gametophyte, but the effects on pollen tube growth may be more delayed, with a delayed bursting effect. Overgrowth is sometimes observed extending beyond the egg apparatus region in these ovules. As discussed in Chapter 2, I believe the overgrowth part of this phenotype may be causing the fertilization failure. The sperm cells may not be released in the correct place to fuse with the egg and central cell.

3.4 Parallels Between Plant Pathogen Defense and Reproduction: Receptor-Like Cytoplasmic Kinases

Shared molecular components of pollen tube reception and pathogen invasion have been reported (Kessler et al., 2010). The discovery that the pattern triggered immunity regulator PCRK1 also functions in pollen tube reception uncovers another link between plant pathogen defense and pollen tube reception. *pcrk1* mutants are more susceptible to pathogen invasion (Sreekanta et al., 2015). However, *pcrk1* gives a reproductive advantage in some cases, such as when NORTIA is knocked out. This reveals another gene with a potential trade-off between pathogen defense and fertility. Similarly, potential trade-offs exist in the roles of FERONIA in pollen tube reception and

powdery mildew susceptibility (Kessler et al., 2010). Considering that both PCRK1 and FERONIA are regulators of the pollen tube reception pathway from the female side, and both associate with the PRR FLS2 in the immune signaling pathway, future studies should investigate whether they function in the same pathway during pollen tube reception.

The role of PCRK1 in plant reproduction was masked by the high fertility in single mutant plants. Only when coupled with *nta-1* were we able to observe its effects on pollen tube reception. PCRK1 may be functioning redundantly with other RLCKs in plant reproduction, which is why double mutants could be required to observe a fertility phenotype. Given this discovery of the RLCK member PCRK1 functioning in the female and male gametophytes during pollen tube reception, future investigations should explore the role of phylogenetically related RLCKs in plant reproduction. Publicly available microarray data shows other RLCKs in subfamily VII expressed in the female and male gametophytes (Table 3.1). Many of these genes have reported roles in plant pathogen defense. It will be interesting to see if these RLCKs of subfamily VII also have roles in plant reproduction.

By studying the links between fertility and disease in plants, such as the shared roles of FERONIA and MLOs in powdery mildew susceptibility and pollen tube reception, we may be able to uncover important implications in potential trade-offs with fertility when breeding for pathogen resistance. In this thesis, another gene described in pathogen defense, *PCRK1*, was identified to have roles in pollen tube reception from both the male and female gametophytes.

Table 3.1 Microarray Data of RLCK Subfamily VII in the Male and Female Gametophytes (Modified from Wuest et al., 2010).

Name	Gene #	Synergid	Egg	Central Cell	Sperm	Pollen
PBL5	AT1G07870.2	M	M	P	M	M
PBL6	AT2G28590.1	M	P	P	A	P
PBS1	AT5G13160.1	A	M	M	M	P
PBL27	AT5G18610.1	A	A	A	A	A
PBL41	AT1G61850.1	P	P	P	P	P
PBL23	AT3G20530.1	A	A	A	A	P
LIP2	AT3G02810.1	A	A	A	A	P
LIP1	AT5G16500.1	A	A	A	A	P
PBL26	AT3G07070.1	A	A	A	A	P
PBL25	AT3G24790.1	A	A	P	A	A
PBL24	AT4G13190.1	P	P	P	P	P
PBL21	AT1G20650.1	A	A	A	A	A
PBL22	AT1G76370.1	A	A	A	P	P
CDG1	AT3G26940.1	A	A	A	M	P
PBL26	AT1G24030.1	A	A	A	A	A
PCRK1	AT3G09830	A	A	M	A	P
PCRK2	AT5G03320	A	A	A	A	A
PCRK3	AT2G39110	M	P	A	A	M
PBL37	AT2G28940	A	A	A	A	A
PBL19	AT5G47070.1	A	A	A	A	A
PBL20	AT4G17660.1	A	A	A	A	A
PBL36	AT3G26890.2	P	P	P	P	P
PBL35	AT3G01300.1	ND	ND	ND	ND	ND
PBL34	AT5G15080.1	ND	ND	ND	ND	ND
PBL17	AT2G07180.1	M	P	P	P	A
PBL16	AT5G56460.1	A	A	A	A	A
PBL8	AT5G01020.1	A	P	P	A	A
PBL15	AT1G61590.1	A	A	A	A	A
PBL33	AT1G72540.1	A	A	A	A	A
PBL12	AT2G26290.1	A	A	A	A	A
PBL14 (RIPK)	AT2G05940.1	A	A	A	A	A
PBL13	AT5G35580	A	A	A	A	A
PBL30 (CST)	AT4G35600.2	A	A	A	P	A
PBL31	AT1G76360.1	A	A	A	A	A
PBL32	AT2G17220.1	A	A	A	A	A
PBL9	AT1G07570.3	A	A	A	A	A
PBL10	AT2G28930.1	A	A	A	A	A
PBL11	AT5G02290.2	M	A	A	A	P
BIK1	AT2G39660.1	A	A	M	A	M
PBL1	AT3G55450.2	A	M	A	A	A
PBL29	AT1G74490	M	M	A	P	P
PBL2	AT1G14370.1	A	A	A	A	A
PBL3	AT2G02800.1	A	A	A	A	A
PBL18	AT1G69790	A	A	A	A	A
PBL4	AT1G26970	A	A	A	A	A

Letters indicate Present (P), Absent (A), and Maybe (M) for each column category. Colors correspond to clades from Figure 3.1.

3.5 References for Chapter 3

Boisson-Dernier, A., Franck, C. M., Lituiev, D. S., & Grossniklaus, U. (2015). Receptor-like cytoplasmic kinase MARIS functions downstream of CrRLK1L-dependent signaling during tip growth. *Proceedings of the National Academy of Sciences*, *112*(39), 12211–12216. doi: 10.1073/pnas.1512375112

Boisson-Dernier, A., Roy, S., Kritsas, K., Grobei, M. A., Jaciubek, M., Schroeder, J. I., & Grossniklaus, U. (2009). Disruption of the pollen-expressed FERONIA homologs ANXUR1 and ANXUR2 triggers pollen tube discharge. *Development*, *136*(19), 3279–3288. doi: 10.1242/dev.040071

Huang, G. Sun, J., Bai, J., Han, Y., Fan, F., Wang, S., … Lu, D. (2019) Identification of critical cysteine sites in brassinosteroid-insensitive 1 and novel signaling regulators using a transient expression system. *New Phytologist*. 222(3), 1405-1419. Doi:10.11

Kessler, S. A., Shimosato-Asano, H., Keinath, N. F., Wuest, S. E., Ingram, G., Panstruga, R., & Grossniklaus, U. (2010). Conserved Molecular Components for Pollen Tube Reception and Fungal Invasion. *Science*, *330*(6006), 968–971. doi: 10.1126/science.1195211

Kong, Q., Sun, T., Qu, N., Ma, J., Li, M., Cheng, Y.-T., … Zhang, Y. (2016). Two redundant receptor-like cytoplasmic kinases function downstream of pattern recognition receptors to regulate activation of SA biosynthesis in Arabidopsis. *Plant Physiology*. Doi: 10.1104/pp.15.01954

Lindner, H., Kessler, S. A., Müller, L. M., Shimosato-Asano, H., Boisson-Dernier, A., & Grossniklaus, U. (2015). TURAN and EVAN Mediate Pollen Tube Reception in Arabidopsis Synergids through Protein Glycosylation. PLOS Biology, 13(4). doi: 10.1371/journal.pbio.1002139

Rao, S., Zhou, Z., Miao, P., Bi, G., Hu, M., Wu, Y., … Zhou, J.-M. (2018). Roles of receptor-like cytoplasmic kinase VII members in pattern-triggered immune signaling. *Plant Physiology*. doi: 10.1104/pp.18.00486

Sreekanta, S., Bethke, G., Hatsugai, N., Tsuda, K., Thao, A., Wang, L., … Glazebrook, J. (2015). The receptor-like cytoplasmic kinase PCRK1 contributes to pattern-triggered immunity againstPseudomonas syringaeinArabidopsis thaliana. *New Phytologist*, *207*(1), 78–90. doi: 10.1111/nph.13345

Vogler, F., Schmalzl, C., Englhart, M., Bircheneder, M., & Sprunck, S. (2014). Brassinosteroids promote Arabidopsis pollen germination and growth. *Plant Reproduction*, *27*(3), 153–167. doi: 10.1007/s00497-014-0247-x

Wuest, S. E., Vijverberg, K., Schmidt, A., Weiss, M., Gheyselinck, J., Lohr, M., … Grossniklaus, U. (2010). Arabidopsis Female Gametophyte Gene Expression Map Reveals Similarities between Plant and Animal Gametes. Current Biology, 20(6), 506–512. doi: 10.1016/j.cub.2010.01.051

Ye, Q., Zhu, W., Li, L., Zhang, S., Yin, Y., Ma, H., & Wang, X. (2010). Brassinosteroids control male fertility by regulating the expression of key genes involved in Arabidopsis anther and pollen development. *Proceedings of the National Academy of Sciences*, *107*(13), 6100–6105. doi: 10.1073/pnas.0912333107

Zhang, T., Xu, P., Wang, W., Wang, S., Caruana, J. C., Yang, H.-Q., & Lian, H. (2018). Arabidopsis G-Protein β Subunit AGB1 Interacts with BES1 to Regulate Brassinosteroid Signaling and Cell Elongation. *Frontiers in Plant Science*, *8*. doi: 10.3389/fpls.2017.02225

Figure 2.1 Unfertilized Ovule Percentages in a Segregating Enhancer Line ntaE-14E-6 Population Compared to nta-1											
Seed Number	**Genotype**	**Fertilized**	**Unfertilized**	**Aborted**	**% Infertile**						
RDF240-7	***nta/nta***	62	10		13.889						
		60	15		20						
		46	25		35.211						
		60	13		17.808						
Average					**21.727**						
RDF240-8	***nta/nta***	60	7	1	10.294						
		53	13		19.697						
		58	14		19.444						
		28	32		53.333						
Average					**25.692**						
RDF240-9	***nta/nta***	47	25		34.722						
		51	12	1	18.75						
		52	11		17.46						
		58	16		21.622						
Average					**23.139**						
RDF240-11	***nta/nta***	59	7		10.606						
		55	13		19.118						
		57	11		16.176						
		42	29		40.845						
Average					**21.686**						
RDF240-12	***nta/nta***	62	11		15.068						
		53	19		26.389						
		64	9		12.329						
		53	16		23.188						
Average					**19.244**						

RDF245-2	**ntaE-14E-6 (From ELK6-3 BC2 ⊗)**	43	29		40.278						
		45	30		40						
		40	39		49.367						
		55	17		23.611						
		51	36		41.379						
Average					**38.927**						
RDF245-3	**ntaE-14E-6 (From ELK6-3 BC2 ⊗)**	51	56		52.336						
		31	40		56.338						
		34	41		54.667						
		42	35		45.455						
		39	12		23.529						
Average					**46.465**						
RDF245-4	**ntaE-14E-6 (From ELK6-3 BC2 ⊗)**	53	23		30.263						
		46	35		43.21						
		64	15		18.987						
		63	11		14.865						
Average					**26.831**						
RDF245-7	**ntaE-14E-6 (From ELK6-3 BC2 ⊗)**	36	37		50.685						
		54	16		22.857						
		43	30		41.096						
		61	13		17.568						
Average					**33.051**						
RDF245-9	**ntaE-14E-6 (From ELK6-3 BC2 ⊗)**	48	28		36.842						
		53	24		31.169						
		50	24		32.432						
		48	23		32.394						
Average					**33.209**						
RDF245-10	**ntaE-14E-6 (From ELK6-3 BC2 ⊗)**	57	22		27.848						
		53	22		29.333						
		62	18		22.5						

		61	24		28.235						
Average			=		**26.979**						
RDF245-11	**ntaE-14E-6 (From ELK6-3 BC2 ⊗)**	38	33		46.479						
		54	26		32.5						
		59	18		23.377						
		56	25		30.864						
Average			=		**33.305**						
RDF245-14	**ntaE-14E-6 (From ELK6-3 BC2 ⊗)**	55	12		17.91						
		49	22	1	30.556						
		53	18		25.352						
		52	25		32.468						
Average					**26.571**						
RDF245-15	**ntaE-14E-6 (From ELK6-3 BC2 ⊗)**	31	43	1	57.333						
		37	42		53.165						
		36	41		53.247						
		36	48		57.143						
Average		=			**55.222**						
RDF245-20	**ntaE-14E-6 (From ELK6-3 BC2 ⊗)**	53	20		27.397						
		54	22	1	28.571						
		56	21		27.273						
		58	17	1	22.368						
Average					**26.402**						
RDF245-21	**ntaE-14E-6 (From ELK6-3 BC2 ⊗)**	28	36	1	55.385						
		26	44	1	61.972						
		36	36		50						
		34	36	1	50.704						
Average					**54.515**						
RDF245-22	**ntaE-14E-6 (From ELK6-3 BC2 ⊗)**	34	38	2	51.351						
		41	34	4	43.038						
		39	28	2	40.58						

		35	41	1	53.247						
Avg					**47.054**						
Figure 2.2 Percentage of Unfertilized Ovules in T-DNA Insertion Lines of the Enhancer Candidates											
Seed Number	**Genotype**	**Fertilized**	**Unfertilized**	**Aborted**	**% Infertile**						
RDF 14-5	**Col-0**	56	3		5.0847						
		54	3		5.2632						
		59	0		0						
		57	0		0						
Average					**2.587**						
RDF 14-7	**Col-0**	54	3		5.2632						
		54	0		0						
		64	0		0						
		43	9		17.308						
Average					**5.6427**						
RDF8-2	**Homozygous *pcrk1* (SALK_145629)**	55	9	1	13.846						
		60	10		14.286						
		65	3	1	4.3478						
		61	6		8.9552						
		62	2		3.125						
Average					**8.912**						
RDF 8-4	**Homozygous *pcrk1* (SALK_145629)**	57	5		8.0645						
		57	6	2	9.2308						
		72	1		1.3699						
		63	0		0						

		68	2		2.8571						
Average					**4.3045**						
RDF11-8	**Heterozygous SALK_014609**	54	0		0						
		57	2		3.3898						
		60	0		0						
		54	3		5.2632						
		45	6		11.765						
Average					**4.0835**						
RDF12-16	**Homozygous SALK_036970**	54	2		3.5714						
		57	0		0						
		52	0		0						
		56	0		0						
		56	0		0						
Average					**0.7143**						
RDF 13-1	**Heterozygous *rrp5* CS735776(GK_834C08)**	12	51		80.952						
		18	47		72.308						
		38	32		45.714						
		49	10		16.949						
		43	20		31.746						
Average					**49.534**						
RDF 13-10	**Heretozygous *rrp5* CS735776(GK_834C08)**	15	33		68.75						
		24	40		62.5						
		24	26		52						
		29	25		46.296						
Average					**57.387**						
RDF10-5	**SALK_142406C**	40	14		25.926						
		39	7	4	14						
		41	11	1	20.755						

		45	9	1	16.364						
		42	8	2	15.385						
Average					**18.486**						
Figure 2.3A pcrk1 Pollen Suppresses nta-1 Pollen Tube Overgrowth.											
RDF106-1	**Col-0**	53	2		3.6364						
		60	0		0						
		63	0		0						
		62	0		0						
Average					**0.9091**						
RDF121-3	**Col-0**	53	1		1.8519						
		53	0		0						
		51	2		3.7736						
		56	0		0						
		53	0		0						
		46	0		0						
Average					**0.9376**						
RDF121-4	**Col-0**	49	0		0						
		51	1		1.9231						
		48	0		0						
		44	1		2.2222						
Average					**1.0363**						
RDF121-2	**Col-0**				5.085						
					5.263						
					0						
					0						
Average					**2.587**						
RDF162-1	**Ws**	59	20		25.316						
		64	15		18.987						
		67	11		14.103						
		50	25		33.333						

		66	6		8.3333						
Average					**20.015**						
RDF162-2	**Ws**	61	7		10.294						
		65	6		8.4507						
		57	11		16.176						
		47	23		32.857						
		65	6		8.4507						
Average					**15.246**						
RDF162-3	**Ws**	66	13		16.456						
		51	17		25						
		38	39		50.649						
		65	17		20.732						
		61	18		22.785						
Average					**27.124**						
RDF162-4	**Ws**	64	7		9.8592						
		39	29		42.647						
		60	15		20						
		62	12		16.216						
		68	8		10.526						
RDF108-2	***pcrk1***	55	2		3.5088						
		68	0		0						
		64	0		0						
		64	1		1.5385						
Average					**1.2618**						
RDF108-4	***pcrk1***	59	0		0						
		60	0		0						
		58	0		0						
		57	1		1.7241						
Average					**0.431**						
RDF8-5	***pcrk1***	61	0		0						

		61	1		1.6129						
		57	0		0						
		55	2		3.5088						
Average					**1.2804**						
RDF8-8	***pcrk1***	61	2		3.1746						
		65	0		0						
		62	2		3.125						
		63	1		1.5625						
		67	0		0						
Average					**1.1719**						
RDF107-1	***nta-1/nta-1***	43	17		28.333						
		44	14	2	23.333						
		45	11		19.643						
		45	14		23.729						
Average					**23.76**						
RDF107-2	***nta-1/nta-1***	25	35		58.333						
		43	18	2	28.571						
		39	25		39.063						
		45	13	1	22.034						
Average					**37**						
RDF107-3	***nta-1/nta-1***	48	12	1	19.672						
		43	18	1	29.032						
		42	18		30						
		38	17		30.909						
Average					**27.403**						
RDF107-4	***nta-1/nta-1***	40	16	1	28.07						
		41	26		38.806						
		47	14		22.951						
Average					**29.942**						
RDF97-1	***nta/nta pcrk1/pcrk1***	44	18		29.032						

		36	24		40						
		46	13		22.034						
		48	18		27.273						
		57	3		5						
Average					**24.668**						
RDF97-3	***nta/nta pcrk1/pcrk1***	51	13		20.313						
		58	9		13.433						
		57	10		14.925						
		58	7		10.769						
Average					**14.86**						
RDF97-2	***nta/nta pcrk1/pcrk1***	58	7		10.769						
		49	13	3	20						
		53	11	1	16.923						
		60	6	1	8.9552						
Average					**14.162**						
RDF97-5	***nta/nta pcrk1/pcrk1***	42	22		34.375						
		57	12		17.391						
		49	19		27.941						
		51	10		16.393						
Average					**24.025**						
RDF98-4	***nta/nta* PCRK1/*pcrk1***	52	10		16.129						
		48	13	1	20.968						
		56	6		9.6774						
		55	10	1	15.152						
		53	10		15.873						
Average					**15.56**						
RDF98-5	***nta/nta* PCRK1/*pcrk1***	57	9	2	13.235						
		50	7	1	12.069						
		41	16		28.07						
		54	4	6	6.25						

		51	6	3	10						
Average					**13.925**						
RDF98-6	***nta/nta* PCRK1/*pcrk1***	50	9	1	15						
		56	8		12.5						
		61	5	1	7.4627						
		58	5	2	7.6923						
		64	1		1.5385						
Average					**8.8387**						
RDF98-8	***nta/nta* PCRK1/*pcrk1***	54	1		1.8182						
		56	2		3.4483						
		52	5	2	8.4746						
		51	3	1	5.4545						
		52	5		8.7719						
Average		**Fertiliz ed**	**Unferili zed**	**Aborted**	**5.5935**						
Figure 2.3C					**Unfer**						
RDF236-13	***nta-1* x Col-0**	36	25	4	38.462						
		37	24		39.344						
		38	23	2	36.508						
Average					**38.105**						
236-14	***nta-1* x Col-0**	34	19		35.849						
		31	30		49.18						
		35	18		33.962						
		33	24		42.105						
		30	26		46.429						
		33	24		42.105						
Average					**41.605**						
RDF236-13	***nta-1* x Col-0**	35	28		44.444						
		28	31	4	49.206						
		36	25	2	39.683						

		29	37	5	52.113						
Average					**46.362**						
239-5	***nta-1* x *pcrk1***	37	22	1	36.667						
		34	22		39.286						
		28	23	1	44.231						
		32	15		31.915						
Average					**38.025**						
239-6	***nta-1* x *pcrk1***	49	21		30						
		40	24	3	35.821						
		35	31	2	45.588						
		36	37		50.685						
Average					**40.524**						
Figure 2.6A One Half of T1 Plants Have High Percentages of Unfertilized Ovules Due to Defective Embryo Sacs											
		Fertiliz	**Unfertil**	**Unfertil**							
Seed Number	**Genotype**	**ed**	**ized**	**ized %**							
RDF160-1	***nta-1/nta-1***	56	23	29.114							
		35	43	55.128							
		63	15	19.231							
		56	25	30.864							
		57	22	27.848							
Average				**32.437**							
RDF160-2	***nta-1/nta-1***	55	28	33.735							
		48	35	42.169							
		57	30	34.483							
		57	25	30.488							
		54	24	30.769							
Average				**34.329**							
RDF160-3	***nta-1/nta-1***	32	38	54.286							
		42	25	37.313							

		45	30	40							
		45	23	33.824							
		53	19	26.389							
Average				**38.362**							
RDF160-4	***nta-1/nta-1***	44	27	38.028							
		37	37	50							
		63	13	17.105							
		53	15	22.059							
		58	20	25.641							
Average				**30.567**							
RDF169-1	***nta pcrk1*** **homozygous**	44	20	31.25							
		57	10	14.925							
		54	14	20.588							
		56	12	17.647							
		64	4	5.8824							
Average				**18.059**							
RDF169-2	***nta pcrk1*** **homozygous**	52	9	14.754							
		46	9	16.364							
		46	12	20.69							
		44	7	13.725							
		45	5	10							
Average				**15.107**							
RDF169-3	***nta pcrk1*** **homozygous**	50	22	30.556							
		49	12	19.672							
		50	17	25.373							
		43	19	30.645							
		57	12	17.391							
Average				**24.727**							
RDF169-4	***nta pcrk1*** **homozygous**	47	8	14.545							
		50	10	16.667							

		57	7	10.938							
		46	7	13.208							
		48	8	14.286							
Average				**13.929**							
RDF171-1	***nta pcrk1* dipped with pRDF17-1 (pPCRK1::PCRK1-GFP)**	58	8	12.121							
		59	8	11.94							
		59	9	13.235							
		60	9	13.043							
		71	5	6.5789							
Average				**11.384**							
RDF171-2	***nta pcrk1* dipped with pRDF17-1 (pPCRK1::PCRK1-GFP)**	26	43	62.319							
		13	55	80.882							
		25	44	63.768							
		26	49	65.333							
		15	56	78.873							
Average				**70.235**							
RDF171-3	***nta pcrk1* dipped with pRDF17-1 (pPCRK1::PCRK1-GFP)**	30	43	58.904							
		14	60	81.081							
		25	46	64.789							
		24	49	67.123							
		43	27	38.571							
Average				**62.094**							
RDF171-4	***nta pcrk1* dipped with pRDF17-1 (pPCRK1::PCRK1-GFP)**	51	15	22.727							
		56	22	28.205							
		56	21	27.273							
		63	26	29.213							

		67	12	15.19							
Average				**24.522**							
RDF171-5	***nta pcrk1* dipped with pRDF17-1 (pPCRK1::PCRK1-GFP)**	62	22	26.19							
		59	22	27.16							
		68	12	15							
		71	15	17.442							
		71	14	16.471							
Average				**20.453**							
RDF171-6	***nta pcrk1* dipped with pRDF17-1 (pPCRK1::PCRK1-GFP)**	44	29	39.726							
		61	13	17.568							
		58	18	23.684							
		61	12	16.438							
		65	12	15.584							
Average				**22.6**							
RDF171-7	***nta pcrk1* dipped with pRDF17-1 (pPCRK1::PCRK1-GFP)**	28	37	56.923							
		23	51	68.919							
		22	58	72.5							
		19	53	73.611							
		18	54	75							
Average				**69.391**							
RDF171-9	***nta pcrk1* dipped with pRDF17-1 (pPCRK1::PCRK1-GFP)**	53	15	22.059							
		67	5	6.9444							
		62	8	11.429							
		56	15	21.127							
		63	11	14.865							
Average				**15.285**							

RDF171-10	***nta pcrk1* dipped with pRDF17-1 (pPCRK1::PCRK1-GFP)**	60	19	24.051							
		56	25	30.864							
		57	21	26.923							
		56	26	31.707							
		59	21	26.25							
Average				**27.959**							
RDF162-1	**Ws**	59	20	25.316							
		64	15	18.987							
		67	11	14.103							
		50	25	33.333							
		66	6	8.3333							
Average				**20.015**							
RDF162-2	**Ws**	61	7	10.294							
		65	6	8.4507							
		57	11	16.176							
		47	23	32.857							
		65	6	8.4507							
Average				**15.246**							
RDF162-3	**Ws**	66	13	16.456							
		51	17	25							
		38	39	50.649							
		65	17	20.732							
		61	18	22.785							
Average				**27.124**							
RDF162-4	**Ws**	64	7	9.8592							
		39	29	42.647							
		60	15	20							
		62	12	16.216							
		68	8	10.526							

Average				**19.85**							
RDF171-8	***nta pcrk1* dipped with pRDF17-1 (pPCRK1::PCRK1-GFP)**	24	29	54.717							
		23	23	50							
		28	19	40.426							
		22	28	56							
		22	28	56							
Average				**51.429**							
Figure 2.7 pPCRK1::PCRK1-GFP Complements the *nta-1* Suppression Phenotype of *nta-1 pcrk1* Pollen											
Plant	**Genotype**	**Unfertilized**	**Fertilized**	**Aborted**	**% Infertile**						
Yan513-1 x Yan513-1	***nta x nta***	35	42	0	54.545						
		29	41	0	58.571						
		34	44	0	56.41						
		26	37	4	55.224						
Average					**56.188**						
Yan513-2 x Yan513-2	***nta x nta***	44	24	0	35.294						
		38	33	0	46.479						
		38	33	0	46.479						
		34	35	0	50.725						
		34	27	4	41.538						
Average					**44.103**						
Yan513-4 x Yan513-4	***nta x nta***	35	42	0	54.545						
		47	27	0	36.486						
		33	38	0	53.521						

		20	47	0	70.149						
Average					**53.676**						
Yan513-9 x Yan513-9	***nta x nta***	27	40	0	59.701						
		34	39	0	53.425						
		18	51	0	73.913						
		30	34	0	53.125						
		23	46	0	66.667						
Average					**61.366**						
Yan513-9 x RDF205-2*	***nta* x *nta pcrk1* with PCRK1::PCRK1-GFP T2 homozygous**	24	43	0	64.179						
***Line 1 in Figure**		28	46	0	62.162						
		29	37	0	56.061						
		27	42	0	60.87						
		33	39	0	54.167						
Average					**59.488**						
Yan513-4 x RDF205-15*	***nta* x *nta pcrk1* with PCRK1::PCRK1-GFP T2 homozygous**	47	32	1	40						
***Line 1 in Figure**		36	26	16	33.333						
		33	38	0	53.521						
		36	39	0	52						
		35	35	0	50						
Average					**45.771**						
Yan513-2 x RDF205-7*	***nta* x *nta pcrk1* with PCRK1::PCRK1-GFP T2 homozygous**	39	31	0	44.286						

***Line 1 in Figure**		40	32	0	44.444						
		40	26	0	39.394						
		18	47	0	72.308						
		23	48	0	67.606						
Average					**53.607**						
Yan513-3 x RDF205-14*	***nta* x *nta pcrk1* with PCRK1::PCRK1-GFP T2 homozygous**	38	27	0	41.538						
***Line 1 in Figure**		36	33	0	47.826						
		32	37	0	53.623						
		28	36	0	56.25						
		12	50	0	80.645						
Average					**55.977**						
Yan513-8 x RDF204-3*	***nta* x *nta pcrk1* with PCRK1::PCRK1-GFP T2 homozygous**	38	27	0	41.538						
***Line 2 in Figure**		44	22	0	33.333						
		20	47	0	70.149						
		26	41	0	61.194						
		10	48	0	82.759						
Average					**57.795**						
Yan513-7 x RDF204-6*	***nta* x *nta pcrk1* with PCRK1::PCRK1-GFP T2 homozygous**	32	24	0	42.857						
***Line 2 in Figure**		32	24	5	39.344						
		34	24	2	40						

		31	30	0	49.18						
		16	46	0	74.194						
Average					**49.115**						
Yan513-5 x RDF204-8*	***nta* x *nta pcrk1* with PCRK1::PCRK1-GFP T2 homozygous**	23	35	1	59.322						
***Line 2 in Figure**		21	34	1	60.714						
		21	34	0	61.818						
		13	46	0	77.966						
		0	53		100						
Average					**71.964**						
Yan513-5 x RDF204-10*	***nta* x *nta pcrk1* with PCRK1::PCRK1-GFP T2 homozygous**	35	27	2	42.188						
***Line 2 in Figure**		39	22	0	36.066						
		30	33	0	52.381						
		35	26	0	42.623						
		42	21	0	33.333						
Average					**41.318**						
Yan513-8 x RDF206-6*	***nta* x *nta pcrk1* with PCRK1::PCRK1-GFP T2 homozygous**	35	30	0	46.154						
***Line 3 in Figure**		15	34	0	69.388						
		19	31	0	62						
		30	26	0	46.429						
		18	31	0	63.265						
Average					**57.447**						

Yan513-2 x RDF206-8*	***nta* x *nta pcrk1* with PCRK1::PCRK1-GFP T2 homozygous**	30	30	0	50						
***Line 3 in Figure**		25	34	1	56.667						
		33	33	0	50						
		20	35	0	63.636						
		10	47	0	82.456						
Average					**60.552**						
Yan513-1 x RDF206-16*	***nta* x *nta pcrk1* with PCRK1::PCRK1-GFP T2 homozygous**	30	31	0	50.82						
***Line 3 in Figure**		30	27	0	47.368						
		25	30	1	53.571						
		23	32	0	58.182						
		20	37	0	64.912						
Average					**54.971**						
Yan513-1 x 209-10*	***nta* x *nta pcrk1* with PCRK1::PCRK1-GFP T2 homozygous**	37	30	0	44.776						
***Not included in figure**		44	21	0	32.308						
		28	27	0	49.091						
		38	27	0	41.538						
		29	33	0	53.226						
Average					**44.188**						
Figure 2.10 *nta pcrk1* Female-Side Phenotype is Partially Complemented by pPCRK1::PCRK1-GFP											

Plant	Genotype	Unfertilized	Fertilized	Aborted	% Infertile						
Yan513-1⊗	***nta-1/nta-1***	24	50		67.568						
		40	39		49.367						
		48	18		27.273						
		48	21		30.435						
		40	37		48.052						
Average					**44.539**						
Yan513-2 ⊗	***nta-1/nta-1***	45	24		34.783						
		44	27		38.028						
		39	21		35						
		35	27		43.548						
		50	23		31.507						
Average					**36.573**						
Yan513-4⊗	***nta-1/nta-1***	30	39		56.522						
		18	52		74.286						
		54	19		26.027						
		51	25		32.895						
		48	35		42.169						
Average					**46.38**						
Yan513-7⊗	***nta-1/nta-1***	42	25		37.313						
		40	33		45.205						
		40	19		32.203						
		50	17		25.373						
		48	23		32.394						
Average					**34.498**						
Yan513-6 ⊗	***nta-1/nta-1***	44	29	0	39.726						
		38	34	1	46.575						
		48	25	2	33.333						
		45	21	3	30.435						

		42	32	0	43.243						
Average					**37.968**						
RDF190-1 ⊗	***nta pcrk1***	47	11	0	18.966						
		40	15	0	27.273						
		38	8	1	17.021						
		39	7	0	15.217						
		44	9	2	16.364						
Average					**18.968**						
RDF190-2 ⊗	***nta pcrk1***	41	4	1	8.6957						
		38	9	1	18.75						
		32	7	0	17.949						
		34	8	0	19.048						
		33	7	1	17.073						
Average					**16.303**						
RDF169-1 ⊗	***nta pcrk1***	44	20	0	31.25						
		57	10	0	14.925						
		54	14	0	20.588						
		56	12	0	17.647						
		64	4	0	5.8824						
Average					**18.059**						
RDF169-2 ⊗	***nta pcrk1***	52	9	0	14.754						
		46	9	0	16.364						
		46	12	0	20.69						
		44	7	0	13.725						
		45	5	0	10						
Average					**15.107**						
RDF169-4 ⊗	***nta pcrk1***	47	8	0	14.545						
		50	10	0	16.667						
		57	7	0	10.938						
		46	7	0	13.208						
		48	8	0	14.286						

Average					**13.929**						
RDF205-7 ⊗	***nta* x *nta pcrk1* with PCRK1::PCRK1-GFP T2 homozygous**	41	33		44.595						
***Line 1 in Figure**		69	11		13.75						
		62	11		15.068						
		64	12	2	15.385						
		54	20	1	26.667						
Average					**23.093**						
RDF205-14 ⊗	***nta* x *nta pcrk1* with PCRK1::PCRK1-GFP T2 homozygous**	37	32		46.377						
***Line 1 in Figure**		52	23		30.667						
		53	13		19.697						
		44	25		36.232						
		35	28		44.444						
Average					**35.483**						
RDF205-15 ⊗	***nta* x *nta pcrk1* with PCRK1::PCRK1-GFP T2 homozygous**	46	11	12	15.942						
***Line 1 in Figure**		61	2	9	2.7778						
		59	2	10	2.8169						
		55	9		14.063						
		54	16		22.857						
Average					**11.691**						

RDF205-2 ⊗	***nta* x *nta pcrk1* with PCRK1::PCRK1-GFP T2 homozygous**	47	20	12	25.316						
***Line 1 in Figure**		56	21	2	26.582						
		58	18	0	23.684						
		42	38	3	45.783						
		60	15	0	20						
Average					**28.273**						
RDF204-3 ⊗	***nta* x *nta pcrk1* with PCRK1::PCRK1-GFP T2 homozygous**	53	29		35.366						
***Line 2 in Figure**		70	13		15.663						
		72	18		20						
		56	16		22.222						
		66	19		22.353						
Average					**23.121**						
RDF204-6 ⊗	***nta* x *nta pcrk1* with PCRK1::PCRK1-GFP T2 homozygous**	62	20		24.39						
***Line 2 in Figure**		70	11		13.58						
		60	22		26.829						
		71	10		12.346						
		66	22		25						
Average					**20.429**						
RDF204-8 ⊗	***nta* x *nta pcrk1* with PCRK1::PCRK1-GFP T2 homozygous**	53	23		30.263						

***Line 2 in Figure**		59	17		22.368						
		71	11		13.415						
		70	11		13.58						
		64	11		14.667						
Average					**18.859**						
RDF204-10 ⊗	***nta* x *nta pcrk1* with PCRK1::PCRK1-GFP T2 homozygous**	63	9		12.5						
***Line 2 in Figure**		69	10		12.658						
		51	25		32.895						
		77	9		10.465						
		56	28		33.333						
Average					**20.37**						
RDF206-8 ⊗	***nta* x *nta pcrk1* with PCRK1::PCRK1-GFP T2 homozygous**	50	19		27.536						
***Line 3 in Figure**		55	11		16.667						
		42	21		33.333						
		61	6		8.9552						
		51	20		28.169						
Average					**22.932**						
RDF206-16 ⊗	***nta* x *nta pcrk1* with PCRK1::PCRK1-GFP T2 homozygous**	57	8		12.308						
***Line 3 in Figure**		43	25		36.765						
		51	21		29.167						

		52	19		26.761						
		33	39	2	52.703						
Average					**31.54**						
RDF209-10 ⊗	***nta* x *nta pcrk1* with PCRK1::PCRK1-GFP T2 homozygous**	65	8		10.959						
***Not included in Figure**		52	24		31.579						
		68	1		1.4493						
		46	17		26.984						
		59	6		9.2308						
Average					**16.04**						
Figure 2.10B		**Fertile**	**Infertile**	**Aborted**	**% Infertile**	**% Aborted-Looking**					
RDF206-8 x DCG24-5	***nta pcrk1* with PCRK1::PCRK1-GFP T2 homozygous x Col-0**	15	11	21	23.404	44.681					
		13	2	25	5	62.5					
		17	20	11	41.667	22.917					
		28	16	7	31.373	13.725					
		22	11	20	20.755	37.736					
Average					**24.44**	**36.312**					
RDF206-6 x DCG24-5	***nta pcrk1* with PCRK1::PCRK1-GFP T2 homozygous x Col-0**	26	11	10	23.404	21.277					
		35	17	32	20.238	38.095					
		11	7	13	22.581	41.935					
		36	21	31	23.864	35.227					
		17	40	10	59.701	14.925					

Average					**29.958**	**30.292**					
RDF206-16 x DCG24-5	***nta pcrk1* with PCRK1::PCRK1-GFP T2 homozygous x Col-0**	0	61	0	100	0					
		0	55	0	100	0					
		3	35	18	62.5	32.143					
Average					**87.5**	10.714					
RDF169-2 x Yan398-1	***nta pcrk1* x Ws**	30	2	19	3.9216	37.255					
		22	7	18	14.894	38.298					
		27	11	4	26.19	9.5238					
					15.002	**28.359**					
RDF169-3 x Yan398-1	***nta pcrk1* x Ws**	18	2	25	4.4444	55.556					
		10	1	24	2.8571	68.571					
Average					**3.6508**	**62.063**					
Figure 2.8G *nta pcrk1* Crossed by Wild-Type Pollen Results in Increased Pollen Tube Overgrowth and a POEM phenotype											
Seed Number	**Genotype**	**Fertile**	**No PT Infertile**	**Infertile w/ PT**	**PT OG Infertile**	**PT OG Fertile**	**Fertile %**				
RDF141-8 x 140-5	***nta-1* x Col-0**	33	8	0	13		61.11				
		38	8	0	10		67.86				
		33	4	0	12		67.35				
		37	2	0	13		71.15				
		30	2	1	9		71.43				
141-5 x 140-3	***nta-1* x Col-0**	37	4	0	14		67.27				
		42	12	2	8		65.63				
		53	0	0	8		86.89				
		43	7	0	11		70.49				

		46	7	0	12		70.77				
141-6 x 140-4	***nta-1* x Col-0**	36	2	0	8		78.26				
		31	10	0	7		64.58				
		32	4	0	4		80				
		43	3	0	5		84.31				
		34	2	0	8		77.27				
Avg percentage of genotype		**#REF!**	**#REF!**	**#REF!**	**#REF!**						
144-3 x 140-5	***nta pcrk1* x Col-0**	38	7	0	12	4	68.85				
		32	6	0	12	3	66.04				
		36	6	0	13	0	65.45				
144-2 x 140-3	***nta pcrk1* x Col-0**	34	12	0	10	0	60.71				
		25	13	1	8	0	53.19				
		17	15	0	6	0	44.74				
		20	9	0	8	0	54.05				
		21	4	0	8	8	70.73				
144-4 x 140-4	***nta pcrk1* x Col-0**	21	13	1	13	0	43.75				
		9	18	0	15	4	28.26				
		1	6	0	33	4	11.36				
		22	14	0	18	0	40.74				
		Fertile	**No PT Infertile**	**Infertile w/ PT**	**PT OG Infertile**	**PT OG Fertile**	**Fertile %**	**No PT Infertile %**	**Infertile with PT**	**Infertile PT OG**	**PT OG Fertile %**
144-6 x 140-7	***nta pcrk1* x Col-0**	23	17	0	5	2	53.19	14.81	0	24.1	0
		34	13	0	7	5	66.1	14.29	0	17.9	0
		28	14	0	9	4	58.18	8.163	0	24.5	0
		34	5	0	7	3	75.51	3.846	0	25	0
		25	16	0	8	0	51.02	4.762	2.38	21.4	0

141-5 x 141-5	***nta-1 x nta-1***	36	2	0	11	4	75.47	7.273	0	25.5	0
		15	16	0	5	2	44.74	18.75	3.13	12.5	0
		36	5	0	10	2	71.7	0	0	13.1	0
		29	10	0	10	0	59.18	11.48	0	18	0
percentage		62.703	7.4309	0	19.459			10.77	0	18.5	0
141-7 x 141-5	***nta-1 x nta-1***	41	6	0	12	0	69.49	9.653		17.5	
		33	8	0	8	0	67.35	4.348	0	17.4	0
		26	7	0	7	0	65	20.83	0	14.6	0
		17	10	0	8	0	48.57	10	0	10	0
percentage		65.923	7.3481	0	19.978			5.882	0	9.8	0
141-8 x 141-6	***nta-1 x nta-1***	36	1	1	8	0	78.26	4.545	0	18.2	0
		24	5	0	10	1	62.5	9.122	0	62.5	1.36
		25	4	0	10	3	66.67				
		22	9	0	7	0	57.89	12.28	0	19.7	6.56
percentage		67.747	5.0228	0.3918	21.539			12	0	22.6	5.66
Avg Percentage of Genotype		65.458	6.6006	0.1306	20.326			10.91	0	23.6	0
144-4 x 141-6	***nta pcrk1 x nta***	16	10	1	20	5	40.38				
		14	17	0	17	7	38.18	21.43	0	17.9	0
		20	11	0	19	3	43.4	27.66	2.13	17	0
		8	6	0	20	17	49.02	39.47	0	15.8	0
		21	8	0	18	3	48	24.32	0	21.6	0
percentage		34.956	10.834	0.4425	41.593			12.12	0	19.5	19.5
144-2 x 141-6	***nta pcrk1 x nta***	13	17	0	20	5	32.73				
		23	13	0	13	4	50.94	27.08	2.08	27.1	0
		6	4	0	16	14	50	42.86	0	32.6	8.7
		21	2	0	21	5	53.06	15	0	75	9.09
percentage		38.141	9.9317	0.1723	43.451			25.93	0	33.3	0
144-6 x 141-8	***nta pcrk1 x nta***	17	2	0	22	5	47.83				

		12	16	0	16	7	37.25	37.78	0	10.6	4.26
		17	7	0	21	4	42.86	24.07	0	11.9	8.47
		15	17	0	14	2	35.42	27.45	0	16.4	7.27
percentage		37.035	11.565	0.0644	43.501			10.87	0	14.3	6.12
144-3 x 141-6	***nta pcrk1 x nta***	6	27	0	16	7	23.21	32.65	0	16.3	0
		38	4	0	17	3	66.13				
		17	22	0	16	0	30.91	4.082	0	20.8	7.55
		23	7	0	12	5	59.57	44.44	0	13.2	5.26
		25	14	0	17	5	49.18	9.804	0	18.9	3.77
Figure 2.8H		**Fertile**	**Infertile**	**Aborted**	**% Infertile**	**% Aborted-Looking**		20.41	0	20.4	0
Yan371-2 x yan370-2	***nta* x Ws**	24	16	0	40	0					
		22	20	0	47.619	0			0	20.3	0
		27	17	0	38.636	0		16.33	0	16.3	0
		17	25	2		4.5455		17.5	0	17.5	0
						1.1364		28.57	0	22.9	0
RDF169-2 x Yan398-1	***nta pcrk1* x Ws**	30	2	19	3.9216	37.255					
		22	7	18	14.894	38.298		2.174	2.17	17.4	0
		27	11	4	26.19	9.5238		12.82	0	25	2.5
					15.002	**28.359**		10.26	0	23.8	7.14
RDF169-3 x Yan398-1	***nta pcrk1* x Ws**	18	2	25	4.4444	55.556		23.68	0	18.4	0
		10	1	24	2.8571	68.571					
					3.6508	**62.063**					

Figure 2.12A, B		Fertilized	Unferilized	Aborted	% Unfertilized	% Aborted-Looking		21.28	2.13	38.5	9.62
RDF236-15 x 236-11	**Col-0 x Col-0**	40	11	0	21.569			35.42	0	30.9	12.7
		41	8	0	16.327			22	0	35.8	5.66
		45	0	0	0			17.65	0	39.2	33.3
					12.632			17.02	0	36	6
RDF236-12 x RDF236-12	**Col-0 x Col-0**	54	5		8.4746						
		52	8		13.333			34	0	36.4	9.09
		21	34		61.818			26.53	0	24.5	7.55
					27.875			15.38	0	40	35
RDF236-11 x 236-11	**Col-0 x Col-0**	36	14		28			4.545	0	42.9	10.2
		46	2	2	4						
		36	9		20			4.878	0	47.8	10.9
		30	12	1	27.907			36.36	0	31.4	13.7
					19.977			15.56	0	42.9	8.16
RDF236-12 x 239-6	**Col-0 x *pcrk1***	43	8		15.686			36.96	0	29.2	4.17
		30	13		30.233						
		32	5		13.514			55.1	0	28.6	12.5
					19.811			6.78	0	27.4	4.84
RDF236-11 x 239-6	**Col-0 x *pcrk1***	35	10	2	21.277			40	0	29.1	0
		32	12		27.273			16.67	0	25.5	10.6
		38	5		11.628			25	0	27.9	8.2

		38	8	1	17.021						
					19.3						
RDF236-15 x RDF239-7	**Col-0 x *pcrk1***	33	8	5	17.391						
		27	8	7	19.048						
		30	14	2	30.435						
					22.291						
RDF237-1 x 236-13	***fer-4* x Col-0**	9	35	8	67.308	15.385					
		12	35	11	60.345	18.966					
					63.826						
RDF237-6 x RDF236-13	***fer-4* x Col-0**	16	40	0	**71.429**	**0**					
RDF237-1 x 239-6	***fer-4 x pcrk1***	15	16	24	29.091	43.636					
		9	24	20	45.283	37.736					
		4	45	4	84.906	7.5472					
		6	20	22	41.667	45.833					
					50.237	**33.688**					
RDF237-4 x RDF239-6	***fer-4 x pcrk1***	3	38	16	66.667	28.07					
		2	36	12	72	24					
RDF237-1 x RDF239-6		3	49	4	87.5	7.1429					
					69.101	**23.225**					
Seed Number	**Genotype**	**Fertilized**	**Unfertilized**	**POEM**	**% Unfertilized**	**% POEM**	**% Fertilized**				

DCG52-4 x RDF243-4	***turan* /+ x *pcrk1***	43	4	16	6.3492	25.397	68.25				
		53	1	7	1.6393	11.475	86.89				
		39	6	18	9.5238	28.571	61.9				
x RDF234-2		26	11	18	20	32.727	47.27				
		37	9	15	14.754	24.59	60.66				
Average					**10.453**	**24.552**	**64.99**				
DCG52-3 x RDF234-2	***turan* /+ x *pcrk1***	46	0	16	0	25.806	74.19				
		28	14	8	28	16	56				
		19	18	12	36.735	24.49	38.78				
Average					**21.578**	**22.099**	**56.32**				
DCG52-7 x RDF234-6	***turan* /+ x *pcrk1***	37	6	22	9.2308	33.846	56.92				
		34	4	24	6.4516	38.71	54.84				
		35	5	25	7.6923	38.462	53.85				
		42	15	11	22.059	16.176	61.76				
		39	5	24	7.3529	35.294	57.35				
		49	6	13	8.8235	19.118	72.06				
Average					**10.268**	**30.268**	**59.46**				
DCG52-5 x RDF234-8	***turan* /+ x *pcrk1***	33	10	23	15.152	34.848	50				
		46	6	14	9.0909	21.212	69.7				
		39	4	26	5.7971	37.681	56.52				
		42	2	22	3.0303	33.333	63.64				
Average					**8.2675**	**31.769**	**59.96**				
DCG52-18 x RDF234-8	***turan* /+ x *pcrk1***	50	1	23	1.3514	31.081	67.57				
		49	1	22	1.3889	30.556	68.06				
		55	2	28	2.3529	32.941	64.71				

		34	11	22	16.418	32.836	50.75				
xRDF234-2		40	2	27	2.8986	39.13	57.97				
		27	17	20	26.563	31.25	42.19				
Average					**8.4954**	**32.966**	**58.54**				